



TECHNISCHE
UNIVERSITÄT
WIEN
Vienna University of Technology

GEOWISSENSCHAFTLICHE MITTEILUNGEN

Heft Nr. 92, 2013

**VLBI scheduling strategies
with respect to VLBI2010**

Jing Sun

Veröffentlichung des Departments für Geodäsie und Geoinformation
ISSN 1811-8380

Schriftenreihe der Studienrichtung VERMESSUNG UND GEOINFORMATION



TECHNISCHE
UNIVERSITÄT
WIEN
Vienna University of Technology

GEOWISSENSCHAFTLICHE MITTEILUNGEN

Heft Nr. 92, 2013

VLBI scheduling strategies with respect to VLBI2010

Jing Sun

Veröffentlichung des Departments für Geodäsie und Geoinformation
ISSN 1811-8380

Schriftenreihe der Studienrichtung VERMESSUNG UND GEOINFORMATION

2013

Published by the Department of Geodesy and Geoinformation
of the Vienna University of Technology
Gußhausstraße 27-29
1040 Vienna, Austria

Responsible for this issue: Prof. Dr. Johannes Böhm

Printed by: Grafisches Zentrum HTU GmbH

The digital version of the full document with colored figures is available online:

<http://www.ub.tuwien.ac.at/diss/AC07814953.pdf>

Die Kosten für den Druck wurden vom Department für Geodäsie und Geoinformation übernommen.

Diese Arbeit wurde an der Fakultät für Mathematik und Geoinformation der Technischen Universität Wien zur Erlangung des akademischen Grades einer Doktorin der technischen Wissenschaften eingereicht.

Begutachter:

Prof. Dr. Harald Schuh

Department für Geodäsie und Geoinformation der Technischen Universität Wien

Gußhausstraße 27-29, 1040 Wien, Österreich

Department 1 „Geodäsie und Fernerkundung“, Deutsches Geoforschungszentrum GFZ

Telegrafenberg, 14473 Potsdam, Deutschland

Dr. John M. Gipson

NASA Goddard Space Flight Center, Code 698.2

Greenbelt, MD 20771, USA

Tag der mündlichen Prüfung: 01.02.2013

Auflage: 100 Stück

ISSN 1811-8380

Prüfungssenat:

Prof. Dr. Georg Gartner
Vienna University of Technology

Prof. Dr. Harald Schuh
GFZ German Research Centre for Geosciences

Dr. John M. Gipson
NASA Goddard Space Flight Center

Prof. Dr. Johannes Böhm
Vienna University of Technology

Assoc.Prof. Dr. Rüdiger Haas
Chalmers University of Technology

Abstract

Very Long Baseline Interferometry (VLBI) plays an important role for the realization of global geodetic reference frames. The next generation VLBI system, called VLBI2010, has been developed with a major goal of bridging the gap from the current 5 mm level of accuracy for VLBI position determination to the new sub 1 mm requirement. To reach the goals of VLBI2010, various new facets have been investigated within the International VLBI Service for Geodesy and Astrometry (IVS) including small fast-moving antennas, broadband frequency observations (2-14 GHz), and two or more antennas at a site. In order to exploit the full power of the future VLBI2010 system and to derive the best possible geodetic parameters, a new scheduling package (VIE_SCHED) has been developed at the Vienna University of Technology, which is the main research objective of the thesis.

This scheduling research takes into considerations all present and future VLBI2010 requirements and implements the various specifications of VLBI2010 antennas. Considering a more uniform network and fast moving antennas, one of the strategies is new source-based scheduling, which means that the scheduling program selects radio sources from the catalogue without regard for their direct impact on individual stations. The other strategy is conventional station-based scheduling, i.e. the sky coverage is optimized in short intervals taking into account the rapid atmospheric variability, partly at the expense of the total number of observations. The research also includes radio source structure models, antenna models, and the considerations of antenna maintenance and power saving mode. Schedules of sites with multiple antennas are also considered. The scheduling package offers the possibility to the user to optimize the schedule for various simulations and studies according to different criteria. It also writes .skd file, which contains a complete description of the session, the schedule and the additional information used in scheduling a real IVS session.

Within the doctoral thesis, the new scheduling package VIE_SCHED is developed, implemented

and tested according to the requirements of the VLBI2010 system. To validate the newly developed scheduling algorithms, thorough and realistic Monte Carlo simulations have been carried out. VIE_SCHED is directly connected to Vienna VLBI Software (VieVS) to provide feedback on the quality of the schedule. Different schedules for 24-hour continuous observations are compared in terms of schedule performance and estimated geodetic parameters to evaluate different scheduling strategies, considering both the test VLBI2010 network and the current IVS network. Results of similar quality are achieved with the two scheduling strategies – source-based scheduling strategy and station-based scheduling strategy. The comparisons with other scheduling packages (e.g. SKED software) also show a good agreement. In the last phase of the scheduling research, VIE_SCHED has been accepted by the IVS Coordinating Center for scheduling RD sessions successfully since June 2012.

Zusammenfassung

Acknowledgements

I am profoundly grateful to Prof. Dr. Harald Schuh who offered me a project position and accepted me to perform my PhD at the Vienna University of Technology under his supervision. I admire and respect him for his willingness to share his knowledge and experiences to the people around him. And he always provides the most opportunities he can to the young geodesists. I am also thankful for his constant instructions, supports, encouragements and motivations on my studies.

I am forever grateful to Prof. Dr. Johannes Böhm for his patient instructions on my doctoral studies from the beginning to the end. Dr. Tobias Nilsson is always helpful to me on solving lots of scientific and technical problems. I want to express my appreciation to Dipl.-Ing. Lucia Plank, Dipl.-Ing. Hana Krasna, Dr. Sigrid Böhm, Dipl.-Ing. Matthias Madzak, Dipl.-Ing. Claudia Tierno Ros, Dipl.-Ing. Andrea Pany, and Dr. Kamil Teke whom I closely work together within VLBI group. My PhD study could not have been fruitful without the contributions of my colleagues to Vienna VLBI software. I also want to thank Dipl.-Ing. Gregor Möller and Dipl.-Ing. Fabian Hinterberger who share the biggest and brightest office with me and are always helpful to me. I want to forward my heartfelt thanks to Frau Linsmayer who is our secretary. I also thank Banoub Akladiou for his supports. I thank all my colleagues working together at the Advanced Geodesy Research Group for being always helpful and kind to me and I will remember them forever. I feel very lucky to have experienced a great support and joyful working atmosphere with all cooperative colleagues. I want to thank the Austrian Science Fund (FWF) for supporting this work (P21049-N14) and the expenses for many scientific meetings. Vienna, the metropolis on the Danube, will be in my memory forever.

I want to express my thanks to Dr. John M. Gipson for accepting to be my secondary supervisor. He gives me great supports and encouragements each time when I get an improvement. Moreover he explained the existing scheduling software detailedly and shared his experiences of scheduling

with me. I also want to thank Dirk Behrend for his trust because the participation in real IVS sessions validated and improved the new scheduling package greatly. I'd like to give my thanks to GSFC VLBI group for many communications and discusses and to the IVS stations and correlators for providing feedbacks on my schedules. I also thank the colleagues of VLBI2010 Committee (V2C). The monthly teleconference always gives me many inspirations. Special thanks are given to Bill Petrachenko, Arthur Niell, and the other members of the V2C for many valuable comments and fruitful discussions. I want to thank the users of the new scheduling package for your feedbacks, comments, and questions. I cordially acknowledge the International VLBI Service for Geodesy and Astrometry (IVS) and the other IAG and IUGG services for the data and the numerous authors for their publications that I benefitted from in my doctoral studies.

I also want to forward my special thanks to Shanghai Astronomical Observatory and Beijing Aerospace Control Center where I started the study of VLBI space technique. I'd like to express particular thanks to Prof. Zhihan Qian, Prof. Jinsong Ping and Prof. Geshi Tang who supported my academic studies abroad when I was in need of help.

I also want to thank all reviewers for their useful comments and constructive remarks, which ensure the quality of this thesis.

Finally, I am enormously grateful to my mother and father, and my husband for their endless love, understanding, patience and support.

Contents

Abstract	i
Zusammenfassung	iii
Acknowledgements	iv
Contents	vi
List of Figures	ix
List of Tables	xii
Symbols	xiii
Acronyms	xvi
1 Introduction	1
1.1 VLBI basics	1
1.2 VLBI2010 background and development	2
1.3 Contribution of the thesis and research objectives	4
1.4 Outline of the thesis	6
2 Selection of radio sources for geodetic VLBI	7
2.1 The ICRF2 data	7
2.2 Characteristics of radio sources	8
2.2.1 Radio source positional accuracy	8
2.2.2 Radio source flux density	8
2.2.3 Radio source structure and correction model	10
2.3 Suitable radio sources for geodetic VLBI	12
3 Algorithms and models for a scan	15
3.1 Calculation of scan start time	15

3.1.1	Cable wrap and slew distance of AZEL antenna	15
3.1.2	Slew time of antenna	17
3.1.3	How to calculate the start time of a scan	18
3.2	Calculation of scan length	19
3.2.1	Antenna sensitivity and its elevation-dependent reduction	19
3.2.2	How to calculate scan length	21
3.3	The conditions of a valid scan	22
3.3.1	Horizon mask	22
3.3.2	Definition of a valid scan	23
3.4	Other system considerations	25
3.4.1	Electric power saving	25
3.4.2	Antenna maintenance and antenna life time	25
4	Strategies for automatic scheduling	27
4.1	Source-based scheduling strategy	28
4.1.1	One-source scheduled each time	29
4.1.2	Two-source scheduled simultaneously	30
4.1.3	Four-source scheduled simultaneously	31
4.2	Station-based scheduling strategy	32
4.2.1	Definition of sky coverage	32
4.2.2	Subconfiguration selection algorithm	33
4.2.3	An example of station-based strategy	35
4.3	Fill-in mode	35
4.4	Comparisons and analyses of the scheduling strategy	37
4.4.1	Two solutions for mutual visibility of source-based strategy	37
4.4.2	Different schedules for the VLBI2010 network	38
4.4.3	Different schedules for the IVS R1 network	41
5	Simulations and results	45
5.1	Monte Carlo simulations	45
5.2	Simulations and results for VLBI2010	46
5.2.1	Simulation parameters	46
5.2.2	Estimation parameters	49
5.2.3	Antenna specifications and basic scheduling settings	50
5.2.4	Comparisons of schedule performance	52

5.2.5	Comparisons of estimated geodetic parameters	55
5.3	Simulations and results for CONT11	56
5.3.1	Comparisons of schedule performance	57
5.3.2	Comparisons of estimated geodetic parameters	59
5.3.3	Conclusions	63
6	Applications of scheduling	64
6.1	Interim network consisting of fast and slow antennas	64
6.1.1	Simulations	64
6.1.2	Results	67
6.1.3	Conclusions	68
6.2	Twin telescopes at one site	69
6.2.1	Observing strategies	70
6.2.2	Simulations and results	71
6.2.3	Conclusions	73
6.3	Solar corona study	73
7	Conclusions, future work, and perspectives	77
7.1	Conclusions	77
7.2	Future work	78
7.3	Perspectives	79
	List of references	81
	Curriculum vitae	85
	Appendices	86
A	Appendices	86
A.1	Reference manual of VIE_SCHED program	86
A.1.1	Overview of VIE_SCHED	86
A.1.2	Distribution and installation	87
A.1.3	Input files	88
A.1.4	How to run VIE_SCHED	92
A.1.5	Output files	95
A.1.6	Analyzing tools	95

List of Figures

1.1	VLBI system. The yellow layer represents the stochastic errors due to the atmosphere and the red circles indicate the stochastic errors of the clocks. (by courtesy of Jörg Wresnik)	1
2.1	Distribution of the total 3414 ICRF2 radio sources (blue squares), of the 1217 non-VCS radio sources (green diamonds). The 295 defining radio sources of ICRF2 are marked with red circles.	8
2.2	Formal error of the position estimate vs. declination.	9
2.3	Distribution of the flux for 658 radio sources at X band and S band.	9
2.4	Distribution of the mean structure index for 701 radio sources at X band.	10
2.5	Distribution of the 211 suitable radio sources on celestial sphere.	13
2.6	Skyplot of the grid.	13
2.7	Distribution of the 211 suitable radio sources in segments.	14
3.1	Antenna cable wrap at station KOKEE.	16
3.2	Elevation mask at station TIGOCONC.	23
3.3	Elevation mask at station NYALES20.	24
4.1	An test VLBI2010 network (16 stations).	28
4.2	An typical IVS R1 network (8 stations).	28
4.3	Visibility of one-source configuration for the VLBI2010 network (left) and the IVS R1 network (right).	29
4.4	The example of two-source configuration on the sky.	30
4.5	Visibility of two-source configuration for the VLBI2010 network (left) and the IVS R1 network (right).	30
4.6	The example of four-source configuration on the sky.	31
4.7	Visibility of four-source configuration for the VLBI2010 network (left) and the IVS R1 network (right).	31

4.8	Sky plot at station HartRAO for a schedule with a slowly moving antenna (1.5 deg/sec in azimuth and 0.7 deg/sec in elevation) and no particular algorithm to create uniform sky coverage. The plot shows the observations in a time window of 30 min. As an additional information all observations in a 6 minute time window have the same color.	33
4.9	Sky coverage of one hour at 8 stations of the IVS R1 network	35
4.10	Flowchart of the alternation between standard mode and fill-in mode in scheduling.	36
4.11	Distribution of scans and observations at 8 stations of the IVS R1 network.	37
4.12	Mean sky coverage of one hour at 8 stations of the IVS R1 network.	37
4.13	Eight schedules for the test VLBI2010 network.	40
4.14	Mean subnet size for the test VLBI2010 network.	41
4.15	Eight schedules for the IVS R1 network.	43
4.16	Mean subnet size for the IVS R1 network.	44
5.1	Scheme of the Monte Carlo simulations with VieVS.	47
5.2	Mean on-source time for the VLBI2010 system.	53
5.3	Mean slew time for the VLBI2010 system.	53
5.4	Mean source-switching interval for the VLBI2010 system.	53
5.5	Distribution of scans for the VLBI2010 system.	54
5.6	Distribution of observations for the VLBI2010 system.	54
5.7	Mean subnet size per scan for the VLBI2010 system.	54
5.8	Number of observed sources for the VLBI2010 system.	54
5.9	Mean sky coverage of 10 minutes for the VLBI2010 system.	55
5.10	Required time for the whole sky coverage (sky coverage is of category 13).	55
5.11	Distribution of observed sources on celestial sphere per 15 min for the VLBI2010 system.	55
5.12	RMS of 3D position error for the VLBI2010 system.	56
5.13	Baseline length repeatability for the VLBI2010 system.	57
5.14	The IVS CONT11 network (13 stations).	58
5.15	Distribution of scans for the CONT11 session.	58
5.16	Distribution of observations for the CONT11 session.	58
5.17	Mean subnet size per scan for the CONT11 session.	59
5.18	Number of observed sources for the CONT11 session.	59
5.19	Mean sky coverage of one hour for the CONT11 session.	59

5.20	Distribution of observed sources on celestial sphere per one hour for the CONT11 session.	59
5.21	RMS of 3D position error for the CONT11 session.	61
5.22	Baseline length repeatability obtained from simulations for CONT11. The site-dependent value for C_n was used for each station. Also given are the rates (slopes of the straight lines fitted to the data) in mm Mm^{-1} (ppb).	62
6.1	18 stations network used for the VLBI2010 simulations. Stars denote legacy antennas, circles new fast slewing antennas.	65
6.2	Distribution of observations. Results from SKED are shown with left bar (red), and results from VIE_SCHED are shown with right bar (blue). The station indices are consistent with increasing slew rate.	67
6.3	Idling, slewing, and observing percentage. Results from SKED are shown left, results from VIE_SCHED are shown right.	68
6.4	Sky coverage distribution for 20 minutes interval.	68
6.5	Station position repeatabilities obtained from the simulations. Results from SKED are shown with left bar (red), and results from VIE_SCHED are shown with right bar (blue).	69
6.6	Network used for simulations. The red circle denotes station Wettzell with twin telescopes.	71
6.7	Mean observing duration from “same source observations” mode.	72
6.8	Number of observations from the three observing modes.	72
6.9	Sky coverage from “multidirectional observations” mode.	72
6.10	Station position repeatabilities from “multidirectional observations” mode.	72
A.1.1	The structure of VIE_SCHED within VieVS.	87
A.1.2	VIE_SCHED graphical user interface (GUI).	93
A.1.3	Run options for VIE_SCHED.	94

List of Tables

4.1	Eight schedules for the VLBI2010 network.	38
4.2	Eight schedules for the IVS R1 network.	41
5.1	Simulation parameters for the VLBI2010 system.	47
5.2	Statistics of the schedules for the VLBI2010 system.	52
5.3	Statistics of the schedules for the CONT11 session.	58
5.4	Simulation parameters for the CONT11 session.	60
5.5	Site-dependent Cn for the CONT11 session.	60
5.6	Repeatability and standard deviation of ERP.	62
5.7	Repeatability and standard deviation of Nutation.	62
6.1	Characteristics of the 18 stations used for the simulations. The numbering of the stations (station indices) in the table corresponds to the numbers in Figures 6.2 to 6.5. The slewing rates given are just exemplificative values used for the simulations and do not always agree with the real or projected specifications of the antennas. . .	65
6.2	Statistics of the different schedules.	67
6.3	Schedule performance of RD1205 session.	75
6.4	Schedule performance of RD1206 session.	75
A.1.1	Catalog system files.	88
A.1.2	Minor scheduling options.	91

Symbols

Selection of radio sources for geodetic VLBI

σ	the formal error on the source position estimate
σ_α	the formal error on the right ascension estimate
σ_δ	the formal error on the declination estimate
$C(\alpha, \delta)$	the correlation between estimates of right ascension and declination
F_{obs}	predicted flux density of the component
F	total flux density of the component
θ	size of the major axis of the component
l	effective baseline length
b_x	x component of the baseline
b_y	y component of the baseline
b_z	z component of the baseline
R	axial ratio of the component
pa	position angle of the component major axis with respect to the origin
GHA	Greenwich hour angle of the source
δ	source declination

Algorithms and models for a scan

T_{AZEL}	slew time in both azimuth and elevation axes
T_{AZ}	slew time in azimuth axis
T_{EL}	slew time in elevation axis
T_{HADC}	slew time in both hour angle and declination axes
T_{HA}	slew time in hour angle axis
T_{DC}	slew time in declination axis

$T_{2s}(i)$	the earliest possibly start time for the 2nd observation at the i th station
$T_{1e}(i)$	the end time of the 1st observation at the i th station
$T_{slew}(i)$	the slew time that the i th antenna requires
<i>SOURCE</i>	time for the antenna to settle down
<i>TAPETM</i>	time for the tape
<i>IDLE</i>	time for idling
<i>CALI</i>	time for calibration
$T_{1s}(i)$	start time of the 1st observation at the i th station
$DUR(i)$	observation duration at the i th station
$T_{2s}(scan)$	start time of the 2nd scan
k	Boltzmann's constant
T_{sys}	system temperature
A_{eff}	the effective collecting area of the antenna
D	antenna diameter
η	the VLBI processing factor
<i>SEFD</i>	antenna sensitivity
$f(el)$	a function of the elevation
n	number of terms
el	the elevation of the source
c_i	coefficient for the i th term
y	power of the $\sin(el)$ term
F_{obs}	observed source strength
B	bandwidth
N_{ch}	number of channels
<i>scanlength</i>	scan length for integration
<i>CORSYNCH</i>	time for synchronization

Simulations and results

wzd_1	simulated wet zenith delay at station 1
wzd_2	simulated wet zenith delay at station 2
$clock_1$	simulated clock value at station 1
$clock_2$	simulated clock value at station 2
$mfw_1(el)$	the wet mapping function at station 1

$mfw_2(el)$ the wet mapping function at station 2
 el elevation angle
 wn white noise per baseline

Acronyms

ASD	Allan Standard Deviations
AUSCOPE	the Australian VLBI Network
AZEL	Azimuth-elevation Mount
CRF	Celestial Reference Frame
ECMWF	European Center for Medium-Range Weather Forecasts
EOP	Earth Orientation Parameters
ERP	Earth Rotation Parameters
GGOS	Global Geodetic Observing System
GSFC	Goddard Space Flight Center
GUI	Graphical User Interface
HADC	Hour angle-declination Mount
IAG	International Association of Geodesy
ICRF	the International Celestial Reference Frame
ICRF2	the Second Realization of the International Celestial Reference Frame
IUGG	International Union of Geodesy and Geophysics
IVS	International VLBI Service for Geodesy and Astrometry
NNR	No Net Rotation
NNT	No Net Translation
OPC	Observing Program Committee
RAM	Random-Access Memory
RDV	Research and Development with the VLBA
RFI	Radio Frequency Interference
RMS	Root Mean Square
SEFD	System Equivalent Flux Density
SI	Structure Index

SNR	Signal-to-Noise Ratio
TEC	Total Electron Content
TRF	Terrestrial Reference Frame
TTW	Twin Telescope Wettzell
VCS	Very Long Baseline Array Calibrator Surveys
VieVS	Vienna VLBI Software
VLBA	Very Long Baseline Array
VLBI	Very Long Baseline Interferometry
V2C	VLBI2010 Committee
WG	Working Group
WZD	Wet Zenith Delay

1. Introduction

1.1. VLBI basics

Very Long Baseline Interferometry (VLBI) is a radio astronomical technique in which two or more antennas simultaneously observe the same source of radio emission (Figure 1.1), usually a compact extragalactic object like a quasar, typically billions of light years away. The faint received signals are cross-correlated to determine the difference in their arrival time. Knowing the speed of light, these time delays can be interpreted as the component of the baseline (i.e. the vector connecting two antennas) in the direction of the source. If several radio sources are observed subsequently, all components of the baseline can be determined unambiguously.

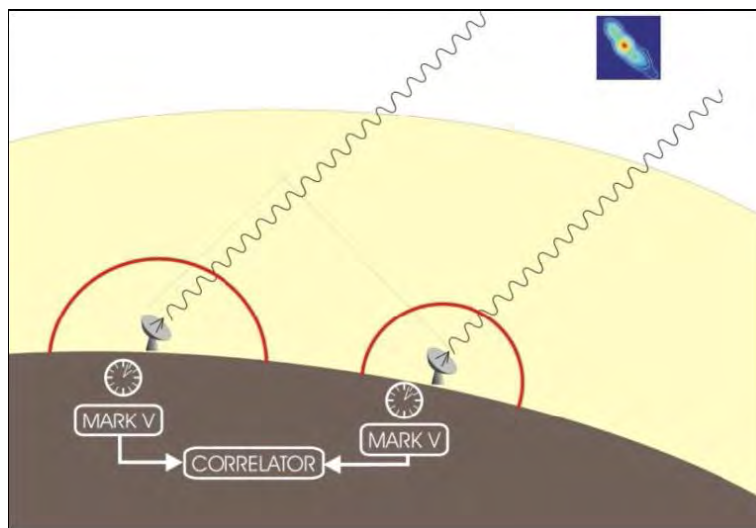


Figure 1.1.: VLBI system. The yellow layer represents the stochastic errors due to the atmosphere and the red circles indicate the stochastic errors of the clocks. (by courtesy of Jörg Wresnik)

The VLBI technique has now been employed in geodesy for over 40 years and it plays an important role for the realization of global geodetic reference frames. In particular, it is a major contributor to the definition of a stable scale of the Terrestrial Reference Frame (TRF) and it has

a unique capability to determine the orientation of the Earth in space, an essential element for all positioning and navigation (Schuh and Böhm, 2013). The current accuracy for VLBI position determination from a 24-hour observing session is on the level of 5 mm (Schlüter and Behrend, 2007). An important element towards achieving this level of accuracy is the development of scheduling algorithms that allow successful separation of the various geodetic parameters in large multi-parameter adjustments (Steffmeier, 1994).

1.2. VLBI2010 background and development

The International VLBI Service for Geodesy and Astrometry (IVS) was inaugurated in February 1999. Since then, the IVS has been coordinating the global VLBI components and resources on an international basis (Schlüter and Behrend, 2007). Within the frame of IAG's (International Association of Geodesy) flagship project GGOS (Global Geodetic Observing System) it has become clear that modern space geodetic techniques should provide station coordinates and/or baseline length time series with an accuracy better than 1 mm. Only then subtle effects like non-linear station motions related to geo-hazards such as earthquakes or sea level rise can be detected and studied (Plag et al., 2009). In September 2003, the IVS formed a Working Group (WG3) to begin a process of modernization with a major goal of bridging the gap from the current 5 mm level of accuracy for VLBI position determination to the sub 1 mm requirement, nearly one order of magnitude improvement. In September 2005 the IVS Directing Board accepted the final report of WG3 entitled "VLBI2010: Current and Future Requirements for Geodetic VLBI Systems" (Niell et al., 2005). This bold vision for the future recommended a review of all current VLBI systems and processes from antennas to analysis and outlined a path to a next-generation system with unprecedented new capabilities:

- 1 mm position accuracy on global scales;
- continuous measurements for time series of station positions and Earth orientation parameters;
- turnaround time to initial geodetic results of less than 24 hours.

Immediately following the acceptance of the WG3 final report, the IVS established the VLBI2010 Committee (V2C) as a permanent body to encourage the implementation of the recommenda-

tions of WG3 in the same year. Since its inception, the V2C has accomplished much towards this goal. The progress of the VLBI2010 efforts is discussed at general VLBI meetings, dedicated workshops and online fora. The V2C investigates the various facets that the new system needs to fulfill the requirements. The major focus is on reducing the main error sources stemming from the atmosphere, the instrumentation, and the structure of the radio sources. The following performance-enhancing strategies are envisaged: (1) a reduction of random errors, e.g. the delay measurement error, the stochastic properties of the clocks, and the unmodeled variation of the atmosphere; (2) a reduction of systematic errors, e.g., thermal and gravitational deflections of the antennas, drifts of the electronics, and radio source structure; (3) an increase in the size and an improvement in the geographic distribution of networks; (4) an increase of observation density, i.e., number of observations per unit time; (5) a reduction of susceptibility to external radio-frequency interference (Niell et al., 2005).

The V2C also works on the design of a new VLBI system based on fast moving, small (≈ 12 m diameter), mechanically reliable antennas that can be replicated economically. In order to shorten the on-source observing time, it is important to find a means for measuring the delay with the required precision even at a modest signal-to-noise ratio (SNR). To do this a new approach is being developed in which several widely spaced frequency bands are used to unambiguously resolve the interferometric phase. The new observable is being referred to as the broadband delay. A four-band system is recommended that uses a broadband feed to span the entire frequency range from 2 to 14 GHz. It includes both the current S-band and X-band frequencies for backwards compatibility, but allows much more agility to avoid RFI and more bandwidth to significantly improve delay measurement precision. In order to detect an adequate number of high-quality radio sources, a total instantaneous data rate as high as 32 Gbps and a sustained data storage or transmission rate as high as 8 Gbps are necessary. It is also recognized that reducing systematic errors (e.g. electronic biases, antenna deformations, source structure, etc.) plays a critical role in improving VLBI accuracy. One of the VLBI2010 strategies for improvement is to achieve a better global coverage of VLBI antennas. Today, most VLBI antennas are located on the northern hemisphere, and are concentrated near areas of high population density. However, VLBI's important contribution of scale and orientation to global reference frames can be improved with a more uniform distribution of sites on the globe. A high priority is placed on increasing the number of stations in the southern hemisphere. At the same time, some of the existing large antennas will be updated for compatibility with the new small-antenna system; this will allow them to co-observe with the small-antenna systems to preserve

continuity with the historical record, as well as to improve the Celestial Reference Frame (CRF) measurements made primarily by the large antennas. The use of multiple antennas at a site is also proposed to share the observing load and hence to reduce the effective source-switching interval. As for operational considerations, it is recommended that a globally distributed network of at least 16 VLBI2010 antennas observes every day to determine Earth Orientation Parameters (EOP), and that other antennas be added as needed for the maintenance of the celestial and terrestrial reference frames. A subset of antennas with access to high-speed fiber networks is also required to enable daily delivery of initial IVS products in less than 24 hours. In order to increase reliability and to reduce the cost of operations, enhanced automation will be introduced both at the stations and in the analysis process (Himwich and Corey, 2009). It should also be mentioned that there are still a number of risks to successful implementation of VLBI2010, the most significant ones include data volume, Radio Frequency Interference (RFI), the broadband delay technique (Petrachenko et al., 2009).

Up to the spring of 2012, a number of VLBI2010 projects are under way; several antennas have been erected and construction of about ten antennas is at various stages of completion. The project of Twin Telescope Wettzell (TTW) is the first rigorous approach to realize a radio telescope system consisting of more than one antenna per site. Further projects are in the proposal or planning stage. The next-generation IVS network is growing organically, with an operational core of stations becoming available within the next few years, plus further growth continuing into the foreseeable future.

1.3. Contribution of the thesis and research objectives

In the final report of WG3, the importance of new observing strategies and scheduling algorithms was clearly recognized. Considering also the recommendations for future IVS products given in the final report of the former IVS Working Group 2 (WG2) “Product Specification and Observing Programs ”(Schuh et al., 2002), a new set of criteria to specify the next generation geodetic VLBI system was established by the V2C.

In practice, it is a great challenge to achieve the geodetic and astrometric quantities with the targeted accuracy. The independent oscillators used as time references at each station and the atmosphere layers above the stations both add unpredictable contributions to the measured signal delay (Sun et al., 2010). To provide the highest-level observations, these phenomena need

to be separated from the geodetic parameters of interest. It has been shown that the accuracy of the estimated parameters directly depends on the observation density of a 24-hour VLBI session. For the VLBI2010 system, the number of observations per day is increased by: (1)decreasing the slew time from source to source; (2)decreasing the time to acquire data while on a radio source; (3)changing the scheduling algorithm.

As for the effect of the first measure, i.e. how the number of observations depends on the slew speed of the antennas, obviously the linear relation of number of observations versus slew speed ends between 4.5 deg/sec and 6 deg/sec. Furthermore it has to be considered that very fast antennas will be more expensive and will definitely need more maintenance. The second measure, i.e. reducing the on-source time, is also limited, as a minimum scan length has to be kept in order to achieve the necessary coherent integration time of an observed radio source. Five seconds on each radio source is assumed to be the absolute minimum. Thus, the only means to further increase the number of observations of a schedule is to improve the scheduling algorithm and strategy, which will be the main target of the thesis. As for the schedule it has to be taken into account that an increased number of observations does not necessarily correspond to an improved geometry. The simulations done so far have shown that more work is needed to optimize the sky coverage in short intervals (<10 minute) taking into account the rapid atmospheric variation, perhaps at the expense of the total number of observations (Wresnik et al., 2009).

This research takes into considerations all present and future VLBI2010 requirements and implements the various specifications of VLBI2010 antenna. The goal of the thesis is to study, optimize and implement new scheduling algorithms to exploit the full power of the future VLBI2010 system, and in this new context derive the best possible geodetic parameters. The various VLBI scheduling strategies and algorithms are carefully investigated, the resulting schedules are thoroughly evaluated based on the Monte Carlo simulations and a new scheduling software (VIE_SCHED) has been developed from scratch. VIE_SCHED is strongly related to current activities within V2C and fully compatible with the VLBI2010 specifications. With the new Matlab software VIE_SCHED it is also very easy to consider any new development and model. Some obsolete and no longer necessary models related to tape, e.g. tape recording and tape speed, are removed from scheduling, because the days when tapes were used to record data was passed and all recording is now done using disks. And some stations are already connected to fast Internet links.

1.4. Outline of the thesis

In Chapter 2 of this thesis, the characteristics of radio sources are studied and a preliminary list of suitable radio sources for geodesy is established. In Chapter 3 the basic algorithms and models used in scheduling are described. Chapter 4 explains the different scheduling strategies in detail. The results from various VLBI scheduling strategies and algorithms are compared and analyzed in Chapter 5. In Chapter 6 the application in various studies to better understand the scheduling strategy is presented. Chapter 7 summarizes the research and proposes next steps for the study. Appendix A is the reference manual of the new scheduling software (VIE_SCHED), including the graphical user interface (GUI).

2. Selection of radio sources for geodetic VLBI

This chapter reports on the establishment of a preliminary list of suitable radio sources for geodetic VLBI based on their positional stability, flux density, source structure indices, and distribution on the sky. It has to be noted that the characteristic values mentioned below represent a snapshot of the available data at the time this work was carried out and that these values may evolve with time. And the characteristics of radio sources are still studied at dual bands (S/X band) because the complete data for the radio sources at wide VLBI2010 frequencies (2-14 GHz) is unavailable now.

2.1. The ICRF2 data

The second realization of the International Celestial Reference Frame (ICRF2) is generated at radio wavelengths using nearly 30 years of VLBI observations. The ICRF2 contains precise positions of 3414 compact radio astronomical sources. Compared to the first ICRF, the second ICRF has more than 5 times as many sources, is roughly 56 times more accurate, and is nearly twice as stable. The ICRF2 is found to have a noise floor of only $\approx 40 \mu\text{as}$ and an axis stability of $\approx 10 \mu\text{as}$. Of the total 3414 sources, 2197 sources are observed only in one (or a few) sessions, e.g. in Very Long Baseline Array (VLBA) Calibrator Surveys (VCS) sessions. Among the remaining 1217 sources, 295 sources have been designated as defining sources on the basis of their positional stability and a lack of any known extensive source structure (Ma, 2009). The total 3414 ICRF2 sources, the 1217 non-VCS sources, and the 295 defining sources are displayed in Figure 2.1. It is found that the amount of data begins to drop off quickly for sources south of around -30° declination. With the development of new antennas in the southern hemisphere, e.g. the Australian VLBI network (AUSCOPE), more and more new sources in the far south will be observed. On the basis of the ICRF2 data, various characteristics of radio sources are investigated and ranked in the next section.

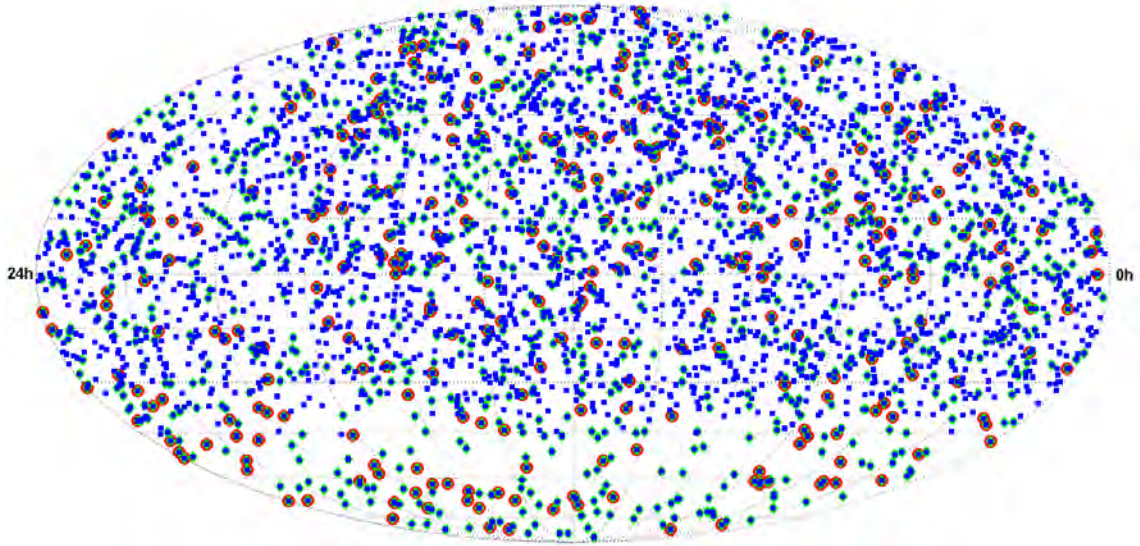


Figure 2.1.: Distribution of the total 3414 ICRF2 radio sources (blue squares), of the 1217 non-VCS radio sources (green diamonds). The 295 defining radio sources of ICRF2 are marked with red circles.

2.2. Characteristics of radio sources

2.2.1. Radio source positional accuracy

An overall formal error on the radio source position estimate σ can be computed with Equation (2.1).

$$\sigma = \sqrt{\sigma_\alpha^2 + \sigma_\delta^2 + \sigma_\alpha \sigma_\delta C(\alpha, \delta)}. \quad (2.1)$$

where σ_α is the formal error on the right ascension estimate, σ_δ the formal error on the declination estimate. $C(\alpha, \delta)$ is the correlation between estimates of right ascension and declination. The 617 ICRF2 sources shown in Figure 2.2 have a positional accuracy of better than $200 \mu\text{as}$ which is considered sufficient for geodesy. For the 406 radio sources in the north, the average position accuracy ($89.6 \mu\text{as}$) is better compared with that ($105.1 \mu\text{as}$) of 211 southern radio sources. As a radio source is observed in more and more sessions, its accuracy will most likely be improved.

2.2.2. Radio source flux density

Strong radio sources that are well distributed over the sky are required for any session to generate a schedule with good sky coverage. From the catalog system file (flux.cat) at Goddard Space

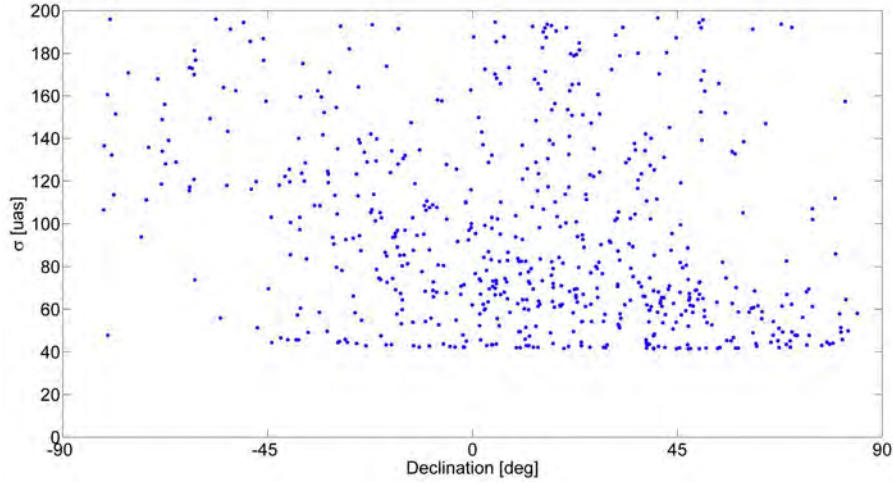


Figure 2.2.: Formal error of the position estimate vs. declination.

Flight Center (GSFC), source strength and source structure information are provided, which are determined from recent VLBI geodetic experiment data. Source strength is described by flux density and it is used to calculate scan length. These algorithms will be discussed in more detail in Chapter 3. From the latest flux.cat file, source flux density at X band and S band are provided for 658 radio sources, which are shown in Figure 2.3. The reduction of source strength on long baseline isn't taken into account in this subsection. The numbering of the radio sources (source indices) is by flux density at X band in Figure 2.3. Among the total 658 radio sources, 355 radio sources have a strength better than 0.3 Jy at both X and S band. 479 radio sources are stronger than 0.2 Jy, while only 36 radio sources are weaker than 0.1 Jy.

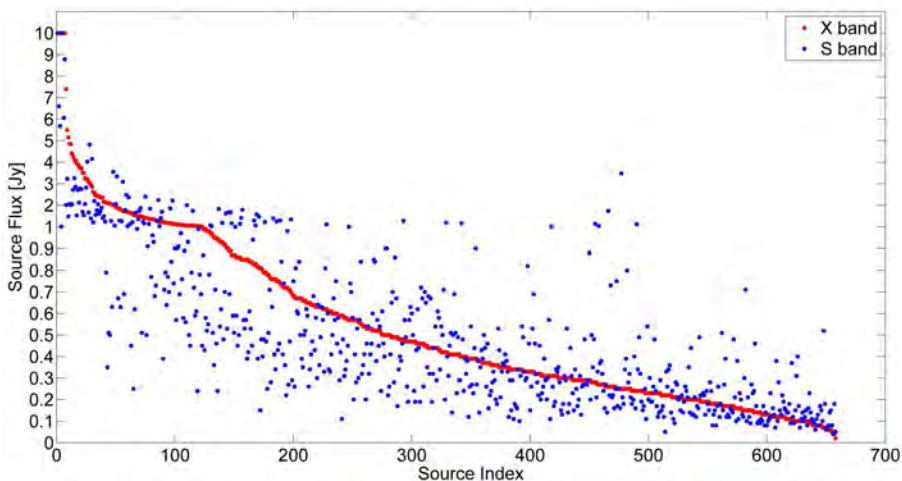


Figure 2.3.: Distribution of the flux for 658 radio sources at X band and S band.

2.2.3. Radio source structure and correction model

In order to describe the astrometric quality of the sources, the definition of structure index (SI) used in IERS technical note is described (Ma, 2009), which is a continuous structure index scale. The structure index indicates the expected magnitude of the effects of intrinsic source structure on VLBI delay observations. The SI value of 4 corresponds to a value of 30 ps for the delay structure correction. SI value at 3 is equivalent to 10 ps, and SI value at 2 means 3 ps. Compact radio sources with good structure index ($SI < 3.0$) are found to be suitable for the highest astrometric accuracy (Ma, 2009). From the USNO Radio Reference Frame Image Database and the Bordeaux VLBI Image Database for epochs between 1994 and 2008, structure indices were derived for 701 different radio sources by using a total of 3046 X-band VLBI images, as plotted in Figure 2.4. The source indices are consistent with increasing SI in Figure 2.4. 128 out of 701 radio sources are very compact sources ($SI < 2$), while 86 radio sources have an SI larger than 4. The number of radio sources which have SI between 2 and 3 is 273, and the number of radio sources which have SI between 3 and 4 is 214.

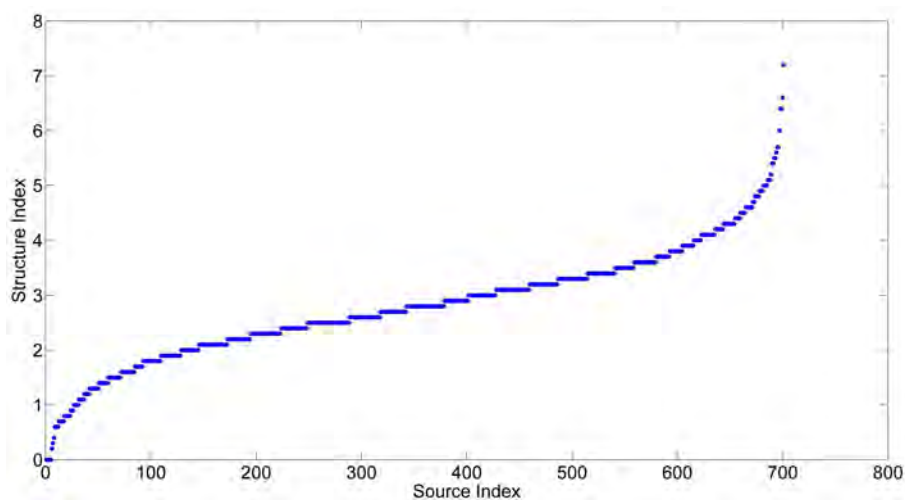


Figure 2.4.: Distribution of the mean structure index for 701 radio sources at X band.

The effect of observing sources with extended structure is that the observed flux is reduced on long baselines. There are usually two kinds of flux models. In baseline models, indicated by “B”, the flux is modeled as a series of step functions. In elliptical models, indicated by “M”, the source is modeled as a sum of ellipses. It may happen that some of the sources are missing fluxes. Sources without complete fluxes on the selected frequency band(s) can not be scheduled.

1. Step function model

If the source is described by step function of baseline length, the flux information are baseline/flux pairs as shown below.

$$Base_1 \ Flux_1 \ Base_2 \ Flux_2 \ Base_3 \ Flux_3 \ Base_4 \ \dots \ Base_{14} \ Flux_{14} \ Base_{15} \quad (2.2)$$

Fluxes are in Jy; baselines are in kilometers. Flux1 is the source strength valid for baseline lengths between Base1 and Base2, Flux2 is the source strength for baseline lengths between Base2 and Base3, Flux3 applies between lengths Base3 and Base4. Up to fourteen fluxes and fifteen baseline lengths can be read in VIE.SCHED. No interpolation is done for intermediate baseline lengths.

2. Source structure model

If the source is described by structure model, the flux information are six model parameters for one component. Parameters for up to three components may be specified in flux.cat file. All components are added to get the total source flux for calculations. Source structure model is used in scheduling to calculate the predicted observed flux on each baseline of a scan. The current implementation uses elliptical gaussian model. The effect of observing sources with extended structure is that they are partially resolved on long baselines, thus reducing the observed flux. The appropriate baseline length is the projected baseline. The equations below are used to compute the observed flux density for a given baseline (Gipson, 2012). All angles are in radians, u and v components are in wavelengths, and flux density is in Jy. The observed flux for all components is added to obtain the total observed flux. The offsets of components from a centroid is not implemented. Separate calculations are done for each band. The observed flux for one component is calculated from the following equation:

$$F_{obs} = F \times \exp\left(\frac{-(\pi\theta l)^2}{4\ln 2}\right) \quad (2.3)$$

$$l^2 = (v \cos(pa) + u \sin(pa))^2 + R^2 \times (u \cos(pa) - v \sin(pa))^2 \quad (2.4)$$

$$u = b_x \sin(GHA) + b_y \cos(GHA) \quad (2.5)$$

$$v = b_z + \sin \delta (-b_x \cos(GHA) + b_y \sin(GHA)) \quad (2.6)$$

Where

F_{obs} = predicted flux density that will be seen for this observation, for one component

F = total flux density of the component, Jy

θ = size of the major axis of the component, milli-arcsecond

l = effective baseline length, taking into account the baseline projection and the position angle of the component. For a circular source, l is the projected baseline.

b_x, b_y, b_z = components of the baseline

R = axial ratio of the component (1.0 for circular)

pa = position angle of the component major axis with respect to the origin, range -180 to 180

GHA = Greenwich hour angle of the source

δ = source declination

2.3. Suitable radio sources for geodetic VLBI

As mentioned before, the ICRF also includes very weak sources and sources with complex and variable structure. In the 1980s, more than 100 radio sources used for geodetic VLBI observations are frequently observed during various experiments. This source list was mainly generated by choosing the brightest sources. At that time the knowledge about source structure was limited. Today, images of more than 3000 objects are available. For the VLBI2010 system, these images have been used to determine a new source list of objects by analyzing source maps at X and S band and then selecting the most compact and symmetric sources.

The preliminary list of sources is established here based on their positional stability, flux density, source structure indices, and distribution on the sky. Using the data files listed above, a list of 211 ICRF2 sources is compiled that are met the criteria below and suitable candidate sources for geodesy. They have positional accuracies of better than 200 μas , have an X-band structure index of < 3.0 , and are stronger than 0.25 Jy at both X and S band. Their uniform sky distribution is shown in Figure 2.5. Among the listed sources, some that have long been used for geodetic and earth orientation sessions have more than 10,000 observations and a few even have more than 100,000 observations. 172 sources in the list are ICRF2 defining sources.

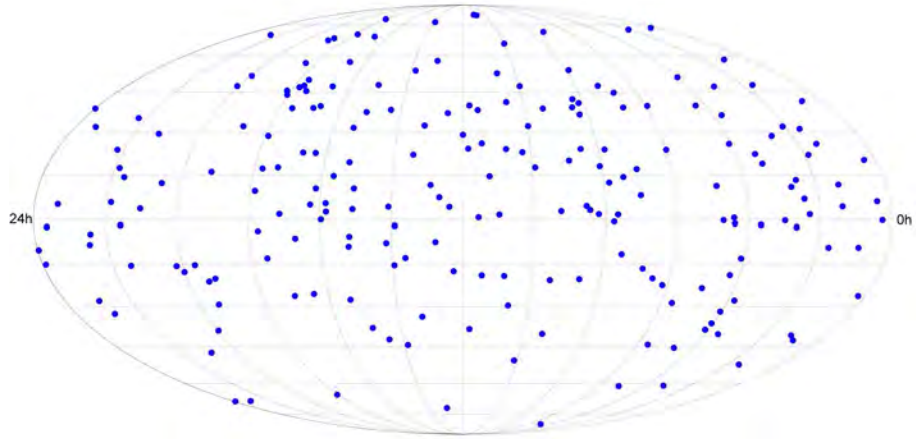


Figure 2.5.: Distribution of the 211 suitable radio sources on celestial sphere.

One method to define the source distribution on the sky clearly and quantitatively could be to split the sky into 64 areas by right ascension and declination (see Figure 2.6). In order to make each segment with equivalent area, the declination interval is set 20 degree invariantly, while the right ascension interval is changed with the declination. The number of sources in each segment is plotted in Figure 2.7.

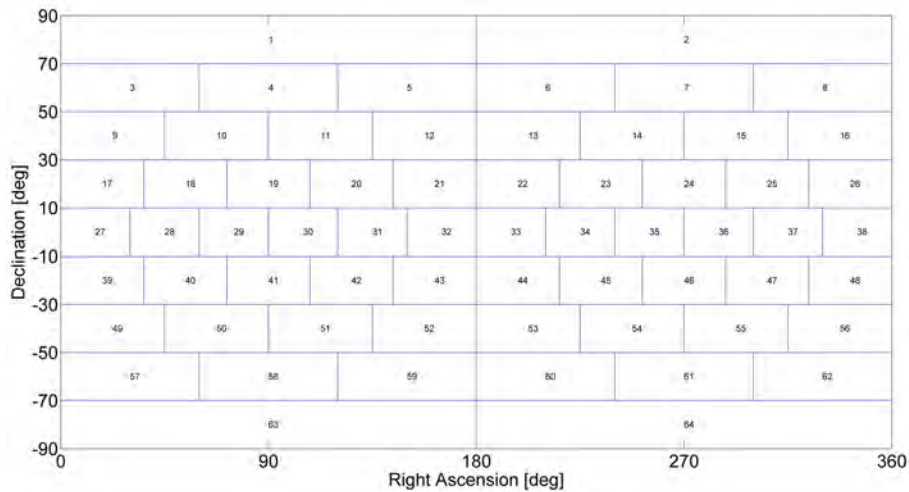


Figure 2.6.: Skyplot of the grid.

On the other side, special sessions are generated to provide astrometric observations. Every 3-4 weeks, CRF sessions are dedicated to provide astrometric observations that are useful in improving and extending the current CRF by observing new sources. Bi-monthly RDV (Research and Development with the VLBA) sessions using the ten stations of the VLBA and ten geodetic stations, provide state-of-the-art astrometry as well as information for mapping CRF sources.

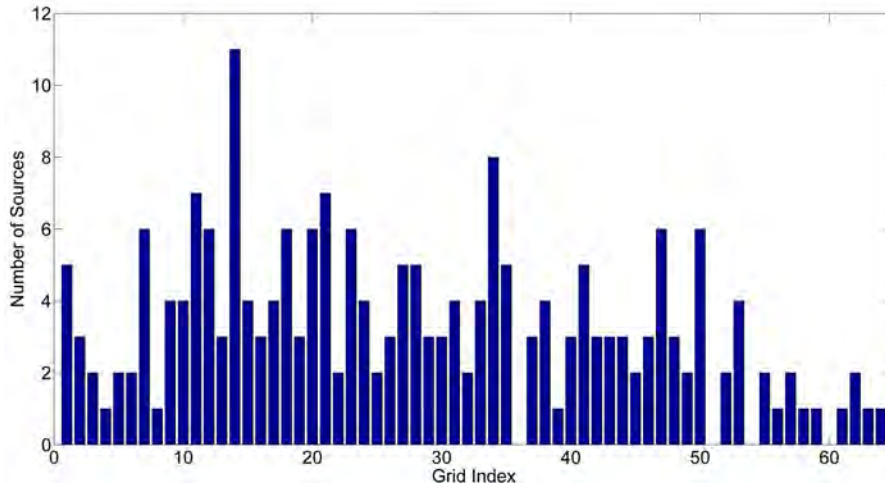


Figure 2.7.: Distribution of the 211 suitable radio sources in segments.

And some particular sessions may be observed for solar corona events. Also, the upcoming Gaia mission will require much more precise radio-optical transfer sources. In VIE_SCHED it is easy to edit the source parameters or add new sources to the list by various requirements.

3. Algorithms and models for a scan

This chapter describes the basic algorithms and models used for a new scan. In scheduling a scan means the time period during which a network of stations observes the same source simultaneously. This chapter focuses on the determination of various scan features, e.g. start time and scan length. A new scan will start as soon as possible, taking into account the time required for the antennas to move to the new source. A scan should begin at the same time at all stations participating in the scan as required for correlation. Each station observes for a different length of time to achieve the SNR target considering its antenna sensitivity, i.e. the scan ends at different times at all stations. Source flux densities and antenna sensitivities can be used, along with user-specified minimum SNRs, to compute scan times for each station. Furthermore, many limitations are imposed on the new scan and various conditions should be satisfied. This chapter also discusses the definition of a valid scan and introduces error conditions processing. Whether either scheduling strategy is used, all of these scan features are fully calculated. The algorithms, models and detailed equations related to a scan are explained in the next sections separately.

3.1. Calculation of scan start time

3.1.1. Cable wrap and slew distance of AZEL antenna

For AZEL (azimuth-elevation mount) telescopes the entire cable is viewed as a single continuous wrap which begins at a certain azimuth and proceeds clockwise through ever-increasing azimuths to the end of the cable. In order to track a source and to slew between sources efficiently with an AZEL antenna, the antenna's range of motion in azimuth should be determined definitely. The cable wrap algorithms are critical to calculate slew distance and slew time for AZEL antenna. This subsection elaborates on details related to the cable wrap of the AZEL antenna.

The values of cable limits are contained in antenna.cat catalog file, which typically depend on the antenna. If the total angular range isn't more than 360° , there is no overlap and cable wrap position can be determined unambiguously. Station WESTFORD is such an example with cable range from 100° to 460° . If the total angular range is greater than 360° , there are some azimuths that correspond to two (or more) values of the cable wrap and the ambiguity of 360° should be calculated. Using station KOKEE as an example, the cable can move between 270° to 810° and the total angular range is 540° , as shown in Figure 3.1. If the azimuth angle is between 90° and 270° , it can be determined definitely that the cable position should be located in the range of 450° to 630° . If the azimuth angle is between 0° to 90° , there are two possibilities of cable position, i.e. 360° to 450° or 720° to 810° . The similar case is for the azimuth range of 270° to 360° .

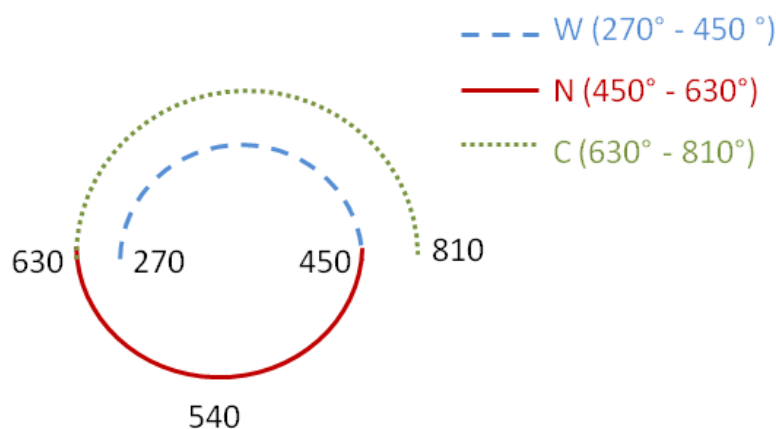


Figure 3.1.: Antenna cable wrap at station KOKEE.

In the output scheduling file (.skd file), the three letters (“-” / “W” / “C”) are used to differentiate which wrap the telescope is positioned. The so-called “neutral point” is located halfway between the azimuth travel limits of the telescope. Antenna is usually oriented so that “neutral point” is towards pole of hemisphere in which the antenna is located. In the above Figure 3.1, it is located at 540° azimuth. For the azimuth between 450° to 630° , it is an unique portion of the cable (“neutral region”) and it is tagged by a letter “-”. The two parts of the cable, one on either side of the neutral point, are designated by the letters “C” (clockwise) and “W” (counter-clockwise), where clockwise and counter-clockwise are the direction of travel from the neutral point looking down on the antenna. In the case of station KOKEE, if the telescope azimuth falls into the 270° - 450° portion of the cable, it is tagged by a letter “W”. And if the telescope azimuth falls into

the $630^\circ - 810^\circ$ portion of the cable, it is tagged by a letter “C”.

In scheduling, cable wrap and slew distance of AZEL antennas are handled in the following manner. When the telescope pointing position is calculated, the azimuth is in the range 0° to 360° . In the second step the azimuth will be converted to the limits of cable wrap. For the non-unique portion of cable, the cable position will be determined unambiguously considering the shortest distance that the telescope moves to that wrap for the scheduled observation. There are always several ways of travelling the distance between two successive azimuth points and the slew distance is decided by the shortest one of all the possible cable movements in scheduling. Because it strongly relies on the cable wrap position of the previous observation, VIE_SCHED keeps track of the cable state of each antenna in scheduling. In the above example of station KOKEE, because some ranges of azimuth are in two cable wrap regions (the azimuth region 0° to 90° and 270° to 360°), there may be two ways of moving from a given azimuth point to the next azimuth point. Let's suppose that the first point is in the neutral region at, say $AZ = 180^\circ$ (cable wrap 540°), and the next point is also in the neutral region, $AZ = 120^\circ$ (cable wrap 480°). There is only one way of moving from point one to point two, and the slew distance is 60° . The unambiguous cable position is 480° . If the next point is in the overlap region at $AZ = 280^\circ$. There are two possible values of cable wrap: 280° and 640° . One of these involves travelling 260° , while the other involves travelling 100° . According to the short-distance criterion, the cable position without ambiguity is 640° and slew distance is 100° .

To avoid potential problems with cable wrap edge, the observations which occur close the edge of cable wrap are always avoided in scheduling. The edge value can be specified in param.txt local control file (“PARA.MARGEL1”). For example, if the upper limit is 810° and the edge is 5° , the upper limit is actually 805° . If an observation is scheduled for 808° , the antenna will move to the cable wrap position of 448° , which differ by 360° .

3.1.2. Slew time of antenna

In VIE_SCHED, the two axis types of antennas are considered, i.e. AZEL (azimuth-elevation mount) and HADC (hour angle-declination mount), which are usual antenna types within the IVS network. In the following the calculation of the required slew time for each antenna type is described. For AZEL antennas, it depends on the time required to move in both azimuth and elevation. The calculation of cable slew distance is mentioned in the above subsection. The

slew distance of elevation is decided by the difference between two successive elevation points. For HADC antennas, the slew distance of each axis is calculated separately from the hour angle difference and the declination difference between two successive points. The slew speed for each axis is also hold in antenna.cat file. In practice, the antenna can't slew with full speed at the start and stop immediately at the end. Hence the acceleration and deceleration should be applied to caculate the slew time. The acceleration value for each axis can be specified in param.txt file separately (“PARA.RATE1A” and “PARA.RATE2A”). Since the antenna can be moving in both axes at the same time, the slew time is the maximum of the slew times in both axes, as shown in Equation 3.1 and Equation 3.2.

$$T_{AZEL} = \max(T_{AZ}, T_{EL}) \quad (3.1)$$

$$T_{HADC} = \max(T_{HA}, T_{DC}) \quad (3.2)$$

For the recommended VLBI2010 antenna, the azimuth and elevation slew speeds are 12 deg/s and 6 deg/s, respectively. The acceleration value in both azimuth and elevation is 3 deg/s². The required time to move a maximum of 180° in azimuth is 19 s and that to move a maximum of 90° in elevation is 17 s. In a word, each sky position can be reached within 20 s with VLBI2010 fast antennas. A particular situation is that the slew distance of cable will be up to 360° occasionally because of cable wrap range, the maximum of slew time in azimuth is 39 s correspondingly.

3.1.3. How to calculate the start time of a scan

There are many things that influence when a scan is started, among them the adequate time required to slew and the time required to perform various conditions.

In the first step, the earliest possible start time of a new observation at the *ith* station is determined as follows.

$$T_{2s}(i) = T_{1e}(i) + T_{slew}(i) + SOURCE + T_{APETM} + IDLE + CALI \quad (3.3)$$

Where $T_{2s}(i)$ is the earliest possible start time for a new observation, $T_{1e}(i)$ is the end time of previous observation at this station which is determined by the actual start time of previous observation ($T_{1s}(i)$) and observation duration ($DUR(i)$).

$$T_{1e}(i) = T_{1s}(i) + DUR(i) \quad (3.4)$$

$T_{slew}(i)$ is the slew time that the antenna requires to slew from the previous source to the new source, as described in the above subsection. The time allowed for settling down (*SOURCE*), tape (*TAPETM*), idling (*IDLE*), and calibration (*CALI*) after slewing and before observation start time are applied in scheduling and can be set in param.txt file.

In the second step, the maximum of start times of participating antennas is taken as the scan start time, as shown in Equation 3.5. The start time of this scan would be appropriate for all participating stations.

$$T_{2s}(scan) = \max(T_{2s}(1), T_{2s}(2), \dots, T_{2s}(n)) \quad (3.5)$$

For any participating station of the scan, it will be excluded from the scan if its slew time is longer than a certain limitation. The maximum of slew time is given in param.txt file (“*PARAMAXSLEWTIME*”). Among the remaining stations, there is an antenna that arrives last. That means the other antennas have to wait for this late antenna to start the scan together. If the waiting time is too long, the last antenna to arrive will be dropped from the scan. The limitation of waiting time is also contained in param.txt file (“*PARAMAXWAIT*”).

Calculations of telescope pointing position and slew time should be computed iteratively, taking into account motion of the source during the slew. An example of antenna with AZEL mounts is that if the source is on one portion of the cable wrap at the beginning of the slew, but by the end of the slew, it has moved onto the other portion of the wrap. Hence the telescope pointing position, slew time, and scan start time are required to be calculated with an iterative process.

3.2. Calculation of scan length

3.2.1. Antenna sensitivity and its elevation-dependent reduction

When the scan length is calculated to achieve a minimum SNR, the antenna sensitivity and its dependence on elevation is applied. The sensitivity information on the equipment at stations is contained in equip.cat catalog file. The parameters for dependence of SEFD on elevation are also held in the equip.cat file. Refer to the catalogs manual (Vandenberg, 1997a) for the way the value of c_i and y are entered into the equip.cat catalog file.

1. Antenna sensitivity

The sensitivity of a VLBI receiver is generally characterized by System Equivalent Flux Density (SEFD), which is the flux density corresponding to the system temperature. It is calculated as follows (Equation (3.6) and Equation (3.7)).

$$SEFD = \frac{2 \times k \times T_{sys}}{A_{eff} \times \eta \times 10^{-26}} \quad (3.6)$$

$$A_{eff} = \pi \times \left(\frac{D}{2}\right)^2 \quad (3.7)$$

k is Boltzmann's constant ($1.38 \times 10^{-23} \text{ m}^2 \text{ kg s}^{-2} \text{ K}^{-1}$), T_{sys} is system temperature (K), A_{eff} is the effective collecting area of the antenna (m^2), D is antenna diameter (m), and η is the VLBI processing factor (0.5 - 1.0). The unit of SEFD is Jy (Jansky).

Using the recommended VLBI2010 antenna as an example, the system temperature is 50 K, which includes all sources of noise. The diameter of the small antenna is 12 m, the effective collecting area is 113 m^2 . The VLBI processing factor is set to be 0.5. Hence the SEFD is calculated as 2440 Jy.

2. Elevation-dependent sensitivity

Due to the atmosphere's contribution to the system temperature, an elevation-dependent reduction in sensitivity is calculated and applied in scheduling. The algorithm was developed by Dave Shaffer that scales the zenith SEFD to compute an elevation dependent SEFD, which accounts for the system temperature contribution to an antenna's sensitivity. The form of the Equation (3.8) and the meaning of the coefficients are shown below.

$$SEFD(el) = SEFD_{zenith} \times f(el) \quad (3.8)$$

where $f(el)$ is a function of the elevation involving powers of $1/\sin(el)$:

$$f(el) = \sum_{i=0}^n \frac{c_i}{(\sin(el))^y} \quad (3.9)$$

where n is number of terms and it is usually 1 to 3. el is the elevation of the source. c_i is coefficient for the i th term. Up to five coefficients may be entered, while usually two are sufficient. y is power of the $\sin(el)$ term and it is generally within the range between 0 and 1.

In addition, some antennas have an elevation-dependent sensitivity due to changes in the amount of ground pickup caused by feed spillover, which is ignored in scheduling.

3.2.2. How to calculate scan length

The scan length is calculated to meet the minimum SNR targets at all participating stations. The SNR per baseline per band depends on the observed source strength (F_{obs}), antenna SEFD ($SEFD_1, SEFD_2$), and the total number of recording bits. Stronger sources give higher SNR. The SNR can also be increased by bandwidth (B), the number of channels (N_{ch}) or the integration time ($scanlength$), which increases the number of bits. The fundamental equations related to SNRs and scan lengths are displayed below.

$$SNR = \frac{F_{obs}}{\sqrt{SEFD_1 \times SEFD_2}} \frac{\sqrt{2 \times B \times N_{ch} \times scanlength}}{1.75} \quad (3.10)$$

which can be inverted to yield scan length:

$$scanlength = \left(\frac{1.75 \times SNR}{F_{obs}}\right)^2 \times \left(\frac{SEFD_1 \times SEFD_2}{2 \times B \times N_{ch}}\right) \quad (3.11)$$

The actual scan length scheduled in practice is

$$scanlength = \left(\frac{1.75 \times SNR_{min}}{F_{obs}}\right)^2 \times \left(\frac{SEFD_1 \times SEFD_2}{2 \times B \times N_{ch}}\right) + CORSYNCH \quad (3.12)$$

The detailed information on observed source strength is in Subsection 2.2.3. The CORSYNCH parameter gives the correlators extra time to synchronize up, which is specified in param.txt local control file (“PARA.CORSYNCH”). Using the fast slew antennas with SEFD 2440, the recording rate is set to 8 Gbps ($2 \times B \times N_{ch}$), the minimum SNR (SNR_{min}) specified as 10, and CORSYNCH set to be 0 s, hence the required scan length is 5 s for stronger source ($F_{obs} = 0.3$ Jy). For the future VLBI2010 system, it is feasible that the on-source time will be reduced to 5 s. While an VLBI2010 antenna is on source, data is being acquired at a very high rate and placed into RAM (Random-Access Memory). Data is then taken from RAM and written to media at the max record rate or transmitted via optical fiber cables (called e-VLBI), that can be done not only during the on source period but also while the antenna is slewing. This allows for shorter on source periods, which is particularly important for smaller antennas.

In scheduling the scan length at individual stations is calculated as follows.

- Step 1: For each baseline of the scan, calculate number of seconds required to achieve minimum SNR for all the bands, using the observed flux density on that baseline, elevation-dependent SEFD for each antenna of this baseline, number of channels, bandwidth and SNR targets (Equation 3.12).

Step 2: For each station of the scan, find the longest duration, for all bands, of all baselines the station participates in. This is the duration assigned to the station.

Step 3: The limits on minimum and maximum of scan length are set in param.txt file (“PARA.MIN_SCAN”, “PARA.MAX_SCAN”). If the scan duration is shorter than the minimum, the minimum value will be assigned to this station. If scan length is longer than the maximum, the station will be marked with failure once.

Step 4: Rank stations by number of failures and drop the worst station from the scan.

Step 5: Repeat the calculations from step 1 to step 4 with the remaining stations until no station is dropped from the scan. And the scan length is sufficient to achieve the specified minimum SNR at each antenna of the scan.

3.3. The conditions of a valid scan

For a valid scan, an important criterion is that the source should be up at participating stations during the observation. The simplicity of these calculations is complicated by the station horizon mask, as described in the next subsection.

3.3.1. Horizon mask

A station can have a horizon mask, a coordinate mask, or both of them. Only horizon mask, which describes the surrounding mountains, is taken into consideration in the scheduling. Horizon masks are represented as either step functions or a series of line segments, which can be found in mask.cat catalog file.

1. Step functions

For step functions, the elevation mask is between the two azimuths; the elevation begins with 0° and ends with 360° usually. As a concrete example, the horizon mask at TIGOCONC is:

```
H TIGOCONC TG 0 2 21 8 106 4 123 12 131 8 150 6 194 10 215 8 224 5 241 4 266 8 284 8 348
2 352 4 360
```

The numbers following the two letter station code “TG” give the mask. Azimuths and minimum elevation angles alternate. The minimum elevation angle is assumed to be constant between azimuth angles. In this example the minimum elevation is 2° between azimuth 0° and 21°. Between azimuth 21° and 106° it is 8°. Between azimuth 106° and 123° it is 4°, etc. Figure 3.2 below is a graphical representation of the elevation mask at station TIGOCONC.

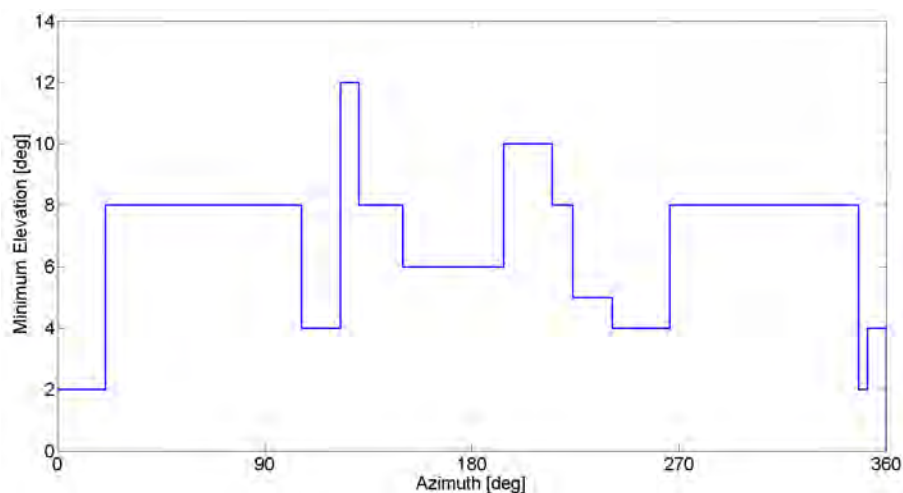


Figure 3.2.: Elevation mask at station TIGOCONC.

2. Line segments

For line segments, the lines are entered as ordered pairs of azimuth and elevation; there are always matching pairs of az and el. For example, the mask at station NYALES20 is below:

```
H NYALES20 NY 0 2 10 4 60 4 65 2 120 2 128 5 150 5 152 7 162 9 176 12 190 5 226 8 230 6
250 6 256 7 266 12 270 12 290 4 310 2 360 2
```

That means the minimum elevation angle is decided by linear function between the two pairs of azimuth and elevation. Figure 3.3 below is a graphical representation of the elevation mask at station NYALES20.

3.3.2. Definition of a valid scan

When scheduling a new scan, VIE_SCHED performs more checks to make sure that the scan is valid. There are several criteria which must be met in order for a scan to be valid. In the

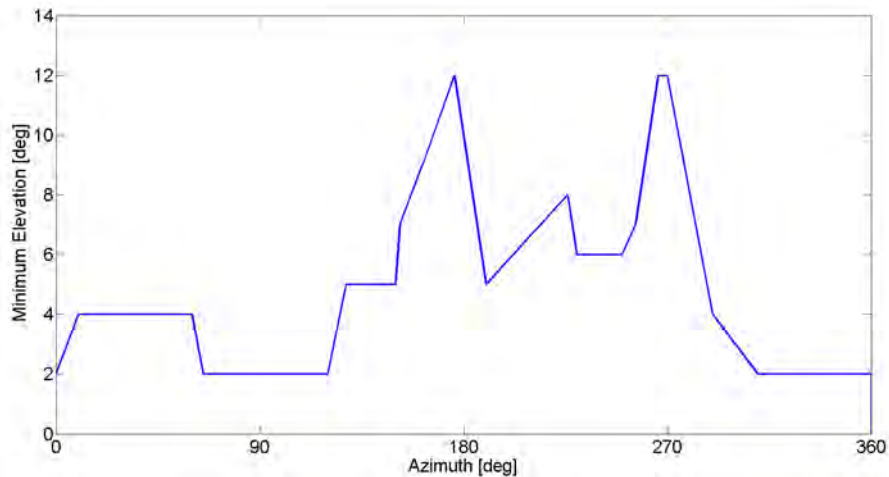


Figure 3.3.: Elevation mask at station NYALES20.

following some limitations and error conditions are described. VIE_SCHED will eliminate the station if it finds any condition isn't met.

1. The valid scan has at least two stations.
2. The source is visible at all the stations which are to participate in the scan and that the scan can be completed at all stations. The source must be within antenna axis limits during the scan, i.e. from the start of the scan to the end of the scan. The source position during the scan is calculated and checked per 5 seconds in scheduling.
3. At stations with AZEL antenna, the continuity of the scan is checked to ensure that it begins and ends on the same cable wrap during the observation.
4. There is enough slew time for each antenna and it isn't longer than the parameter of "PARA.MAXSLEWTIME". To start the scan together, the waiting time isn't longer than "PARA.MAX_WAIT" value.
5. All baselines in a scan must meet user-specified SNR targets and the scan length is between the minimum ("PARA.MIN_SCAN") and maximum ("PARA.MAX_SCAN").
6. Any antenna must not be unavailable during any part of the scan, so the downtime of station is also checked.

3.4. Other system considerations

3.4.1. Electric power saving

Another aspect which has to be considered when optimizing the schedules of VLBI experiments is the usage of electric power. Operation of the whole VLBI system costs very intensively, in particular electric power usage is high for each station. Most power is used by moving the antennas as fast as possible with the highest slewing speed and acceleration. On the one hand, the antenna slewing rate can be set in antenna.cat file, and the acceleration value can be specified in param.txt file for each axis. On the other hand, to reduce usage and cost of electric power, the antenna could move with an adapted speed (with lower power consumption) to the next source, but arriving at the source still in time. Consequently, the idle time must be minimized and the slew speed and acceleration of the antenna must be changed for every single movement at stations. Such a dynamic antenna motion will reduce the consumption of electric power along with wear and tear on the systems. Considering continuous VLBI observations planned for the next decade, it is obvious that energy is an important topic.

3.4.2. Antenna maintenance and antenna life time

For continuous observations of VLBI antennas it is essential that frequent maintenance times are kept for the hardware components of the antennas, e.g. refresh the cryogenic cooling system, maintain the mechanical parts of the radio telescope, and perform system checks and pointing tests. This may cause frequent maintenance periods, which is in contradiction to the plan of continuous VLBI observations. It is also an important issue for the scheduling strategy, because the scheduler has to exclude some stations from the network for a certain time. To consider this option, the scheduling package can read in a station report file (down.txt), where all planned maintenance periods for a particular station are listed. Then, the scheduling package will automatically ignore these stations during this interval. Further considerations are to use a nearby antenna to substitute the antenna during its maintenance, which ensure the loss of the antenna during this time does not critically influence the estimation of the geodetic parameters.

By observing almost continuously, the life time of each antenna will be reduced, but the VLBI system should provide stable reference points over a long time period. Therefore, in principle a gentle treatment of the antenna, which is a physical reference point of the International

Terrestrial Reference Frame (ITRF), should be considered in the schedules, e.g. by avoiding too many rapid accelerations. Increased station reliability and unattended operations can improve temporal coverage of Earth rotation monitoring by VLBI and also allow substantial savings in operating costs.

4. Strategies for automatic scheduling

This chapter describes how scheduling operates in automatic mode. The schedule is generated scan by scan, until there is a scan that ends past the end of the session. One subconfiguration is to be scheduled each time, which means a group of scans that could start the observation at about the same time. Each of the scans is on a different radio source and with a different subnet of stations. Two scheduling strategies are investigated and implemented for VLBI2010 – source-based scheduling strategy and station-based scheduling strategy. Automatic scheduling is governed by the two optimization criteria which determine the next scan to be selected. After standard automatic subconfiguration scheduling either with the source-based strategy or the station-based strategy, the fill-in mode is considered if there are more than one station idling at this given time. The schedule alternates between standard mode and fill-in mode. When the scheduled subconfiguration comes into being and the sources and network of stations are selected, the calculations of various parameters for each scan are followed, e.g. scan start time and scan length, as described in Chapter 3. If the scan is confirmed to be valid, it will be added to the schedule.

The different scheduling strategies and modes are well illustrated by sketches of principle, comparisons of results, and detailed analyses. For the practical generation of the schedules, catalogs of suitable radio sources and stations are required. As the basis for all the schedules in this chapter, the preliminary list of 211 strong and compact radio sources created in Chapter 2 is used for scheduling. The two networks of stations are employed to compare the schedules which are obtained from different strategies and options. One is the test VLBI2010 network of 16 stations plotted in Figure 4.1 which was agreed upon within V2C, including 13 IVS stations and 3 fictitious stations. The selection of stations was driven by a good coverage on all major tectonic plates and the network is only for test purposes. The other is a typical network of IVS R1 session (see Figure 4.2). In practice the source-switching interval is decided by the on-source time needed to make a precise delay measurement and the time required to slew between sources. In order to separate the influence of scheduling strategy from the strength of sources

and the performance of antennas, the subconfigurations are scheduled at a fixed interval in this chapter. In the following, the source-switching interval is set to 5 minute which means there are 12 subconfigurations scheduled in one hour. In VLBI each antenna can only observe one source at a time epoch and the maximum number of scans one antenna can participate in is 12 in one hour. So both the achieved sky coverage at stations and distribution of sources over the celestial sphere are shown for the time interval of one hour. The cut-off elevation angle is 5° in this chapter.

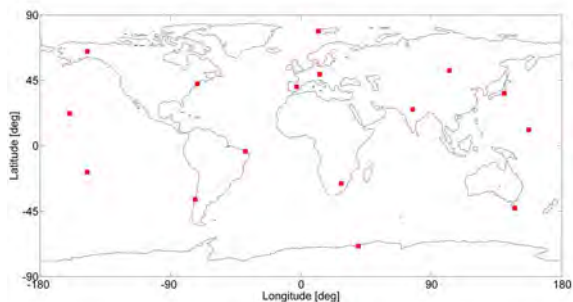


Figure 4.1.: An test VLBI2010 network (16 stations).

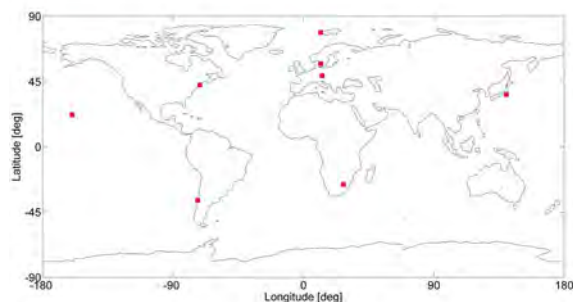


Figure 4.2.: An typical IVS R1 network (8 stations).

4.1. Source-based scheduling strategy

One of the strategies that comes up with a more global station distribution and fast moving antennas is source-based scheduling, which means that the schedule program selects radio sources from the catalogue without regard for their direct impact on individual stations (personal communications with Bill Petrachenko and Harald Schuh). This simplification can be applied effectively for large globally distributed networks and greatly increases the efficiency of the scheduling software. This strategy includes forming different subnets throughout the session in order to optimize geometry and number of observations. Thus, all possible baselines of the network are observed. Roughly speaking, there won't be large holes in the distribution of observed sources on the sky.

In order to evaluate the distribution of sources on the sky clearly, an mathematical approach is developed. As mentioned in Chapter 2, the sky is divided into 64 segments by right ascension and declination (see Figure 2.6). The segments which contain one (or more) observed sources in a certain time interval are counted. If the schedule has 64 observed sources in a certain time

window and they are distributed on all 64 segments, the distribution of sources on the sky is 100%: the best distribution of sources. The worst case would be if all 64 sources are concentrated in one segment. There are three options for source-based strategy as described below.

4.1.1. One-source scheduled each time

Only one radio source is considered for scheduling at each time epoch and as many stations as possible will participate in the scan. Hence the subconfiguration consists of only one scan in this case. As for the radio source of subconfiguration, the segment of sky will be considered sequentially by its grid index, i.e. the loop from grid₁ to grid₆₄ is repeated in scheduling. If there is no radio source in the grid to be considered, the next grid which contains radio sources will be used as substitute. If there are more than one radio sources in this considered grid, these radio sources will be selected one by one when this grid is considered repeatedly. For example, the observed radio source of previous subconfiguration is the first radio source in the grid_{*i*}, the next radio source to be observed should be in the grid_{*i+h*} (*h* is the step length). When the grid_{*i*} is considered for the second time, the second radio source in the grid_{*i*} will be chosen.

The visibility of the one-source configuration at stations in a 24-hour session is calculated per 5 minute and shown in Figure 4.3. The average visibility is 7.5 and 3.8 for the two networks, respectively. That is, less than half of the stations can be observing one source at the same time on average. The visibility percentage is also shown in the right column of figure. It can be found that the visibility varies largely and it is related to the source position and scheduling time epoch.

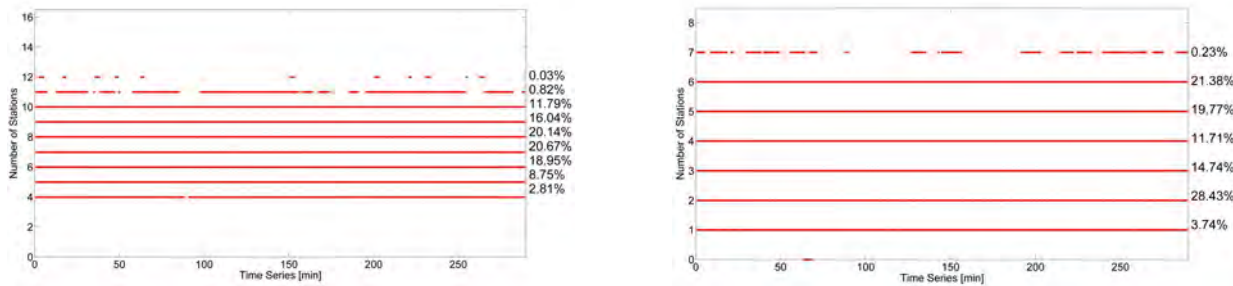


Figure 4.3.: Visibility of one-source configuration for the VLBI2010 network (left) and the IVS R1 network (right).

4.1.2. Two-source scheduled simultaneously

If a pair of sources is considered simultaneously, the two sources should be as far apart as possible on the sky, i.e. they are located on opposite parts of the sky. Figure 4.4 shows the first, the ninth, and the thirty-second pairs graphically as examples. For instance, if one source is located in the cell_{1-a}, the other one should be in the cell_{1-b}. They constitute the two-source configuration on the sky.

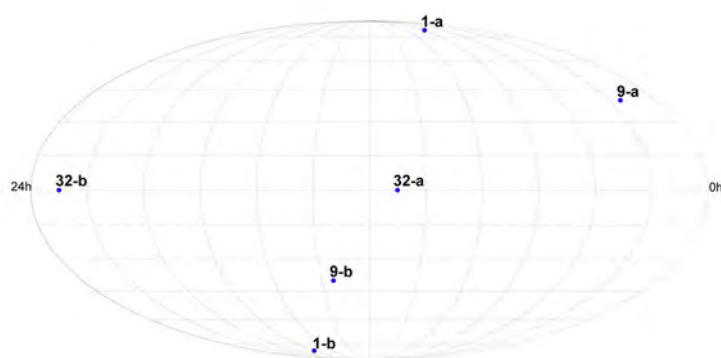


Figure 4.4.: The example of two-source configuration on the sky.

The visibility of each pair of sources at stations in 24-hour session is also calculated per 5 minute, which is shown in Figure 4.5. The average visibility of the two-source configuration is 14.4 and 7.2 for the VLBI2010 network and the IVS R1 network, respectively. From the visibility percentage on the right of each figure, it is found that there are at least 2 stations idling with the probability of 51.36% for the VLBI2010 network and 18.86% for the IVS R1 network during the 24-hour session.

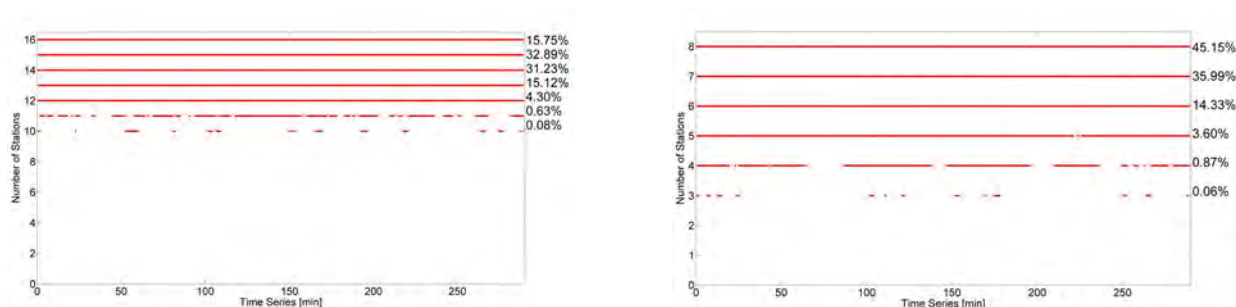


Figure 4.5.: Visibility of two-source configuration for the VLBI2010 network (left) and the IVS R1 network (right).

4.1.3. Four-source scheduled simultaneously

When four sources are considered simultaneously, this is realized by a configuration of regular tetrahedron. One example is shown in Figure 4.6. If the first source has the declination of 90° , the other three sources are in the same plane with declination of -19.5° and they are 120° apart in right ascension.

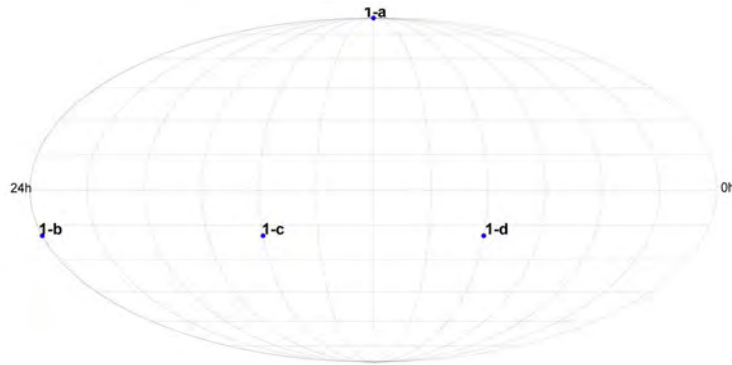


Figure 4.6.: The example of four-source configuration on the sky.

The visibility of each group of four sources at stations in 24-hour session is also calculated per 5 minute and plotted in Figure 4.7. The average visibility of the four-source configuration for the two networks is 15.993 and 7.989, respectively. It means that 99.9% of the stations can be observing at least one of the four sources on average during the session. With four-source configuration, it is found from the visibility percentage that there are 2 stations idling during 0.01% period of the 24-hour session for the VLBI2010 network. And there are not more than one stations idling during the 24-hour session for the IVS R1 network.

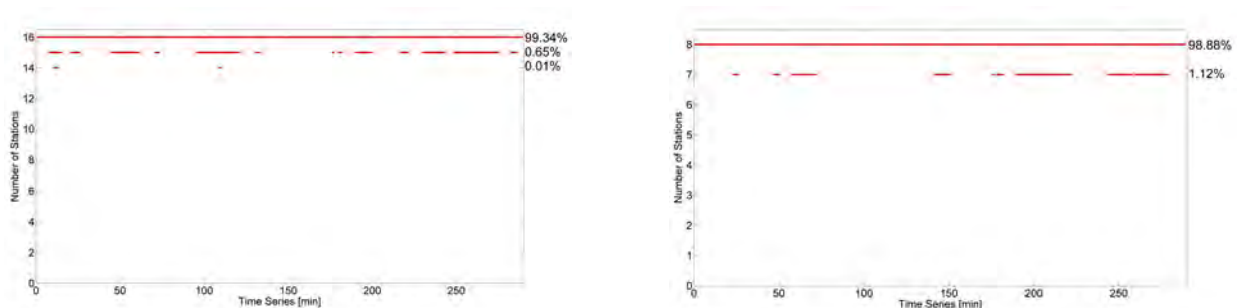


Figure 4.7.: Visibility of four-source configuration for the VLBI2010 network (left) and the IVS R1 network (right).

4.2. Station-based scheduling strategy

Another scheduling strategy is to achieve uniform sky coverage at each station, which is essential to de-correlate wet zenith delay (WZD), clock parameters, and station heights. This subsection gives the definition of sky coverage first. The algorithm used in subconfiguration selection follows. An example is used to illustrate the station-based scheduling strategy.

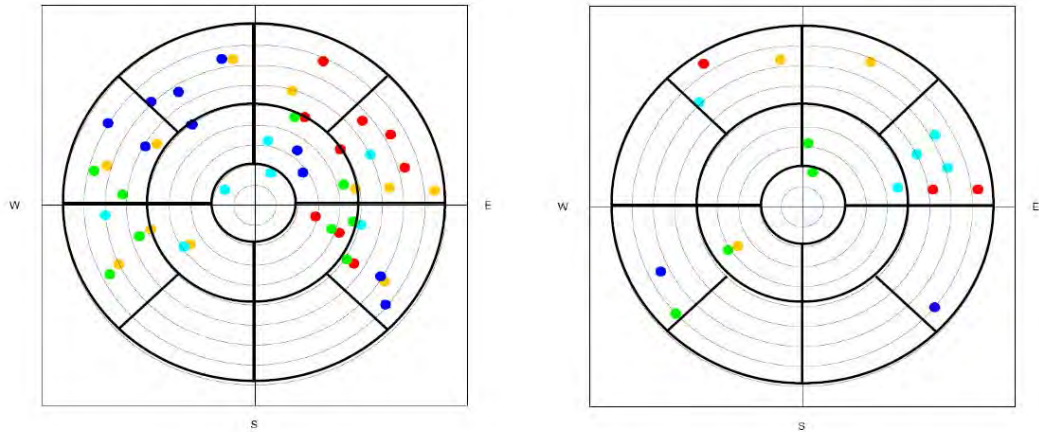
4.2.1. Definition of sky coverage

In all cases of schedule optimization, the sky coverage is one of the most important factors. However it is not clearly defined yet what a uniform sky coverage or a sound geometric radio source distribution is. Some (weak) restrictions which guarantee a fairly good uniform sky distribution are that a nearby radio source should not be observed after each other, and that the time between observations of the identical source should exceed a certain time interval. One possible method to clearly define uniform sky coverage and to get a corresponding statistical number could be to divide the sky into segments and count the segments which contain an observed source in a certain time interval. In principle this method is similar to that used to define the distribution of sources on the sky. Segments and rules for counting could look like in the following example:

- o The sky above the antenna is divided in three different elevation segments: low, middle, and high elevation observations.
- o The middle segment is divided into four azimuthal segments and the low segments into eight parts.
- o 13 segments are available now (see Figures 4.8, (a) and (b)).

Figure 4.8 (a) and (b) show sky coverage plots in a 30 min interval at station HartRAO. In Figure 4.8 (a) the allocation of the observed radio sources is rather uniform and the category of uniform sky coverage is 11 out of 13. The requirement is not fully achieved in Figure 4.8 (b), where the category of uniform sky is 8.

If for one station the schedule has 13 observations for a time window distributed on all 13 segments, the sky coverage is of category 13: the best possible sky coverage. The worst case



(a) *Schedule of category 11.*

(b) *Schedule of category 8.*

Figure 4.8.: Sky plot at station HartRAO for a schedule with a slowly moving antenna (1.5 deg/sec in azimuth and 0.7 deg/sec in elevation) and no particular algorithm to create uniform sky coverage. The plot shows the observations in a time window of 30 min. As an additional information all observations in a 6 minute time window have the same color.

would be if all 13 observations are concentrated in one segment, sky coverage 1. The evaluation of the sky coverage can only be done for a certain time window, i.e. usually the time window of sky coverage should correspond to the sampling of the parameters. For instance, if WZD and clock parameters are estimated every hour, the time window of sky coverage should be one hour, too. If the additional information about sky coverage is provided by the scheduling software, the analyst of the VLBI session will be able to choose the best time window for estimating WZD and clock parameters.

4.2.2. Subconfiguration selection algorithm

During automatic subconfiguration selection with station-based strategy, VIE_SCHED considers many possible subconfigurations of the full network as it decides which subconfiguration should be selected. VIE_SCHED considers two sources observed simultaneously at most, in order to limit the total amount of calculations. The full network can be scheduled to observe one source, or it can be divided in two subnets on two different sources. For example, with a six-station network, five possible subconfigurations include:

- (1) All 6 stations observing the same source.

- (2) 5 stations observing the same source, and 1 station not participating.
- (3) 4 stations observing one source, 2 stations observing another source.
- (4) 3 stations observing one source, 3 stations observing another source.
- (5) 3 stations observing one source, 2 stations observing another source, and 1 station idling.

Considering all the up and available sources at this given time, the number of possible sub-configurations will be up to hundreds, thousands and even ten thousands. Based on a set of criteria, the number of possible subconfigurations is reduced and the selection procedure is more efficient. For example, generally speaking, you do not want to observe the same source twice in a row. This leads to a rule saying do not observe a source if it has been observed in the last X minutes, where X can be set by the user in param.txt file (“PARA.MIN_SRCRP”). When the subconfiguration consists of two sources, they should be far enough and the minimum of angular distance is also specified in param.txt file (“PARA.MIN_SRC2ANG”). The minimum size of network is also specified in param.txt file (“PARA.MIN_STANUM”), i.e. the minimum number of stations should participate in the subconfiguration.

The critical process of scheduling a subconfiguration with station-based strategy involves several steps. It starts with the calculation of what sources are up at which free stations. After a set of criteria is implemented as filter, some trial subconfigurations are generated. The procedure of ranking and selection is followed. The first criterion for ranking the subconfigurations is the sky coverage. VIE_SCHED calculates the sky coverage category for all the stations and adds up for each subconfiguration. VIE_SCHED ranks the subconfigurations internally by sky coverage improvement. The larger the value, the larger the score. VIE_SCHED chooses the subconfiguration that improves the sky coverage at most stations. If more than one subconfigurations have the same sky coverage improvement, the subconfiguration with more observations will be selected. The time window for sky coverage is slid during the scheduling and it can be set in param.txt file (“PARA.SKYDT”).

4.2.3. An example of station-based strategy

A schedule for the IVS R1 network of 8 stations is generated with station-based scheduling strategy and the sliding time window of sky coverage is set to one hour. As said above, the scheduling interval is set to 5 minute which means there are 12 subconfigurations scheduled in one hour and the most scans one antenna can participate in is 12 in one hour. So the best sky coverage category in this example will be 12.

The sky coverage achieved in one hour is displayed in Figure 4.9 as example, where we can see clearly that for the schedule created with the station-based scheduling strategy, the observations are not clustered and they are distributed well. It is also found from Figure 4.9 that each station takes part in all the 12 subconfigurations. At station TIGOCONC and WESTFORD, the 12 observed sources are distributed in 12 segments, which is the best sky coverage obtained from station-based strategy in this example. At station HARTRAO, 11 segments contain at least one observed source. For the remaining 5 stations, the sky coverage of 10 is obtained with station-based strategy.

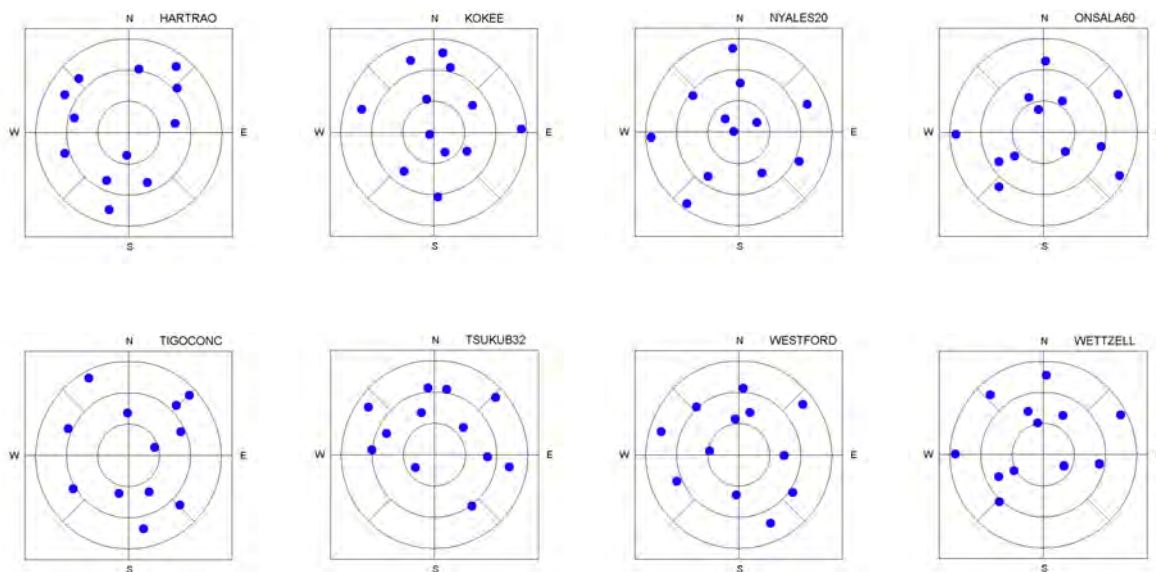


Figure 4.9.: Sky coverage of one hour at 8 stations of the IVS R1 network

4.3. Fill-in mode

By default VIE_SCHED schedules one subconfiguration each time epoch with either source-based strategy or station-based strategy. Thus, it is possible that there are still more than one

stations idling because of visibility or other constraints, as shown in Figure 4.3, Figure 4.5, and Figure 4.7. This can lead to periods of time in the schedule when many stations are idling. So the fill-in mode is introduced to reduce the amount of idle time. The functionality of fill-in mode can be switched on/off in local control param.txt file (“PARA.FILLINMODE”). When VIE_SCHED operates in fill-in mode each time, only one source is considered and only one scan is determined from fill-in mode. Figure 4.10 depicts the flowchart of alternation between standard mode and fill-in mode in the scheduling procedure.

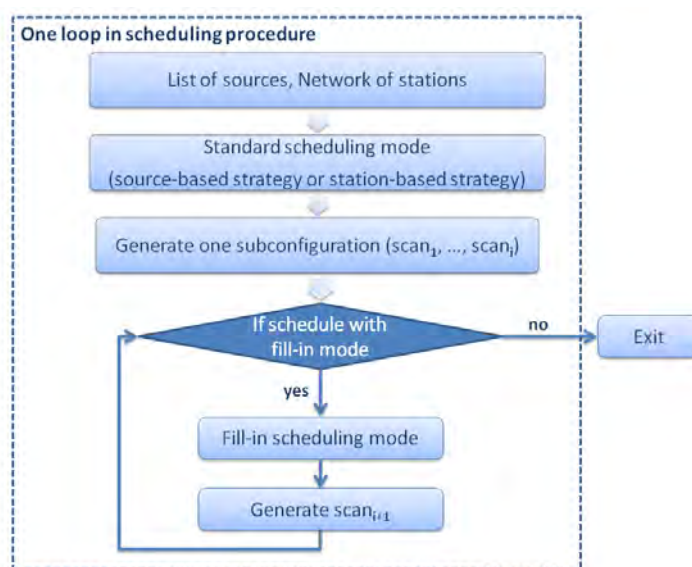


Figure 4.10.: Flowchart of the alternation between standard mode and fill-in mode in scheduling.

As for the fill-in scan scheduling, the detailed steps are followed. There are still a lot of possible scans considered for ranking, VIE_SCHED attempts to schedule this scan using as many idling stations as possible. Hence the first criterion is that the most idling stations participate. The sky coverage criterion will be applied if more than one scan has the same number of idling stations. While there are still many possible scans with the same number of idling stations and same sky coverage improvement, VIE_SCHED will preferentially select the scan which starts first. The fill-in scan shouldn't end much later than the scans from standard scheduling mode. The limitation is specified in param.txt file (“PARA.FILLENDET”).

4.4. Comparisons and analyses of the scheduling strategy

4.4.1. Two solutions for mutual visibility of source-based strategy

For the two-source or the four-source configuration of the source-based strategy, if a station can observe more than one source at the given time, there are two possible solutions to govern which source the station will observe definitely. One is to observe the source which can improve the sky coverage at the station and it is called “Better sky coverage” solution. The other approach considers the number of observations of the subconfiguration, which is called “More observation” solution. Next the IVS R1 network and the two-source configuration are used for comparing the schedules from the two different solutions. The station indices are consistent with increasing latitude everywhere in this chapter.

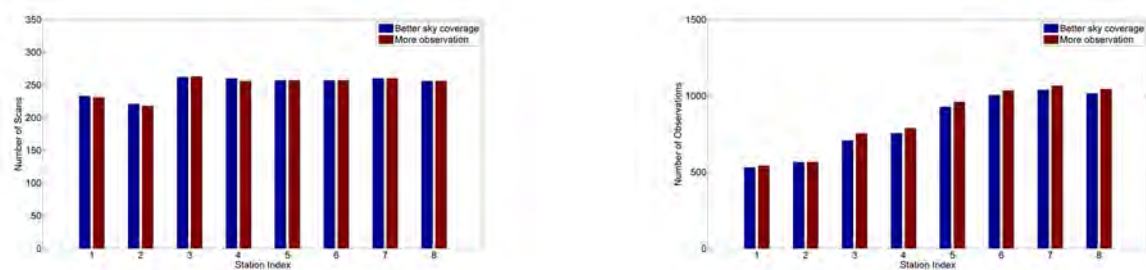


Figure 4.11.: Distribution of scans and observations at 8 stations of the IVS R1 network.

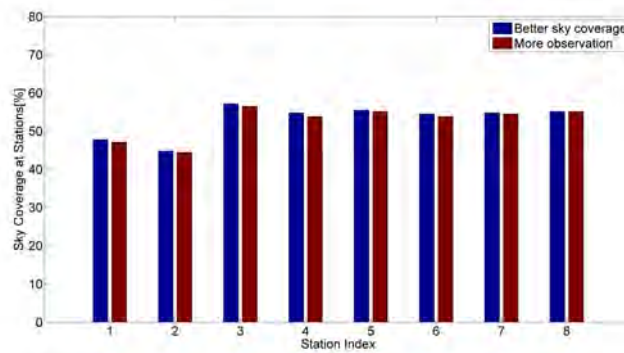


Figure 4.12.: Mean sky coverage of one hour at 8 stations of the IVS R1 network.

The number of scans and observations from the “More observation” solution are 545 and 3377, and that from “Better sky coverage” solution are 561 and 3272. From Figure 4.11 and Figure 4.12, it is found that there is not much difference between the two solutions. Slightly more scans are obtained and less observations are achieved with “Better sky coverage” solution. Because

much more total calculations with “More observation” solution need to be done, the “Better sky coverage” solution is chosen.

4.4.2. Different schedules for the VLBI2010 network

Normally scheduling is an iterative process. After the schedule is generated, it will then be evaluated to see how well it did at each station. There are a lot of criteria for evaluating the schedule. Quite often, different criteria are in conflict. On the one hand you want schedules that have good sky distribution - that sample as much of the sky as possible in a short period of time. To approach uniform spatial coverage over the celestial sphere, the next source should be the one that is furthest from its nearest neighbor. This can lead to schedules where the antennas spend a lot of time slewing from one source to another. On the other hand, you want to maximize the number of observations, which means you want to reduce slewing time. The improvement for the estimated geodetic parameters related to these two somewhat competing factors will be studied with Monte Carlo simulations in Chapter 5. In this chapter a variety of evaluation is employed, e.g. number of scans and observations. The idling stations caused by scheduling strategy are also investigated in depth, and the advantages of fill-in mode will be pointed out. Moreover, mathematic methods are employed to evaluate the sky coverage at stations and the distribution of observed sources on the celestial sphere quantitatively, as described in details above, and the time window required for statistical comparison is also set to one hour. The results which are obtained from different strategies and modes are compared and analyzed below.

For the test VLBI2010 network, eight schedules are created with the different strategies and modes. The two optimization criteria, source-based strategy and station-based strategy, will be considered. The schedules with or without fill-in mode are also compared. The first six schedules are obtained with source-based strategy and the last two schedules are generated using station-based strategy. The influence of fill-in mode is also studied by comparing the results. The total number of observed sources, scans, and observations are summarized in Table 4.1. Since one subconfiguration is generated every 5 minutes, there are 288 scheduled subconfigurations totally in the 24-hour session. The average number of idling stations that don't participate in any scan at the given time epoch is calculated and is shown in the last column in Table 4.1.

Table 4.1.: Eight schedules for the VLBI2010 network.

Num of observed sources	Num of scans	Num of observations	Average of idling stations
------------------------------------	-------------------------	--------------------------------	---------------------------------------

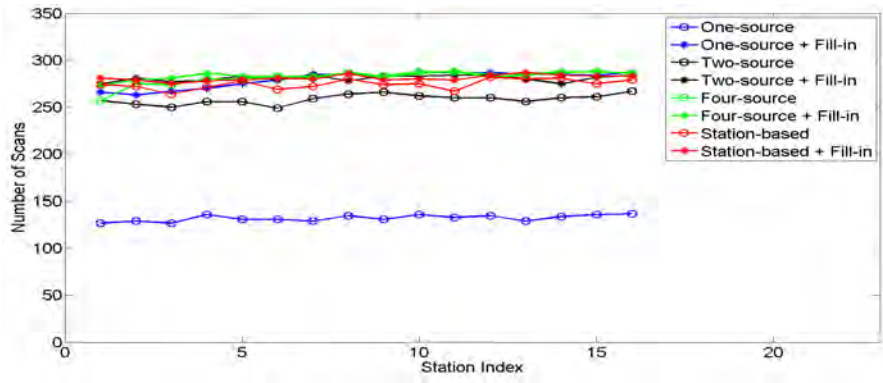
One-source	183	288	7076	8.7
One-source + Fill-in	204	606	15473	0.5
Two-source	210	576	13534	1.6
Two-source + Fill-in	210	722	13826	0.4
Four-source	208	1075	8450	0.4
Four-source + Fill-in	208	1098	8411	0.2
Station-based	187	576	15387	0.7
Station-based + Fill-in	188	599	15746	0.4

In order to study the schedules in depth, Figure 4.13(a) and Figure 4.13(b) show the distribution of scans and observations at each station. Figure 4.13(c) gives the sky coverage percentage for each station. The sky coverage for each station is calculated per hour and the mean value is obtained from the 24-hour session. Because the subconfiguration is scheduled every 5 minutes and there are 12 scans at most for stations per hour, the best sky coverage percentage is 92.3%. The number of grids on the sky containing observed sources is counted per hour and the distribution of sources on the sky is expressed as a percentage of the total 64 grids (See Figure 4.13(d)).

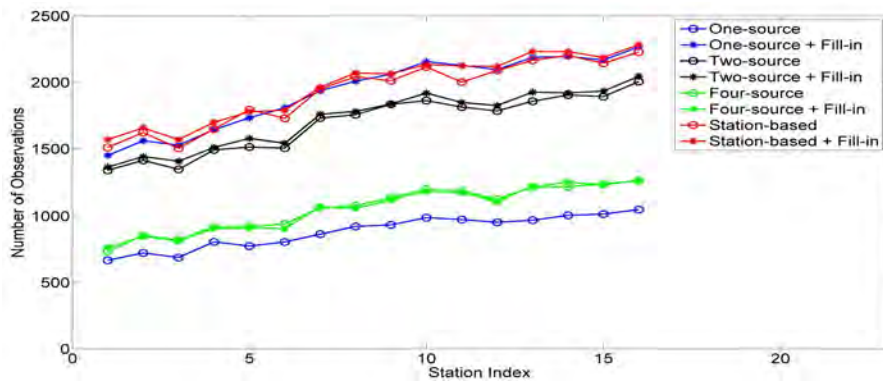
(1) The schedule from the one-source configuration of the source-based strategy (“One-source”) is the worst in terms of number of scans and observations, sky coverage, and source distribution. For the schedule from the four-source configuration of the source-based strategy (“Four-source”), more scans but less observations are received because the network is always divided into four subnets (as shown in Figure 4.14). Because there are the most radio sources observed per hour, the best distribution of observed source on the sky is obtained with “Four-source” mode.

(2) For each schedule, the distribution of scans seems uniform at stations, while the stations in the northern hemisphere have more observations. Figure 4.14 gives detailed information on the mean subnet size at each station, which decides the number of observations gotten from one scan at this station. In this example, 10 out of 16 stations are located in the northern hemisphere. And 132 of 211 sources have the declination in the range from 0° to 90° . To make the number of observations per station more uniform, the global distribution of stations and uniform distribution of sources on the sky are very essential.

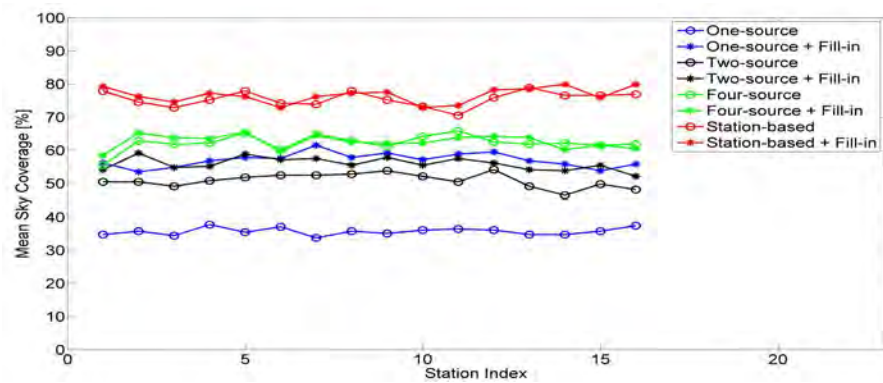
(3) The mode “One-source + Fill-in” brings great improvements compared with “One-source” schedule, where fill-in mode contributes 318 scans to the schedule. Comparing the schedules “Two-source” and “Two-source + Fill-in”, slight improvements are achieved with fill-in mode (146



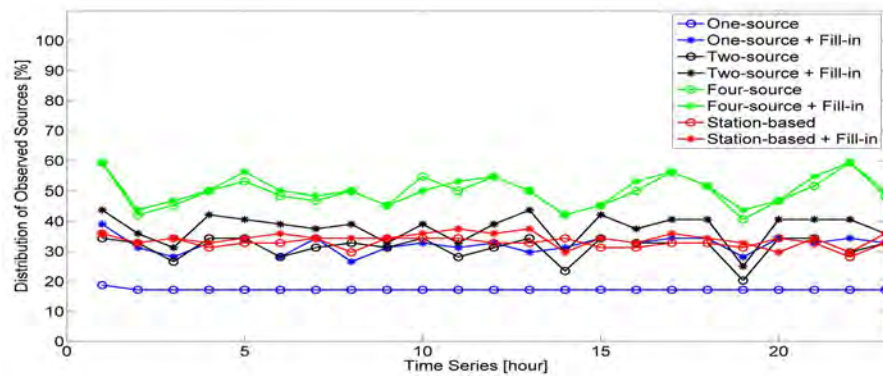
(a) Distribution of scans



(b) Distribution of observations



(c) Mean sky coverage at stations per hour



(d) Distribution of observed sources on the celestial sphere per hour

Figure 4.13.: Eight schedules for the test VLBI2010 network.

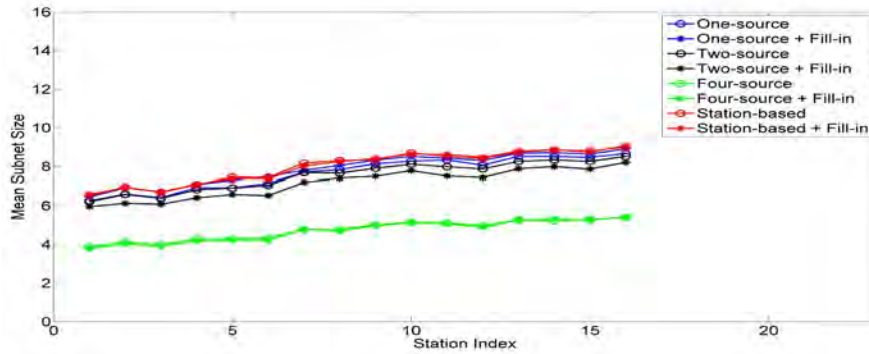


Figure 4.14.: Mean subnet size for the test VLBI2010 network.

scans from fill-in mode). And in the schedule of “Four-source + Fill-in”, 23 scans are generated with fill-in mode. There is not much difference between “Station-based” and “Station-based + Fill-in”. That is, fill-in mode plays an important role to decrease the idling time and make use of stations efficiently, especially when the scheduling parameters are not set up well.

(4) For both schedules “Station-based” and “Station-based + Fillin”, the sky coverage is much better while the number of scans and observations are similar to the schedules from source-based strategy. One disadvantage with station-based strategy is time consumption. For all the above schedules with source-based strategy the entire time required to generate a 24-hour schedule is around ten minutes or less, but the entire process to generate a 24-hour schedule with station-based strategy takes more than 3 hours.

4.4.3. Different schedules for the IVS R1 network

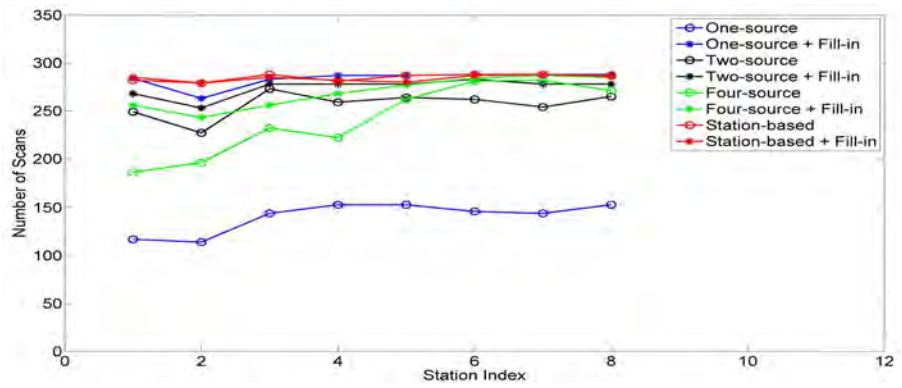
The same procedure is done for the IVS R1 network and Table 4.2 shows the number of observed sources in 24-hour sessions, the number of scans and observations, and the average idling stations. The comparisons of the eight schedules are plotted in Figure 4.15 and Figure 4.16.

Table 4.2.: Eight schedules for the IVS R1 network.

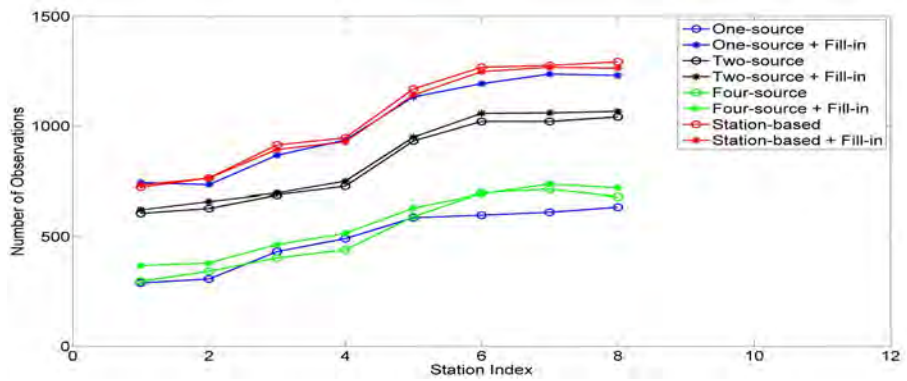
	Num of observed sources	Num of scans	Num of observations	Average of idling stations
One-source	191	288	1974	4.1
One-source + Fill-in	204	575	4036	0.1
Two-source	208	561	3332	0.9
Two-source + Fill-in	209	625	3430	0.4

Four-source	200	685	2081	1.3
Four-source + Fill-in	204	787	2252	0.5
Station-based	174	576	4175	0.1
Station-based + Fill-in	182	578	4118	0.1

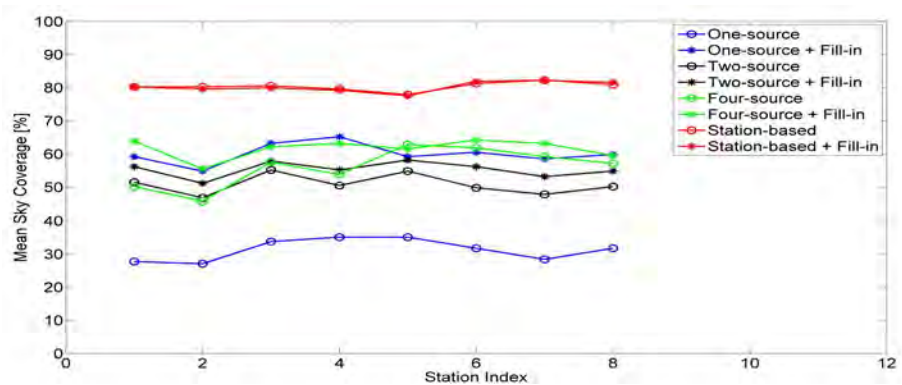
For the IVS R1 network, the schedules from “One-source + Fillin”, “Station-based”, and “Station-based + Fillin” have similar scan distribution and observation distribution. Due to the paucity of continental land-mass in the southern hemisphere, the distribution of stations is worse there than in the north. Hence less observations are always taken at southern stations. Figure 4.16 also shows detailed information on the mean subnet size in scheduling for IVS R1 network. On the other hand, the sky coverage is increased greatly with “Station-based” and “Station-based + Fillin”. The distribution of sources with “Four-source” is better slightly compared with the other schedules because of the smaller network size of IVS R1 session. Scheduling with station-based strategy for IVS R1 network automatically would require one hour.



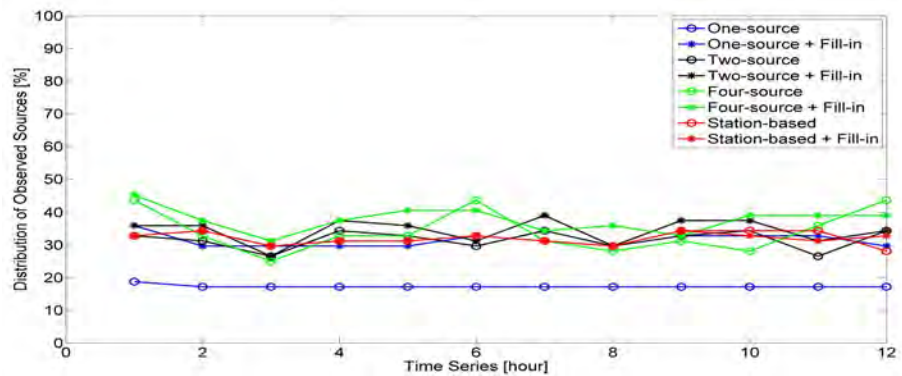
(a) Distribution of scans



(b) Distribution of observations



(c) Mean sky coverage at stations per hour



(d) Distribution of observed sources on the celestial sphere per hour

Figure 4.15.: Eight schedules for the IVS R1 network.

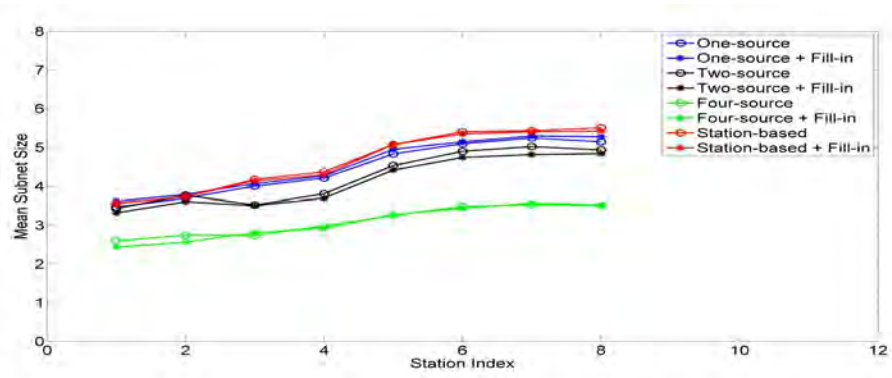


Figure 4.16.: Mean subnet size for the IVS R1 network.

5. Simulations and results

In this chapter the Monte Carlo simulations are employed to study the relationship between the schedules and final products of geodetic parameters. The studies focus on the investigations of the impact of different scheduling optimization criteria on the accuracy of estimated station position.

5.1. Monte Carlo simulations

Simulation studies play a critical role for the development of a future geodetic VLBI system. There have been a lot of simulations in recent years how VLBI could exploit its present resources more efficiently and how future VLBI networks should look like to achieve this general goal of sub-mm accuracy (MacMillan, 2007). In previous studies within V2C, the antenna slew speed (Wresnik et al., 2008), network size, network geometry (Wresnik, 2009), recording rate, and other system specifications have been investigated for achieving 1 mm position accuracy. The main goal of the Monte Carlo simulations here is to study the impact of scheduling strategy on the quality of VLBI products and develop the optimum scheduling strategies for VLBI2010 system. These impacts are difficult to evaluate analytically due to complex interactions in the VLBI analysis process and are impractical to evaluate with real data due to the high cost of VLBI systems and operations. Monte Carlo simulators are developed to fill this gap, which are used extensively to study the benefit of new scheduling approaches for reaching the VLBI2010 target of 1 mm position accuracy. Simulation studies provide the advantage over real observations that the input contributions from each single effect are known and can be compared directly with the output estimates.

The new scheduling package (VIE_SCHED) is directly connected to the other packages of VieVS (Vienna VLBI Software) and the simulation studies are realized by running a sequence of different packages of VieVS software, as shown in Figure 5.1. After scheduling the observations

with VIE_SCHED, they are transformed to NGS format and used as input to the VieVS simulator (VIE_SIM). Simulated VLBI observables are generated taking into account the three most important stochastic error sources in VLBI, i.e. wet troposphere delay, station clock, and measurement error (Böhm et al., 2007). VIE_SIM produces wet zenith delay and clock values as well as white noise for each individual station at each scheduled epoch and sets up the o-c vector (observed minus computed) of the least-squares adjustment at each epoch. The artificial observations from VieVS simulator are also transformed to databases in NGS format and entered into VieVS estimator, which allows the estimation of geodetic parameters with a classical least-squares solution and provides feedbacks on the quality of schedule with distinct numbers and illustrative figures. The scheduler will decide if the target parameters can be achieved according to the goals set before, e.g. whether the errors in the estimated geodetic parameters from the scheduled VLBI session are below a certain threshold. If not, the scheduler can run VIE_SCHED again with another setting of scheduling strategies and rules. This process is repeated until the user is satisfied with the schedule. It is absolutely necessary to define standard interfaces (like NGS files) to be able to cross-check the results by other softwares, too. The performance of the Monte Carlo simulator has been evaluated and validated, which was mainly done with the comparison to real data from the CONT05 continuous VLBI campaign (Pany et al., 2011).

For the Monte Carlo simulations, at least 25 sessions are simulated using the same 24-hour schedule but different realizations of noise delays, each time creating new values for wet zenith delay, clocks and white noise. The analysis is performed for each of the simulated files, and the sample of output parameters is analyzed statistically. Based on physical properties of the troposphere and clocks, the simulations are run to investigate the influence of the scheduling strategy on VLBI analyses, and to gain information about the role of optimization criteria in the process of reaching VLBI2010's goal of 1 mm position accuracy on a global scale.

5.2. Simulations and results for VLBI2010

5.2.1. Simulation parameters

As mentioned above, group delay observables are calculated containing the following three main stochastic error sources in VLBI: wet troposphere delay, station clock, and measurement noise (see Equation 5.1). The wet troposphere delays have the largest impact of these three error sources (Wresnik et al., 2007; Pany et al., 2009). As the simulations presented here are supposed

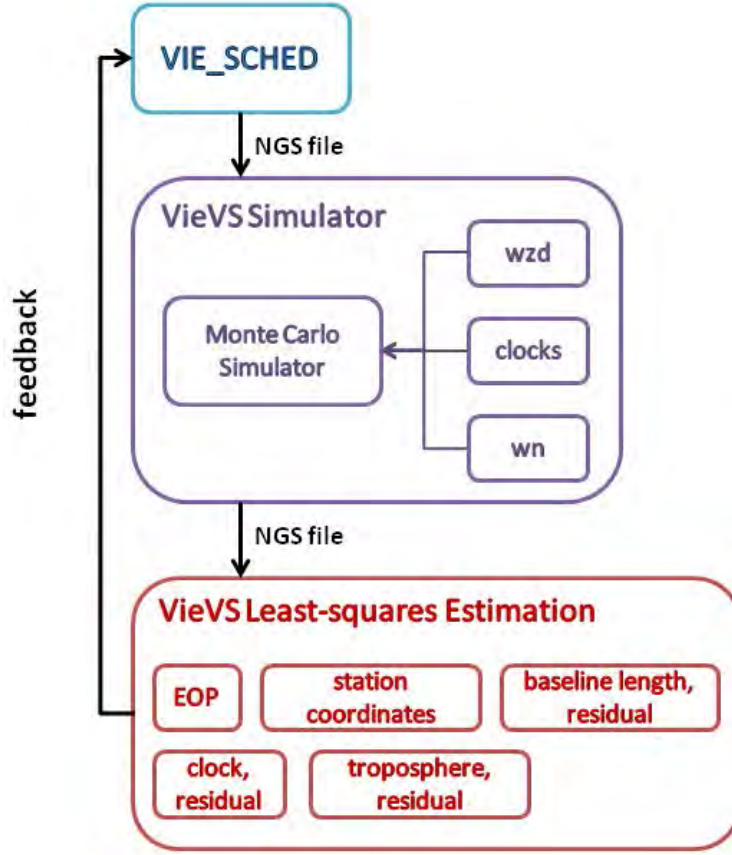


Figure 5.1.: Scheme of the Monte Carlo simulations with VieVS.

to reveal the influence of scheduling, it is decided to use the same set of simulation parameters for all sites and for all the VLBI2010 schedules. The simulation parameters are set to the following values (Table 5.1) and described in details below, which have been accepted within V2C.

$$o - c = (wzd_2 \times mfw_2(el) + clock_2) - (wzd_1 \times mfw_1(el) + clock_1) + wn. \quad (5.1)$$

$wzd_{1,2}$ and $clock_{1,2}$ are the simulated equivalent wet zenith delays and clock values at the station 1 and 2, and $mfw_{1,2}(el)$ are the corresponding wet mapping functions for the elevation angles el which are assumed to be error-free in the studies. wn is the white noise that accounts for random instrumental errors, and it is added per baseline.

Table 5.1.: Simulation parameters for the VLBI2010 system.

$Cn[10^{-7}m^{-1/3}]$	1.0
H[m]	2000.0
Vn[m/s]	0.0
Ve[m/s]	10.0
wzd0[mm]	250

dhseg[h]	2
dh[m]	200
clock ASD	10^{-14} @ 50 min
wn[ps]	4

1. Parameters for simulating wet zenith delay

In order to simulate the wet delays as realistically as possible, the turbulence theory (Treuhaft and Lanyi, 1987) and particular strategy proposed by Nilsson (Nilsson et al., 2007; Nilsson and Haas, 2010) are employed. The wet delays from turbulence theory also include the azimuthal variation which is taken into account with the covariance information between all observations at a station. The output of these calculations is a time series of equivalent zenith delays that include the dependency on elevation, azimuth and time epoch (w.r.t. the first epoch) of the observation. There are several parameters that are very important when creating the turbulent delays. These are:

(1)The refractive index structure constant (C_n). It could be estimated using high resolution radiosonde data, but the set of site-dependent VLBI2010 turbulence parameters are not used because it would be difficult to evaluate the impact of the schedule parameters when each station is assigned different values. The case of $C_n = 1.0 \times 10^{-7} m^{-1/3}$ corresponds to typical atmospheric conditions at mid-latitudes (Nilsson et al., 2007).

(2)The effective height of wet troposphere (H).

(3)The components of wind velocity (V_n and V_e). Realistic values of the wind speed and wind direction are taken from the ECMWF (European Centre for Medium-Range Weather Forecasts) models. For the VLBI2010 simulations the wind velocity is assumed to be constant. It is not realistic that the wind is blowing towards the same direction at all VLBI sites in a network. However, it was decided within the V2C to consider this simplified scenario for the simulations.

(4)The wet zenith delay (wzd_0) at the beginning of the time series.

(5)The correlation interval ($dhseg$) and the height increment for the numerical integration (dh).

2. Parameters for simulating station clock

Stochastic errors of station clocks can be simulated as the sum of random walk and integrated random walk stochastic processes (Herring et al., 1990). The simulations are performed with power spectral densities corresponding to Allan Standard Deviations (ASD) of 1×10^{-14} at 50 minutes, which is the typical frequency stability of current H-masers.

3. Parameters for simulating white noise

The contribution of the measurement error to the simulated delay observables is small compared to the contributions of troposphere and clock. A typical measurement precision for today's VLBI system is 10-30 ps (Behrend et al., 2007), while VLBI2010 is aiming at a measurement error as low as 4 ps by significantly increasing the data rate and the recording bandwidth. In this VLBI2010 simulations the white noise of 4 ps 1-sigma Gaussian random variable is used to represent all the system errors.

5.2.2. Estimation parameters

The main goal of the estimation process in the simulations is to investigate the impact of scheduling strategies on the estimates of geodetic parameters. The parameters to be estimated are troposphere parameters, clock parameters, and station position residuals, as well as daily Earth Orientation Parameters (EOP).

1. The tropospheric slant wet delay is modeled with a zenith wet delay and superimposed gradients as proposed in the IERS Conventions 2010 (Petit and Luzum, 2010). The troposphere parameters to be estimated are wet zenith delays and gradients, all of which are parameterized as piecewise linear offsets. The variations between the offsets are loosely constrained to zero by introducing pseudo observations. For the wet zenith delay the piecewise linear offsets every 6 minutes are used which are relatively constrained with 19 ps. And for gradients, piecewise linear offsets every 10 minutes are modeled which are relatively constrained with 1.4 mm and are absolutely constrained with 1 mm.
2. Station clocks are modeled with a second order polynomial superimposed with piecewise linear offsets. The quadratic function and piecewise linear offsets every 60 minutes are used which are relatively constrained with 42 ps.

3. The components of station position are treated as offsets and are estimated once per 24-hour session. No-Net-Rotation (NNR) and No-Net-Translation (NNT) conditions are employed for all priori station coordinates.
4. The EOP offsets are also estimated once per 24-hour session.
5. The source coordinates are fixed to ICRF2.

The choice of the constraints will have a slight impact on the obtained results. The length of the estimation intervals of station specific and global piecewise linear offset parameters can be chosen between five minutes and one day with VieVS (Teke et al., 2009). While the estimation intervals should be selected according to the number of observations in a session. Too short estimation intervals for every parameter will cause too many unknowns which will decrease the degrees of freedom of the adjustment and may lead to several singularity problems. The huge amount of VLBI2010 observations compared to present sessions provides enough degrees of freedom to select short estimation intervals and appropriate constraints for each parameter properly and to determine the short-term variations of the VLBI estimates more accurately.

The following criteria can be used to evaluate the potential of the VLBI system: baseline length repeatabilities, the root mean square (rms) of the 3D station position residuals, formal errors and standard deviations of the EOP, and the standard deviation between the simulated stochastic processes (troposphere delays, clocks) and their estimates. In the VLBI2010 simulations, the rms of the 3D station positions is mainly used to evaluate and compare different observing strategies and scenarios.

5.2.3. Antenna specifications and basic scheduling settings

To analyze the different scheduling strategies and modes, the typical VLBI2010 schedules are generated. The preliminary list of 211 compact sources created in Chapter 2 is still used here to get a sufficiently dense schedule. The antenna specifications are set up in scheduling according to the recommendations of VLBI2010 antennas within V2C. Four different 24-hour schedules for exactly the same network (see Figure 4.1) are prepared with VIE_SCHED, each with different scheduling strategies and modes described in Chapter 4. The first schedule is generated using source-based strategy with one source observed each time. The second schedule is from

source-based strategy with a pair of sources observed simultaneously. The third schedule is also generated with source-based strategy with four sources observed simultaneously. The fourth schedule is created with station-based strategy. The fill-in mode is employed for all the four schedules. The various scan parameters are fully calculated, the detailed information on algorithms and models are described in Chapter 3. The test VLBI2010 network (Figure 4.1) with existing VLBI sites and simulated ones is assumed to contain 16 identical antennas. The antenna specifications are summarized below, which correspond to the VLBI2010 antenna specifications (Petrachenko et al., 2008).

(1) The AZEL (azimuth-elevation) mount type is considered with azimuth range of -270° to $+270^\circ$ and elevation range of 5° to 88° . The slew rate parameters are 12 deg/s and 6 deg/s in azimuth and elevation axes, respectively. The slew acceleration in both axes is 3 deg/s^2 .

(2) The same SEFD of 2440 (assuming $D = 12 \text{ m}$, $\text{eff} = 0.5$ and $T_{\text{sys}} = 50 \text{ K}$) is used for all the 16 antennas.

(3) The data rate is 8 Gbps (assuming bandwidth 256 MHz, sample rate 512 MHz, 16 channels, and 1 bits quantification).

The basic settings employed in schedules are determined empirically and summarized below.

(1) The minimum SNR of 10 is required to ensure successful detection of signals.

(2) The cut-off elevation angle of 5° is used.

(3) The same source will not be observed within 15 minutes.

(4) The time window of uniform sky coverage is set to 10 minutes.

(5) The minimum of correlated source flux is set to 0.15 Jy for each baseline. The minimum of 5 s and maximum of 20 s are set for scan length.

5.2.4. Comparisons of schedule performance

Table 5.2 gives an overview of the key-parameters of the four schedules. The other results are analyzed and plotted in figures below. A typical IVS R1 session involves 7 or 8 stations observing 60 sources for 24 hours and has on the order of 500-1000 scans. The VLBI2010 session will have more than 10 times as many observations, compared to the current VLBI sessions.

Table 5.2.: Statistics of the schedules for the VLBI2010 system.

	Num of observed sources	Num of scans	Num of observations	Average of idling stations
One-source + Fill-in	208	8444	148504	0.46
Two-source + Fill-in	206	7592	135318	0.36
Four-source + Fill-in	210	13361	78819	0.44
Station-based + Fill-in	208	6845	139988	0.38

1. Mean on-source time

On-source time, the minimum time required to ensure successful application of the broadband delay technique, is based on the correlated flux of observed source on each band at the longer baselines. According to Equation 3.12, the scan length of 44.5 s, 19.8 s, 11.1 s, 7.1 s, and 4.9 s is required for sources with correlated strengths of 0.1 Jy, 0.15 Jy, 0.2 Jy, 0.25 Jy, 0.3 Jy (assuming minimum SNR of 10, SEFD 2440, recording rate 8 Gbps). From Figure 5.2, it is found that the mean on-source time is a little bit less for the schedule with “Four-source + Fill-in” mode. Because four sources are scheduled simultaneously, the network of 16 stations is always divided into four subnets. Because the mean baseline lengths of these subnets are shorter, the correlated flux of sources is less reduced for the shorter baselines. Thus, a shorter on-source time is obtained from this scheduling strategy. That is the same reason for the shorter on-source time at southern stations. It can be said that the on-source time with VLBI2010 antennas is reduced to be less than 10 seconds from Figure 5.2.

2. Mean slew time

As discussed in subsection 3.1.2, the VLBI2010 fast antennas can reach each sky position in 20 s. Figure 5.3 plots the mean slew time of the four schedules. It is found clearly that the longer inter-scan slew time is required for uniform sky coverage with “Station-based + Fill-in” mode.

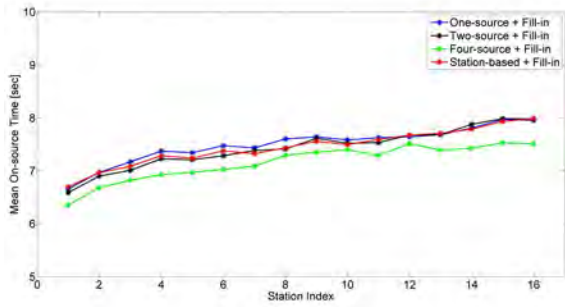


Figure 5.2.: Mean on-source time for the VLBI2010 system.

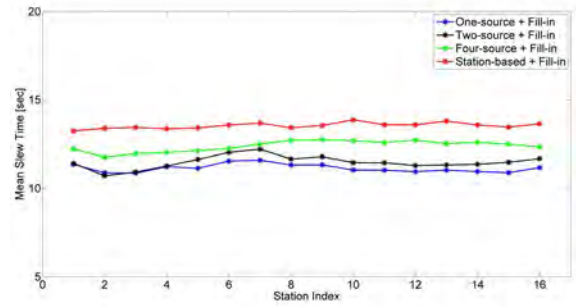


Figure 5.3.: Mean slew time for the VLBI2010 system.

3. Mean source-switching interval

Source-switching interval refers to the time between the start of one scan and the start of the next scan (including on-source time, slew time between sources, and even idling time). The average source-switching interval is calculated for each schedule and plotted in Figure 5.4. In case the network consists of fast moving antennas the number of observations per hour is a very huge increase, compared to today's 10 to 20 scans/hour. The larger source-switching interval at southern stations results from the longer idling time.

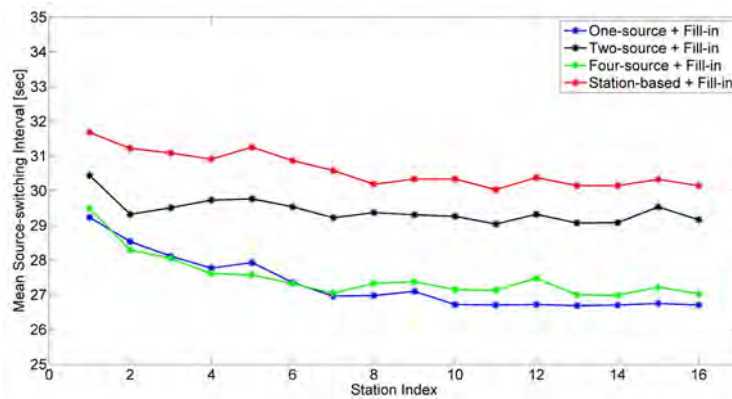


Figure 5.4.: Mean source-switching interval for the VLBI2010 system.

4. Observations at each station

Figure 5.5 shows the homogeneous distribution of scans at stations achieved from each of the four schedules. In Figure 5.6, the number of observations begins to drop off along with the decrease of station latitude in all the four schedules, as the consequence of the smaller subnet size (see Figure 5.7). It is also found that the number of observed sources at stations (from

southern to northern latitudes) is strongly related to the station latitudes in Figure 5.8.

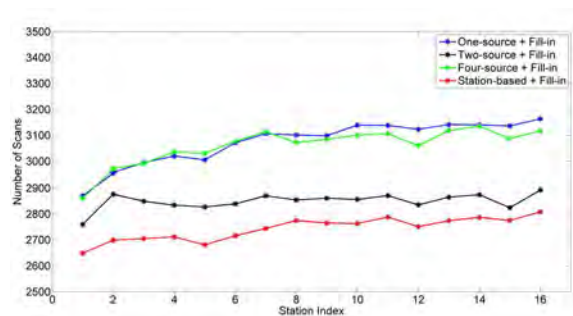


Figure 5.5.: Distribution of scans for the VLBI2010 system.

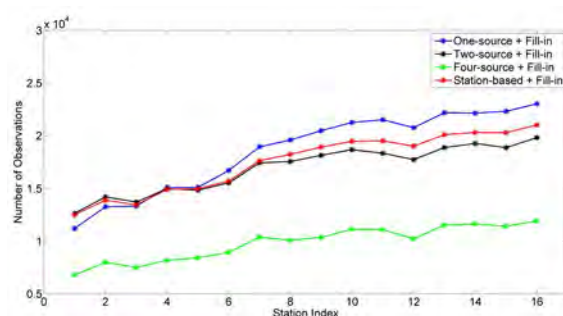


Figure 5.6.: Distribution of observations for the VLBI2010 system.

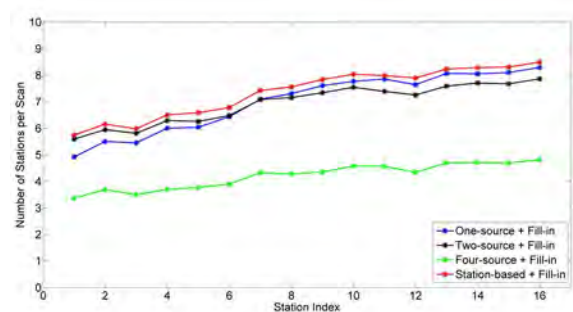


Figure 5.7.: Mean subnet size per scan for the VLBI2010 system.

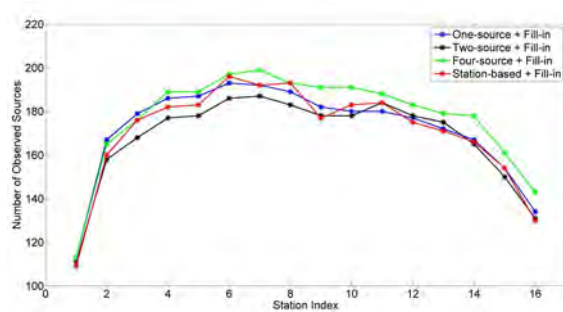


Figure 5.8.: Number of observed sources for the VLBI2010 system.

5. Sky coverage at stations

The sky coverage is calculated every 10 minutes and is shown in Figure 5.9. The sky coverage is 77.3%, 74.3%, 78.5%, and 89.3% for the four schedules on average, and the best one is achieved from “Station-based + Fill-in” mode. The comparisons plotted in Figure 5.3, Figure 5.5 and Figure 5.9 show that the uniform sky approach takes longer slew time and gets less scans within 24 hours. To have a closer look at the achieved sky coverage at stations, Figure 5.10 shows the required time for the whole sky coverage (sky coverage is of category 13).

6. Distribution of observed sources on celestial sphere

The distribution of observed sources on celestial sphere is calculated every 15 minutes, as is shown in Figure 5.11. For the four schedules, source distribution of 80.1%, 76.6%, 88.2% and 72.0% are obtained, respectively. As expected, “Four-source + Fill-in” mode has great advantages to

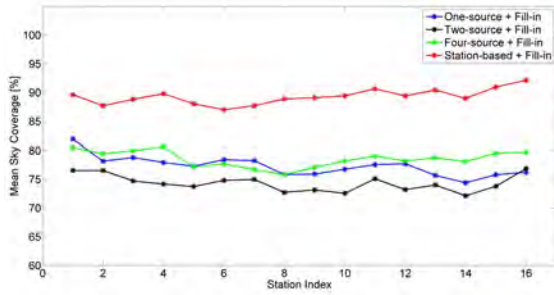


Figure 5.9.: Mean sky coverage of 10 minutes for the VLBI2010 system.

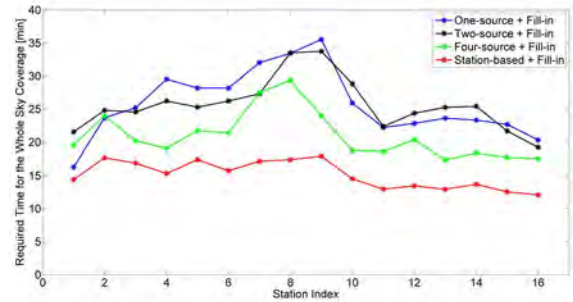


Figure 5.10.: Required time for the whole sky coverage (sky coverage is of category 13).

provide the better source distribution.

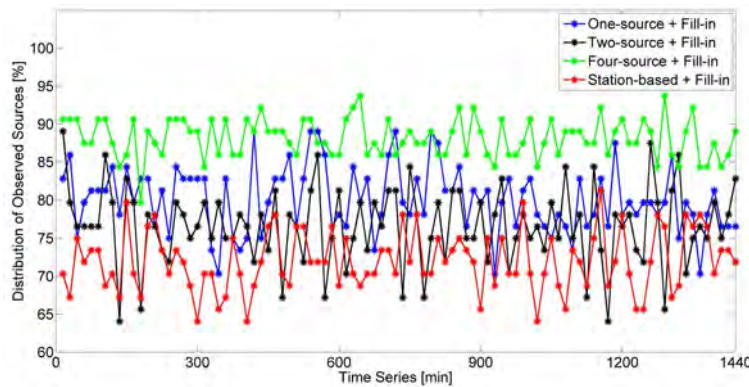


Figure 5.11.: Distribution of observed sources on celestial sphere per 15 min for the VLBI2010 system.

5.2.5. Comparisons of estimated geodetic parameters

1. Station position error

For each station and each of the 25 days of data, a 3D position error was computed. To obtain a single value for comparisons, the rms of 3D position error was computed over the 25 days for each station, as shown in Figure 5.12. Though worse station position repeatabilities for a couple of stations can be found, any significant impact of different schedules on the 3D position error can't be observed. The primary quantity that has been used throughout the simulation studies to characterize performance is the mean of the rms 3D position errors for all the 16 stations. That values obtained from the four schedules are 1.17 mm, 1.12 mm, 1.19 mm, and 1.13 mm, respectively. Their performance with respect to position error is nearly identical.

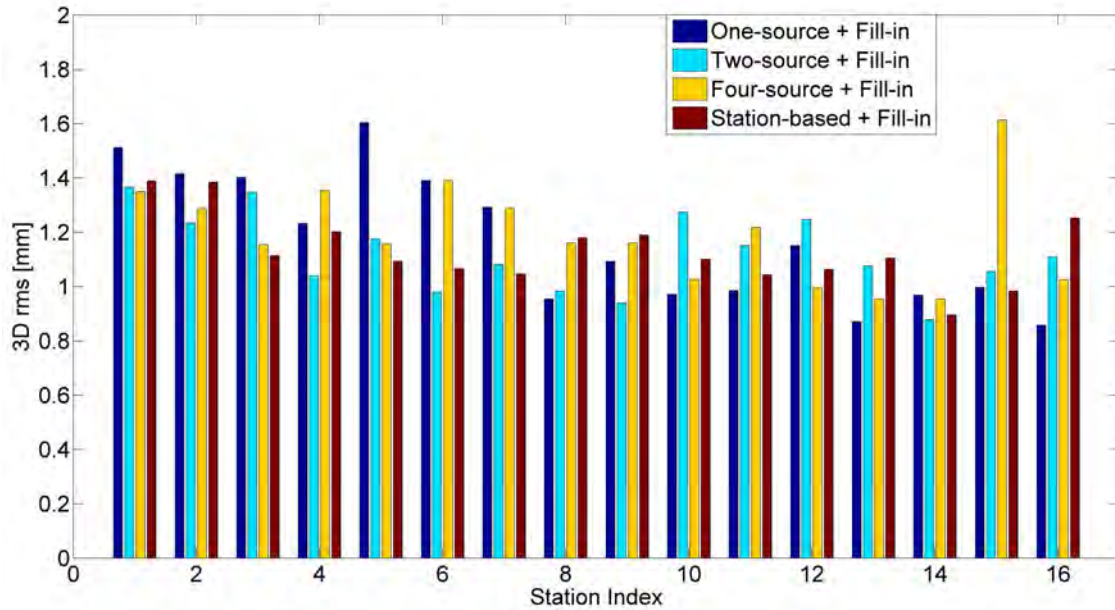


Figure 5.12.: RMS of 3D position error for the VLBI2010 system.

2. Baseline length repeatability

The baseline length repeatability corresponds to the standard deviation of the 25 determinations of the baseline lengths. These values represent the lower limit of the variations of the stochastic processes, thus giving the possibility to see the influence of the different schedules. Figure 5.13 shows the baseline length repeatabilities for the four different schedules described above. The mean baseline length repeatabilities are 1.17 mm, 1.09 mm, 1.17 mm, and 1.13 mm, respectively. It can be seen from this plot that there is no big improvement with respect to baseline length repeatability between schedules.

5.3. Simulations and results for CONT11

To validate the new scheduling package (VIE_SCHED), the comparisons with the current scheduling software (SKED) are performed in this subsection. SKED was originally developed in the late 1970s at Goddard Space Flight Center (GSFC), Greenbelt (USA), which has been employed for scheduling VLBI observations for more than 30 years. CONT11 is the best existing VLBI data set consisting of 15 days of continuous observations, observed 15-29 September 2011. The plan for the CONT11 campaign is to acquire state-of-the-art VLBI data over a time period of about two weeks to demonstrate the highest accuracy of which the current VLBI system is

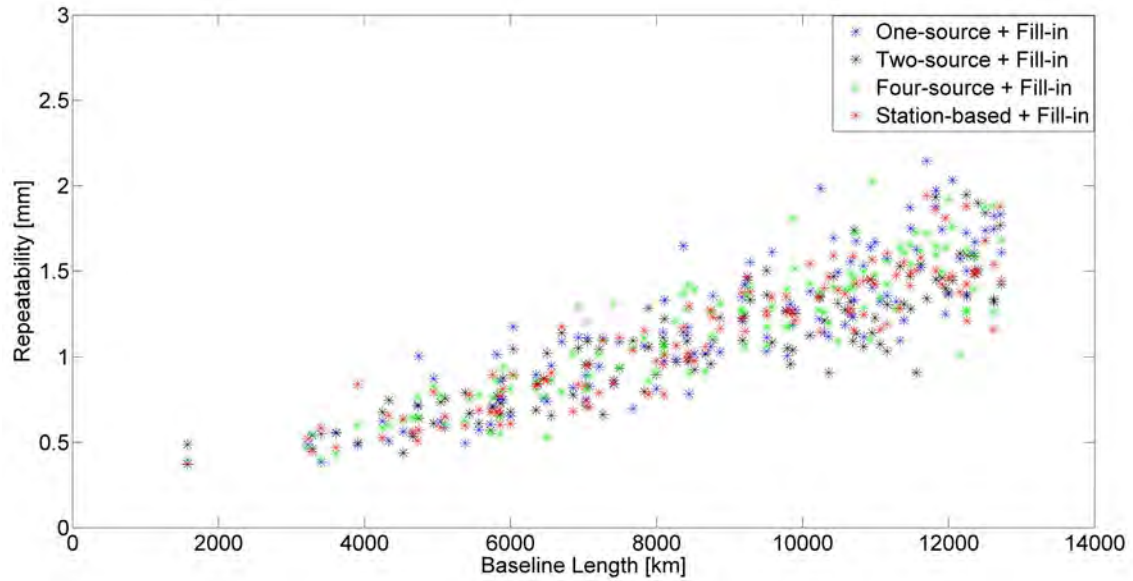


Figure 5.13.: Baseline length repeatability for the VLBI2010 system.

capable. In this subsection, the first 24-hour of CONT11 continuous observations (“C1101”) is used as an example to provide comparability between the two scheduling softwares. The original schedule file (c1101.skd) for this 24-hour continuous observations was prepared with the SKED software. The other four schedules are generated with VIE_SCHED considering the different strategies and modes. The same station catalog files, source parameters, and CONT11 frequency setup (512 Mbps data rate) are also employed in VIE_SCHED. To be consistent with the original C1101 schedule file, the four schedules are generated with VIE_SCHED using SNRs of 15 at X-band and 12 at S-band for all stations except TIGO which is scheduled with values of 10 and 9. The cut-off elevation angle of 5° is used. The minimum of 20 s and maximum of 200 s are set for scan length. The same source will not be observed within 30 minutes. The time window of uniform sky coverage is set to 60 minutes. The minimum of correlated source flux is set to 0.15 Jy for each baseline. From the operational point, the time for the antennas to settle down and calibration are 5 seconds and 10 seconds, respectively. The time to allow the correlator to synchronize tapes is set to 3 seconds. Figure 5.14 shows the CONT11 network of 13 stations.

5.3.1. Comparisons of schedule performance

Table 5.3 gives an overview of the key-parameters of the five schedules, which are generated with SKED and VIE_SCHED, respectively.

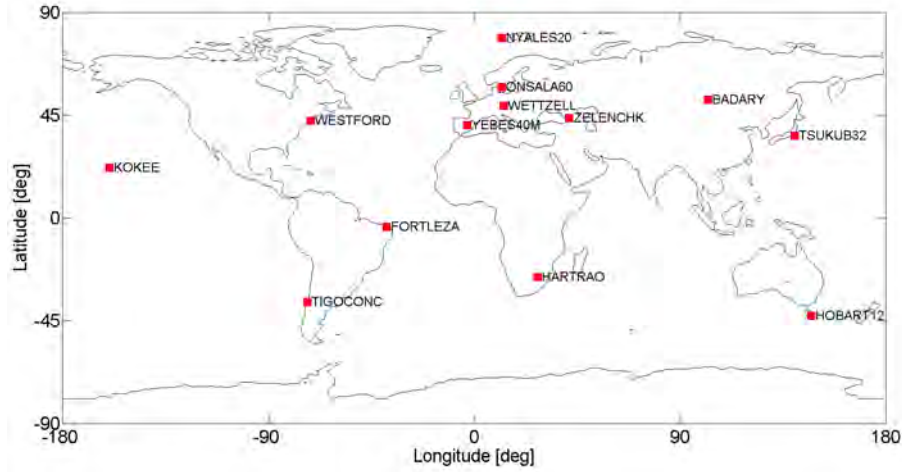


Figure 5.14.: The IVS CONT11 network (13 stations).

Table 5.3.: Statistics of the schedules for the CONT11 session.

		Num of observed sources	Num of scans	Num of observations
SKED		103	1196	11344
VIE_SCHED	One-source + Fill-in	99	1316	11155
	Two-source + Fill-in	98	1391	10045
	Four-source + Fill-in	98	1645	7915
	Station-base + Fill-in	105	1399	9095

1. Observations at each station

Figure 5.15 shows the number of scans at stations. In Figure 5.16, the number of observations begins to drop off along with the decrease of station latitude in all the five schedules, as the consequence of the smaller subnet size (see Figure 5.17). It is also found that the number of observed sources at stations (from southern to northern latitudes) is related to the station latitudes in Figure 5.18. It can be seen that VIE_SCHED tends to have fewer scans for smaller stations (here station TIGO).

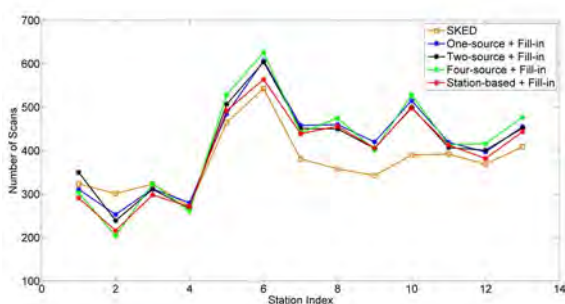


Figure 5.15.: Distribution of scans for the CONT11 session.

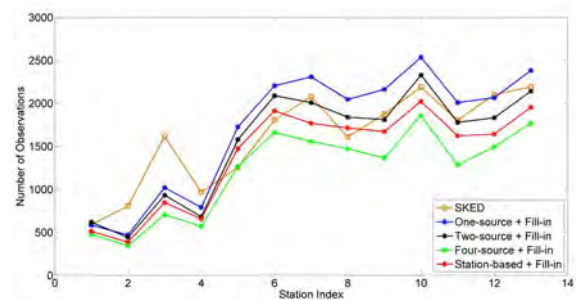


Figure 5.16.: Distribution of observations for the CONT11 session.

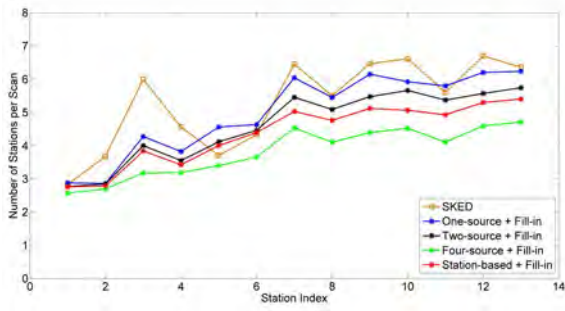


Figure 5.17.: Mean subnet size per scan for the CONT11 session.

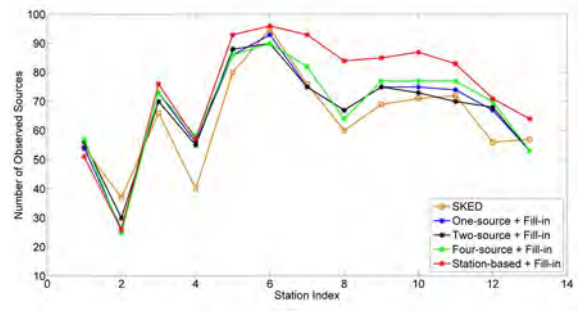


Figure 5.18.: Number of observed sources for the CONT11 session.

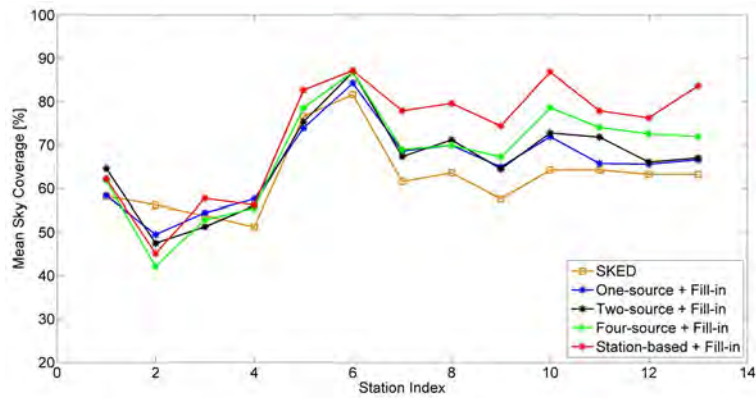


Figure 5.19.: Mean sky coverage of one hour for the CONT11 session.

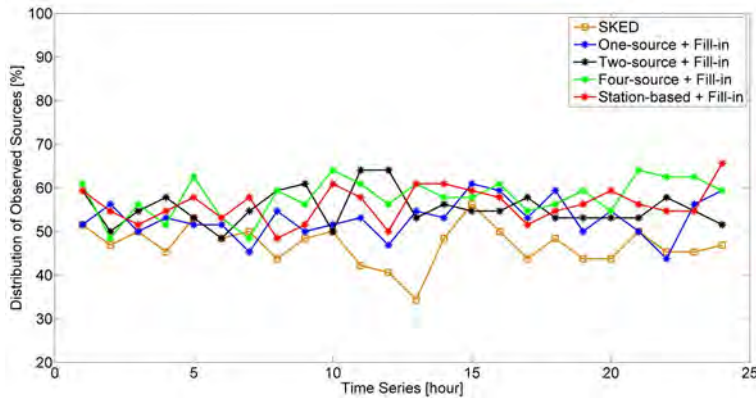


Figure 5.20.: Distribution of observed sources on celestial sphere per one hour for the CONT11 session.

5.3.2. Comparisons of estimated geodetic parameters

1. Simulation parameters

Table 5.4 lists the simulation parameters for C1101 session. In order to get realistic delays

these simulation parameters have values typical for the site of interest. In this study, the site-dependent Cn value are derived using GPS ZTD data (provided by Tobias Nilsson), which are listed in Table 5.5. For the Monte Carlo simulations of CONT11, 50 sessions are simulated using the same 24-hour schedule but different realizations of noise delays.

Table 5.4.: Simulation parameters for the CONT11 session.

Cn[$10^{-7}\text{m}^{-1/3}$]	site-dependent value
H[m]	2000.0
Vn[m/s]	0.0
Ve[m/s]	8.0
wzd0[mm]	250
dhseg[h]	2
dh[m]	200
clock ASD	10^{-14} @ 50 min
wn[ps]	32

Table 5.5.: Site-dependent Cn for the CONT11 session.

Site Name	Cn[$10^{-7}\text{m}^{-1/3}$]	Site Name	Cn[$10^{-7}\text{m}^{-1/3}$]
BADARY	1.37	TSUKUB32	3.45
KOKEE	1.39	NYALES20	0.65
HOBART12	1.60	FORTLEZA	2.46
YEBES40M	1.48	HARTRAO	1.34
TIGOCONC	2.08	WETTZELL	1.50
ZELENCHK	1.86	ONSALA60	2.19
WESTFORD	2.30		

2. Estimation parameters

1. The troposphere parameters to be estimated are wet zenith delays and gradients, all of which are parameterized as piecewise linear offsets. The variations between the offsets are loosely constrained to zero by introducing pseudo observations. For the wet zenith delay the piecewise linear offsets every 60 minutes are used which are relatively constrained with 1.5 cm. And for gradients, piecewise linear offsets every 360 minutes are modeled which are relatively constrained with 0.05 cm.
2. Station clocks are modeled with a second order polynomial superimposed with piecewise

linear offsets. The quadratic function and piecewise linear offsets every 60 minutes are used which are relatively constrained with 1.3 cm.

3. The components of station position are treated as offsets and are estimated once per 24-hour session. No-Net-Rotation (NNR) and No-Net-Translation (NNT) conditions are employed for all priori station coordinates.
4. The EOP offsets are also estimated once per 24-hour session.
5. The source coordinates are fixed to ICRF2.

3. Station position error

For each station and each of the 50 days of data, a 3D position error was computed. To obtain a single value to compare, an rms of 3D position error was computed over the 50 days for each station. From Figure 5.21, any significant impact of different schedules on the 3D position error can't be observed. The mean of the rms 3D position errors from the five schedules are 9.49 mm, 9.87 mm, 9.33 mm, 9.34 mm, and 9.64 mm, respectively.

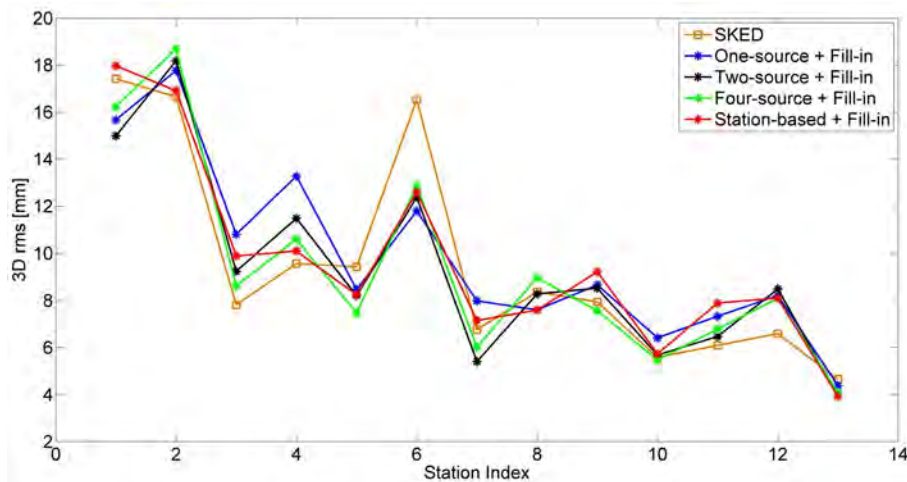


Figure 5.21.: RMS of 3D position error for the CONT11 session.

4. Baseline length repeatability

Figure 5.22 shows the baseline length repeatabilities for the five different schedules described above. The mean baseline length repeatabilities are 9.02 mm, 8.91 mm, 8.63 mm, 8.83 mm, and 9.02 mm for each schedule. From this plot it can be deduced that the baseline length

repeatabilities from the four schedules (generated with VIE_SCHED) fit well with the original schedule (generated with SKED).

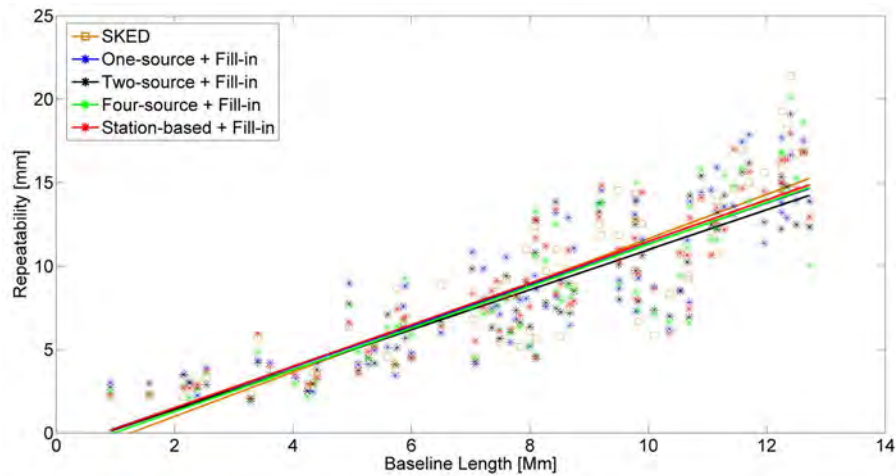


Figure 5.22.: Baseline length repeatability obtained from simulations for CONT11. The site-dependent value for C_n was used for each station. Also given are the rates (slopes of the straight lines fitted to the data) in mm Mm^{-1} (ppb).

5. EOP estimation

Table 5.6 and Table 5.7 give the statistics of ERP estimation and Nutation for each schedule.

Table 5.6.: Repeatability and standard deviation of ERP.

	Rep. of Xp [μas]	St. dev of Xp [μas]	Rep. of Yp [μas]	St. dev of Yp [μas]	Rep. of (UT1-UTC) [μs]	St. dev of (UT1-UTC) [μs]
SKED	63.20	52.57	70.31	44.38	3.81	2.33
VIE_SCHED						
One-source + Fill-in	101.05	55.85	87.66	45.00	3.30	1.86
Two-source + Fill-in	85.23	57.72	72.30	45.92	3.03	1.95
Four-source + Fill-in	79.29	59.38	63.82	47.64	3.43	2.09
Station-based + Fill-in	90.20	62.09	82.21	49.94	3.27	2.25

Table 5.7.: Repeatability and standard deviation of Nutation.

Rep. of Nutation X	St. dev of Nutation X	Rep. of Nutation Y	St. dev of Nutation Y
-------------------------------------	--	-------------------------------------	--

	$[\mu\text{as}]$	$[\mu\text{as}]$	$[\mu\text{as}]$	$[\mu\text{as}]$
SKED				
	28.01	17.29	29.20	17.90
VIE_SCHED				
One-source + Fill-in	28.80	16.36	28.52	15.99
Two-source + Fill-in	28.74	16.62	28.39	16.20
Four-source + Fill-in	24.70	17.71	31.04	17.88
Station-based + Fill-in	29.40	18.57	30.37	18.84

5.3.3. Conclusions

The schedules for CONT11 session are prepared with the software packages SKED and VIE_SCHED respectively, which are compared in terms of schedule performance and geodetic products. Results of similar quality are achieved. Compared with SKED, further improvements of VIE_SCHED will be the introduction of station weights for selection of stations.

6. Applications of scheduling

With the new scheduling package, various studies on VLBI system can be carried out. In this chapter, a few examples of investigations that have been performed with VIE_SCHED are presented.

6.1. Interim network consisting of fast and slow antennas

With the goal to design VLBI2010 system, Monte Carlo simulations are carried out at the Vienna University of Technology and Goddard Space Flight Center (GSFC). Since IVS products must be delivered without interruption, a transition period to VLBI2010 operations is required in which there will be a mix of current system (big slow-slewing antennas) and next-generation system (small fast-slewing antennas). Schedules for 24-hour continuous VLBI2010 observations with this interim network have been prepared with the software packages VIE_SCHED and SKED (developed at GSFC and recently updated for VLBI2010 scheduling) respectively. These are compared in terms of scheduled sources, number of observations, idling percentage, sky coverage, and station position repeatabilities. This study has been published in proceedings of the 20th meetings of the European VLBI group for geodesy and astrometry (Sun et al., 2011).

6.1.1. Simulations

1. Network

The interim network of 18 stations is plotted in Figure 6.1. The network consists of antennas expected to be outfitted with VLBI2010 observing systems in the near future, and also considering political, infrastructural, and economical aspects. The interim network includes legacy antennas (stars) and new fast slewing antennas (circles), as plotted in Figure 6.1 and listed in Table 6.1.

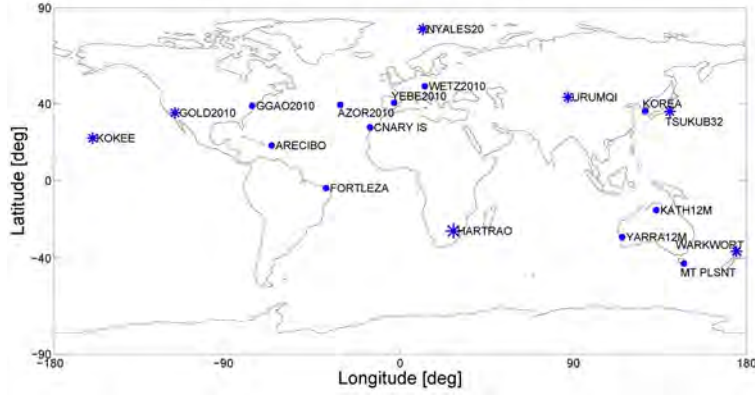


Figure 6.1.: 18 stations network used for the VLBI2010 simulations. Stars denote legacy antennas, circles new fast slewing antennas.

Table 6.1.: Characteristics of the 18 stations used for the simulations. The numbering of the stations (station indices) in the table corresponds to the numbers in Figures 6.2 to 6.5. The slewing rates given are just exemplificative values used for the simulations and do not always agree with the real or projected specifications of the antennas.

Sta Index	Sta Name	Slew Rate	
		AZ (deg/min)	EL (deg/min)
1	*HARTRAO	120	60
2	*KOKEE	120	120
3	*NYALES20	120	120
4	*GOLD2010	180	60
5	*URUMQI	180	60
6	*WARKWORT	180	60
7	*TSUKUB32	180	180
8	°ARECIBO	300	75
9	°FORTLEZA	300	75
10	°GGAO2010	300	75
11	°KATH12M	300	75
12	°MT_PLSNT	300	75
13	°YARRA12M	300	75
14	°KOREA	300	300
15	°AZOR2010	720	360
16	°CNARY_IS	720	360
17	°WETZ2010	720	360
18	°YEBE2010	720	360

2. Schedule parameters

24-hour continuous observing sessions are considered and compared. When creating a schedule for an experiment, VIE_SCHED and SKED read the same catalogue system files for the selection of sources, stations, and observing modes. Source structure models are also used in VIE_SCHED to calculate the predicted observed flux on each baseline of a scan. The minimum of observed flux is 0.3 Jy. The generation of the schedules is done assuming that the observations are carried out with the current S/X system. The recording rate is 8 Gbps (number of channels 16, bandwidth 128 MHz, sample rate 256 MHz and 2 bits quantization). The minimum SNR are 20 (X band) and 15 (S band), respectively. The cut-off elevation angle is 5 degrees. The source-based strategy with two sources scheduled simultaneously is used for this study. The 18 stations are divided into two groups (11 fast antennas plus 7 slow antennas) according to slew rates. The antennas with fast slew rate are given higher priority. The slow antennas take part in the experiment only if they can arrive at the next source in time.

3. Simulation parameters

The simulation values listed were chosen by the V2C to provide comparability between the simulations done at Vienna with VIE_SCHED and those done at GSFC with SKED. The parameters include the refractive index structure constant C_n ($2.5 * 10^{-7} m^{-1/3}$), the effective height of the wet troposphere H (2000 m), and the wind velocity vector v (8.0 m/s) towards east. The stochastic variations of station clocks are computed as sum of a random walk and an integrated random walk, with a power spectral density corresponding to an Allan Standard Deviation (ASD) of 10^{-14} @ 50 min. A white noise of 16 ps per baseline observation is added.

4. Estimation parameters

The parameters used to estimate troposphere parameters, clock parameters, and station positions are listed below.

- NNR/NNT for all a priori station coordinates; source coordinates fixed to ICRF2.
- EOP offsets for each 24-hour session.
- Quadratic function plus 60 min piecewise linear function for clocks with relative constraints of 42 ps.

- 6 min piecewise linear function for zenith wet delays with relative constraints of 19 ps.
- 10 min piecewise linear function for gradients with 1.4 mm relative constraints and 1 mm absolute constraints.

6.1.2. Results

1. The number of observations is shown in Table 6.2 and Figure 6.2.

Table 6.2.: Statistics of the different schedules.

	From SKED	From VIE_SCHED
Number of scheduled sources	200	225
Number of scans	4000	4138
Number of observations	99371	84398

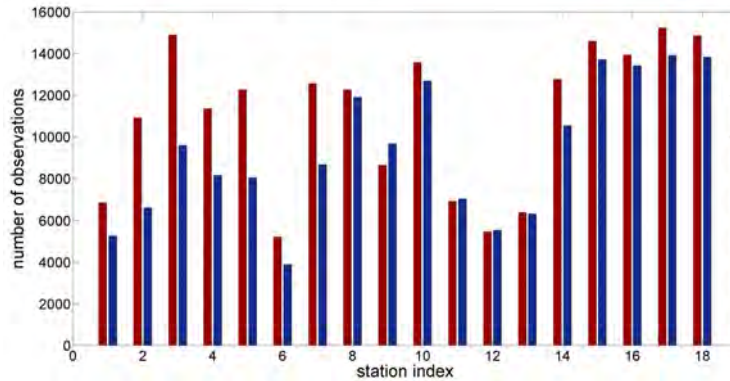


Figure 6.2.: Distribution of observations. Results from SKED are shown with left bar (red), and results from VIE_SCHED are shown with right bar (blue). The station indices are consistent with increasing slew rate.

2. The characteristics of the antenna in the schedule are summarized in Figure 6.3. One of the most striking features is how little time is actually spent on observing. The rest of the time is spent slewing and idling. It is found that the idling percentage is less than slewing percentage in the results from SKED at slow stations.

3. Figure 6.4 shows the difference of mean sky coverage per 20 minutes from the two schedules. Because of less observations, the stations with slow slewing rates (low station indices) have worse sky coverage.

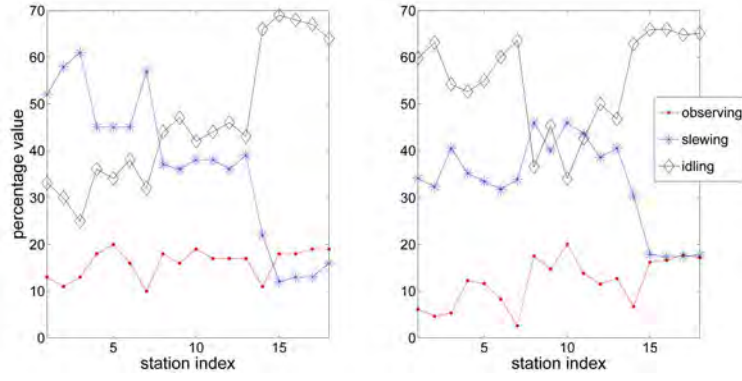


Figure 6.3.: Idling, slewing, and observing percentage. Results from SKED are shown left, results from VIE_SCHED are shown right.

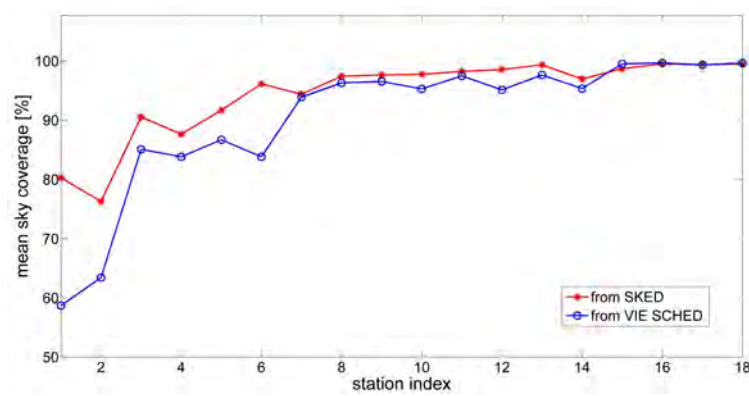


Figure 6.4.: Sky coverage distribution for 20 minutes interval.

4. Figure 6.5 shows station position repeatabilities obtained from the simulations. The median station position repeatabilities derived from SKED and VIE_SCHED are 3.29 mm and 3.72 mm, respectively. The median station position repeatabilities of 7 slow stations are 3.36 mm (from SKED) and 4.29 mm (from VIE_SCHED), respectively. And the median station position repeatabilities of 11 fast stations are 3.25 mm (from SKED) and 3.36 mm (from VIE_SCHED). As a consequence of the difference in terms of observations distribution, idling percentage, and sky coverage distribution, the station position repeatabilities from VIE_SCHED are a little worse than those from SKED at stations with low station indices, i.e., slow slewing rates.

6.1.3. Conclusions

The schedules for 24-hour continuous observation are prepared with the software packages VIE_SCHED and SKED respectively, which are compared in terms of scheduled sources, number of observations, idling percentage, sky coverage, and station position repeatabilities. Results of

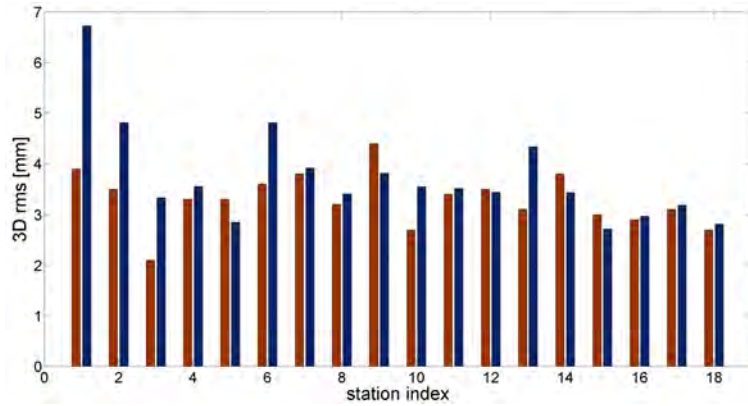


Figure 6.5.: Station position repeatabilities obtained from the simulations. Results from SKED are shown with left bar (red), and results from VIE_SCHED are shown with right bar (blue).

similar quality are achieved. Results of similar quality are achieved and the comparisons with other scheduling software (SKED) show a good agreement.

6.2. Twin telescopes at one site

The IVS WG3 final report suggests a major increase in observation density (or, equivalently, a major decrease in source-switching interval) as a strategy for increasing VLBI position accuracy. The WG3 final report also proposed the use of multiple antennas at a site to share the observing load and hence to reduce the effective source-switching interval (Niell et al., 2005). There are a number of advantages using twin antennas at a geodetic VLBI site, e.g. to increase the total collecting area, to increase the total number of sources observed in a day, to remove the corrupting effect of the reference oscillators through differencing, and to increase redundancy (Petrachenko, 2006). On the other side, to guarantee continuous observations this is only possible with more than one radio telescope per site due to telescope maintenance cycles – if one antenna needs system maintenance or repairs, the second antenna can be used to continue the observation program. This may be a significant benefit in an operational program.

Following the recommendations made by the VLBI2010 vision report of the IVS, the project of Twin Telescope Wettzell (TTW) is the first rigorous approach to realize a radio telescope system consisting of more than one antenna per site. It consists of a pair of identical fast slewing radio telescopes with a 13.2 m main reflector. The aim is to make the first observations at the start of 2013 (Hase et al., 2009).

6.2.1. Observing strategies

The development of the observing strategies for twin telescopes is still an open issue for VLBI2010. The concept of twin radio telescopes enables a lot of new observation strategies. Advantages are obtained by assuming the same troposphere above the two telescopes and connecting them to the same H-maser clock. Assuming both of the two antennas are available for observation, VIE_SCHED can handle three different applications of twin antennas. The careful simulations and the estimated results follow.

1. Same source observations

If the two telescopes point simultaneously to the same radio source and the local tie between them is accurately known, they can be used in the “array mode” to increase the sensitivity. Sensitivity of a VLBI receiver is generally characterized by System Equivalent Flux Density (SEFD), which is calculated with Equation 3.6. A pair of antennas has about twice the collecting area than a single antenna, so it is more sensitive to the very weak signal from a quasar. That is to say, the twin telescope needs less time to achieve the minimum SNR for observing the same sources (see Equation 3.12). Another possible application with this mode is to split high-speed data (e.g. 8 Gbps) recording capability between the antennas.

2. Continuous observations

While one antenna is observing the other antenna is slewing to the next radio source, i.e. one of the two radio telescopes always looks at a source. Hence continuous estimation of EOP can be realized by VLBI, similar to ring laser gyroscopes. In this mode, only one antenna is observing at a time, and the entire recording system can be dedicated to that antenna.

3. Multidirectional observations

The antennas are observing simultaneously in different directions to different sources, i.e. different subnets are tied at the same time. The number of observations could be increased approximately by a factor of two, which is the critical factor for the accuracy of the estimated parameters.

6.2.2. Simulations and results

The interim network of 18 stations (see Figure 6.6) with fast slewing antennas is used in Monte Carlo simulations with VieVS. Different from in Section 6.1, here the azimuth and elevation slewing rates are 12 deg/s and 6 deg/s, respectively, for all stations. The twin telescopes are considered at station Wettzell, which is denoted with a red circle in Figure 6.6. We also do simulations with a single telescope at station Wettzell to provide comparability. Here the source-based scheduling strategy and the option “four-source scheduled simultaneously” are used for this study. Three schedules are generated considering the three observing modes mentioned above.

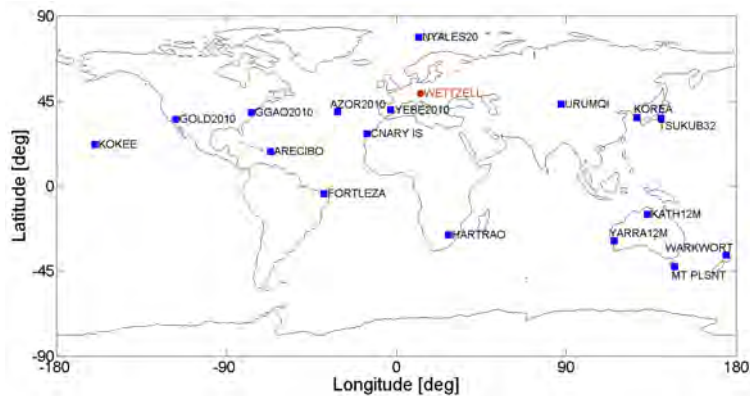


Figure 6.6.: Network used for simulations. The red circle denotes station Wettzell with twin telescopes.

The numbering of the stations (station indices) is by latitude in Figures 6.7, 6.8, 6.9, and 6.10 (Wettzell index is 17). For the “same source observations” mode, the mean observing duration with twin telescope is decreased almost by half, which is shown in Figure 6.7. Though we can get decreased on-source duration from “same source observations” and decreased slewing duration from “continuous observations”, the twin telescope is always waiting for other stations to start the scan because only one station is installed as twin telescope in the simulation network. Consequently, we get similar numbers of observations with the twin telescope, as shown in Figure 6.8. So the performance with one twin telescope in the network is not improved significantly with these two observing modes.

On the other hand with “multidirectional observations” mode, the number of observations is increased by a factor of two and a better sky coverage is obtained, as shown in Figures 6.8 and 6.9. To support the evaluation of “multidirectional observations” mode, Monte Carlo simulations are carried out with VieVS. After scheduling the observations with VIE_SCHED, they are trans-

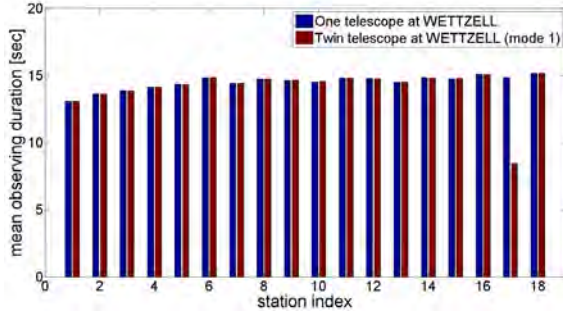


Figure 6.7.: Mean observing duration from “same source observations” mode.

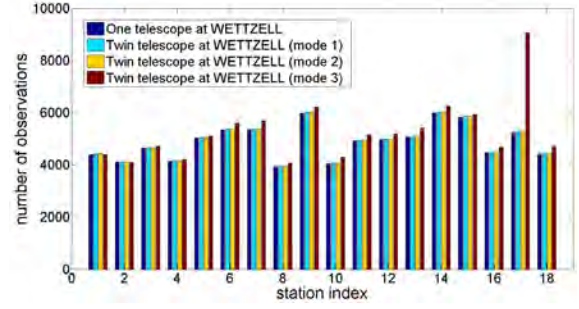


Figure 6.8.: Number of observations from the three observing modes.

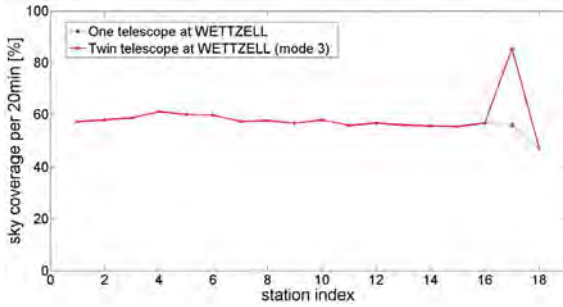


Figure 6.9.: Sky coverage from “multidirectional observations” mode.

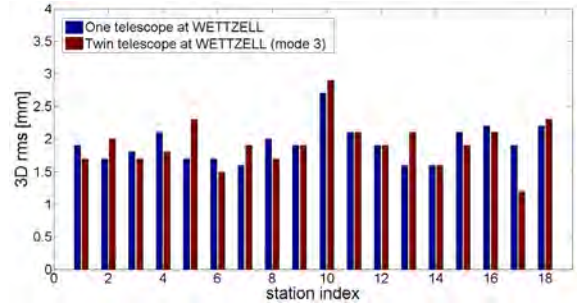


Figure 6.10.: Station position repeatabilities from “multidirectional observations” mode.

formed to NGS format and used as input to the VieVS simulator (VIE_SIM). VIE_SIM sets up the o-c vector (observed minus computed) of the least-squares adjustment with simulated values of zenith wet delays, clocks, and observation noise at each epoch. The simulation parameters include the refractive index structure constant C_n ($1.0 * 10^{-7} m^{-1/3}$, used for all stations), the effective height of the wet troposphere H (2000 m), and the wind velocity vector v (8.0 m/s) towards east. The stochastic variations of station clocks are computed as sum of a random walk and an integrated random walk, with a power spectral density corresponding to an Allan Standard Deviation (ASD) of 10^{-14} @ 50 min. A white noise of 4 ps per baseline observation is added. Additionally, certain modifications have been made with VIE_SIM, e.g. the introduction of condition equations to account for two co-located VLBI antennas using the same clock. Careful simulations were carried out to assess the real benefit of this approach (Wresnik et al., 2006). The simulated NGS data files are entered into the software package VieVS, which computes a classical least-squares solution. The parameters to be estimated are troposphere parameters, clock parameters, and station position residuals (with No-Net-Rotation (NNR) and No-Net-Translation (NNT) conditions on all stations), as well as daily EOP. The simulation process is repeated 50 times to obtain a sample of output parameters that can be analyzed statistically. The station position repeatabilities are compared in Figure 6.10. We find that the

performance generally improves because of more observations per day at Wettzell. 12 out of 18 stations are improved and the most significant improvement is at station Wettzell, while 6 stations are getting worse. We can't count on one twin telescope for the global improvement. There need to be more multiple telescopes for actual global improvement.

6.2.3. Conclusions

The mode “multidirectional observations” improves the sky coverage greatly (53.4%) with almost twice observations, and the station position repeatability is improved correspondingly (22.2%). For the “same source observations” mode and “continuous observations” mode, there is hardly any improvement. In case of more than one twin telescope in a network, these two strategies will be more beneficial.

6.3. Solar corona study

The solar corona is the result of high density and strongly turbulent ionized gases (plasma) being ejected from the Sun. The ionized gas is 1-2 million kilometers thick and it is up to several million kilometers thick during periods of high solar activity (11 year cycle) (Ho, 2010). Assuming the solar corona has similar dispersive effects as ionosphere, the total electron content (TEC) will be different for VLBI measurements close to the Sun or far away from the Sun. With the start of the IVS observing program in 2002, sources were only scheduled when they had an angular distance to the Sun of more than 15 deg. In the previous sessions before 2002, some measurements are found to have 2°-3° solar elongation angle and thus are 4.5-7 million kilometers close to the Sun. The VTECs (Vertical TECs) are estimated at 1 hour intervals. The results show that the effect of solar corona is smaller than observation errors for the measurements far from the Sun. For the observations very close to the Sun, the effects can be detected occasionally but they have very low redundancy and loss of coherence (personal communications with Benedikt Soja).

To probe the solar corona, the IVS Observing Program Committee (OPC) tasked VIE_SCHED to schedule special sessions. This is the first opportunity for VIE_SCHED to schedule a real VLBI session, and the algorithms of sources, antennas, and observing modes can be validated in real-life situation. In 2012, VIE_SCHED generated 7 sessions on the basis of RD session setup, i.e. RD1204, RD1205, RD1206, RD1207, RD1208, RD1209, and RD1210. All these 7

sessions have been observed successfully at stations and the data files of the first four sessions are already available in IVS database after being correlated at Haystack and analyzed by Goddard. The estimation of solar corona effect with the real data is in progress. On the other side, the feedback from stations and IVS coordinating center also gives great help to fix bugs and improve VIE_SCHED finally. Before the full deployment of the VLBI2010 system, it is always necessary and helpful for VIE_SCHED to take part in the current VLBI experiments.

The original purpose of these RD sessions is to include sources closer to the Sun, which can improve the determination of the post-Newtonian parameter γ by 15% (even with a modest number of observations below 15° per session; for instance, 1-2 observations per session). Besides the consideration of γ determination, more dense observations are scheduled on the particular sources closer to the Sun ($< 5^\circ$ elongation angle) to meet the requirements of solar corona study. The list of particular sources and the observation density target are specified in a local control file (psource.txt). During the 24-hour RD session, some stations drop out for participating in an intensive session and then re-enter the RD session. The period that the stations are unavailable is specified in down.txt file. The IVS R1 frequency setup is used for the RD sessions (256 Mbps recording rate). It is generated using SNRs of 20 at X-band and 15 at S-band for all stations except TIGO which is scheduled with values of 18 and 12. Because TIGO is a small insensitive antenna, the SNR requirements need to be loosened to allow for enough scans to be scheduled with this telescope. The source-based scheduling strategy is employed for these RD sessions.

1. RD1204 session

It contains seven stations in the network and it is scheduled to start the observations on June 19. Just before the start of RD1204 session, KOKEE is announced unavailable due to X-band low-noise amplifier failures. Tsukuba missed the start of the session (the first 5.5 hours) due to the passage of a typhoon over Japan. There were very few scheduled observations to TIGO and FORTLEZA and the results there are very poor. Overall 60.6% of scheduled observations are used in analysis.

2. RD1205 session

RD1205 session contains eight stations and has observations less than 15 degrees from the sun for 0656+082, 0657+172, 0743+277, 0745+241, 0748+126, and 0759+183. 94.0% of the scheduled

observations were successfully obtained, more details can be found in Table 6.3.

Table 6.3.: Schedule performance of RD1205 session.

Source Name	Elongation [°]	Num of scheduled obs	Num of correlated obs	Num of used obs
0745+241	6.9	22	22	18
0657+172	7.4	78	78	65
0743+277	8.3	3	3	3
0759+183	10.9	3	3	2
0748+126	12.0	100	100	98
0656+082	15.0	2	2	1

3. RD1206 session

The sixth RD session is scheduled to start the observations on August 28 and eight stations participated. There are nine sources with an angular distance less than 15 deg to the Sun. This resulted in 114 scans and 436 observations with a distance to the Sun ranging from 1.8 deg to 14.7 deg (see Table 6.4). The closest source to the Sun is 1030+074 with an elongation angle of 1.8 deg, which is a real challenge for VLBI system. Unfortunately, the observations at S band for the source 1030+074 is failed. 82.9% of the scheduled observations are used in analysis in total.

Table 6.4.: Schedule performance of RD1206 session.

Source Name	Elongation [°]	Num of scheduled obs	Num of correlated obs	Num of used obs
1030+074	2.3	177	176	0
1023+131	3.7	57	54	35
1015+057	4.9	50	48	25
1013+054	5.5	17	17	14
1022+194	10.0	7	7	6
1055+018	10.4	52	48	43
1111+149	12.1	33	33	29
1049+215	13.1	7	7	7
1012+232	14.2	36	36	34

4. RD1207 session

The RD1207 session is scheduled to start the observations on September 25 and seven stations participated. There are six sources with an angular distance less than 15 deg to the Sun: 1130+009, 1145-071, 1149-084, 1219+044, 1236+077, and 1243-072. This resulted in 44 scans and 93 observations with a distance to the Sun ranging from 6.1 deg to 11.2 deg. The closest source to the Sun is 1219+044 with an elongation angle of 6.1 deg. 99% of the scheduled observations are correlated and 95.4% are used in analysis finally.

7. Conclusions, future work, and perspectives

7.1. Conclusions

To reach the goals of VLBI2010, various new facets have been employed, e.g. small fast-moving antennas, broadband frequency observations (2-14 GHz), and two or more antennas at a site, which are also challenges to the existing scheduling software. At GSFC, the SKED software has been updated for VLBI2010 scheduling. In order to exploit the full power of the future VLBI2010 system and to derive the best possible geodetic parameters, a new scheduling package (VIE_SCHED) has been developed at the Vienna University of Technology. This is the main research objectives of the thesis.

1. The new scheduling package VIE_SCHED has been developed, implemented and tested according to the requirements of the VLBI2010 system. Up to now, all the present VLBI2010 requirements have been employed in VIE_SCHED. The fast slew antennas ensure a maximum slew time of less than 20 seconds. The broadband frequency and the high recording rate decrease the on-source time to as short as 5 seconds. The short source-switching interval increases the amount of VLBI2010 observations by a factor of at least 10 compared to current VLBI sessions, which ensures a more accurate and data-rich geodetic VLBI system.

2. VIE_SCHED provides two major scheduling strategies (source-based strategy and station-based strategy). For the source-based strategy, three options are available for the users. On the basis of VLBI2010 antenna specifications, both strategies with suitable scheduling settings reach the same level of performance. Since it is evaluating sources only, the source-based strategy is time-saving and different strategies can be tested in fairly short time. Along with the extension of network size, e.g. 24 stations, 36 stations, and even more stations in the future, the source-based strategy will be highly advantageous.

3. Three observing modes are developed for twin telescopes at one site. With VIE_SCHED the

operator is able to choose in which observing mode the two-antenna array should be considered for the schedule. The preliminary results with twin telescopes at one site are also shown in this thesis.

4. With integration of VIE_SCHED into the VieVS, it is convenient to connect it with other packages of VieVS, which makes a powerful tool for VLBI simulation studies, e.g. studying schedule strategy, network size, antenna specifications, error sources, analysis strategy, and so on.

5. SKED is a mature scheduling software which has been used for VLBI observations for more than 30 years. The comparisons with SKED have been done in this thesis, considering both a VLBI2010 network and current IVS network, and show a good agreement.

6. In the last phase of the scheduling research, VIE_SCHED is provided to the IVS Operations Center at NASA/GSFC for further tests. From June, 2010, VIE_SCHED takes over the scheduling task for IVS RD sessions. A lot of experiences are obtained and VIE_SCHED is validated with real operations. This is a necessary step to schedule for current IVS sessions before the full deployment of VLBI2010, which ensures that VIE_SCHED can work for future VLBI2010 observations successfully.

7.2. Future work

The development of VIE_SCHED started in 2010 and many changes have been driven by changes in equipment or by user requests to make VIE_SCHED easier to use and less error prone. The VIE_SCHED will be further improved and extended in many aspects along with development activities of the VLBI2010 technique. In future it continues to grow and mature with VieVS. If any future extensions are made to geodetic/astrometric sources, the VIE_SCHED will be updated correspondingly.

With the current VLBI resources, the stations far south do not observe as frequently as the other stations. This can be avoided by selecting more southern radio sources. VIE_SCHED will give one way of increasing the preference for southern stations and southern sources.

The first radio telescope system consisting of two antennas per site has been realized at station Wettzell. Later on, more twin-telescopes in the VLBI2010 network will be set up. And the use of

multiple antennas at a site is one of the future options at many stations, i.e. a small fast-moving antenna will be installed close to a large antenna. For example, all the modes may even include the existing 20m radio telescope in Wettzell as a third contributor to a VLBI2010 observing session. VIE_SCHED will keep up with the development and exploit the advantages of multiple antennas. Twin telescopes offer additional chances, like observing double differences, to remove the effect of the clock entirely and decrease correlation between the vertical component of the baseline and the constant terms of the clock and atmosphere during parameter estimation. On the other hand, the cost efficiency of twin telescopes is also to be investigated in detail.

The new VLBI2010 system is proposing small and fast moving antennas, but the new antennas will be integrated in the existing IVS station network where the slew rates are much slower. In addition the required on-source time for old and new antennas will vary a lot. This is a major task for VIE_SCHED during the transition period. For each antenna of the particular subnet the optimal mixture between dual bands and broadband has to be calculated and considered for scheduling.

To observe continuously within VLBI2010, the full automation from scheduling, observing, and correlating is required. Automated procedures help to improve the timeliness of product delivery. The remote control antenna interface is developed and a subset of antennas with access to high-speed fiber networks is also on construction. The scheduling is also needed to work automatically and the schedule quality should meet the service requirements. It requests VIE_SCHED more stable and robust in terms of operational considerations. The considerations of antenna maintenance and power saving mode should be given great care from a practical point of view.

Last but not least, there are plans to further equip VIE_SCHED with satellite tracking and space VLBI capabilities.

7.3. Perspectives

Since scheduling functionality is completed in VIE_SCHED, it can be used for simulation studies extensively. On the other hand, it is also very helpful to schedule current IVS sessions. The new scheduling package (VIE_SCHED) has more external users now and it will be employed at many other institutes worldwide hopefully. Moreover VIE_SCHED will keep up with the development of the VLBI technique in the future. Along with the deployment of VLBI2010

antennas, VIE_SCHED can schedule for VLBI2010 experiments successfully, even during the transition period. The future VLBI2010 system with high accuracy will contribute to Earth system sciences more greatly.

List of references

- Behrend, D., J. Böhm, P. Charlot, T. Clark, B. Corey, J. Gipson, R. Haas, Y. Koyama, D. MacMillan, Z. Malkin, A. Niell, T. Nilsson, B. Petrachenko, A. Rogers, G. Tuccari, and J. Wresnik (2007). Recent Progress in the VLBI2010 Development. In L. Ubertini, P. Manciola, S. Casadei, and S. Grimaldi (Eds.), *Proceedings of the XXIV IUGG General Assembly*.
- Böhm, J., S. Böhm, T. Nilsson, A. Pany, L. Plank, H. Spicakova, K. Teke, and H. Schuh (2012). The New Vienna VLBI Software VieVS. In S. Kenyon, M. Pacino, and U. Marti (Eds.), *Geodesy for Planet Earth, International Association of Geodesy Symposia 136*, pp. 1007–1011.
- Böhm, J., H. Spicakova, L. Plank, K. Teke, A. Pany, J. Wresnik, S. English, T. Nilsson, H. Schuh, T. Hobiger, R. Ichikawa, Y. Koyama, T. Gotoh, T. Kubooka, and T. Otsubo (2009). Plans for the Vienna VLBI Software VieVS. In G. Bourda, P. Charlot, and A. Collioud (Eds.), *Proceedings of the 19th European VLBI for Geodesy and Astrometry Working Meeting*, pp. 161–164.
- Böhm, J., J. Wresnik, and A. Pany (2007). Simulation of Wet Zenith Delays and Clocks. IVS memorandum. <ftp://ivscc.gsfc.nasa.gov/pub/memos/ivs-2006-013v03.pdf>.
- Gipson, J. (2012). *Sked: VLBI Scheduling Software*. Goddard Space Flight Center. Program Reference Manual.
- Hase, H., R. Dassing, G. Kronschnabl, T. Kluegel, C. Plötz, A. Neidhardt, P. Lauber, and R. Kilger (2009). Status of the Twin Telescope Wettzell Project. In G. Bourda, P. Charlot, and A. Collioud (Eds.), *Proceedings of the 19th European VLBI for Geodesy and Astrometry Working Meeting*, pp. 127–132.
- Herring, T., J. Davis, and I. Shapiro (1990). Geodesy by Radio Interferometry: The Application of Kalman Filtering to the Analysis of Very Long Baseline Interferometry Data. *Journal of Geophysical Research* 95(B8), 12561–12581.
- Himwich, E. and B. Corey (2009). VLBI2010 Antenna Control Recommendations. IVS mem-

- orandum. <ftp://ivscc.gsfc.nasa.gov/pub/memos/ivs-2009-003v01.pdf>.
- Ho, C. (2010). Solar Corona and Solar Wind Effects. DSN telecommunications link design handbook.
- Ma, C. (2009). The Second Realization of the International Celestial Reference Frame by Very Long Baseline Interferometry. IERS Technical Note 35, Verlag des Bundesamts für Kartographie und Geodäsie, Frankfurt am Main.
- MacMillan, D. (2007). VLBI2010 Simulations Using SOLVE. In J. Böhm, A. Pany, and H. Schuh (Eds.), *Proceedings of the 18th European VLBI for Geodesy and Astrometry Working Meeting*, ISSN 1811-8380, pp. 163–167.
- Niell, A., A. Whitney, B. Petrachenko, W. Schlüter, N. Vandenberg, H. Hase, Y. Koyama, C. Ma, H. Schuh, and G. Tuccari (2005). VLBI2010: Current and Future Requirements for Geodetic VLBI Systems. Report of working group 3 to the IVS directing board.
- Nilsson, T. and R. Haas (2010). Impact of Atmospheric Turbulence on Geodetic Very Long Baseline Interferometry. *Journal of Geophysical Research* 115(B03407).
- Nilsson, T., R. Haas, and G. Elgered (2007). Simulations of Atmospheric Path Delays Using Turbulence Models. In J. Böhm, A. Pany, and H. Schuh (Eds.), *Proceedings of the 18th European VLBI for Geodesy and Astrometry Working Meeting*, ISSN 1811-8380, pp. 175–180.
- Pany, A., J. Böhm, D. MacMillan, H. Schuh, T. Nilsson, and J. Wresnik (2011). Monte Carlo Simulations of the Impact of Troposphere, Clock and Measurement Errors on the Repeatability of VLBI Positions. *Journal of Geodesy* 85, 39–50.
- Pany, A., J. Böhm, H. Schuh, T. Hobiger, and R. Ichikawa (2009). Modeling Azimuthal Asymmetries of the Troposphere Delay During a 14-days Typhoon Period in Tsukuba. In G. Bourda, P. Charlot, and A. Collioud (Eds.), *Proceedings of the 19th European VLBI for Geodesy and Astrometry Working Meeting*, pp. 44–48.
- Petit, G. and B. Luzum (2010). IERS Conventions. IERS Technical Note 36, Verlag des Bundesamts für Kartographie und Geodäsie, Frankfurt am Main.
- Petrachenko, B. (2006). The Case For and Against Multiple Antennas at a Site. IVS memorandum. <ftp://ivscc.gsfc.nasa.gov/pub/memos/ivs-2006-019v01.pdf>.
- Petrachenko, B., J. Böhm, D. MacMillan, A. Niell, A. Pany, A. Searle, and J. Wresnik (2008). VLBI2010 Antenna Slew Rate Study. In A. Finkelstein and D. Behrend (Eds.), *The 5th IVS General Meeting Proceedings*, pp. 410–415.
- Petrachenko, B., A. Niell, D. Behrend, B. Corey, J. Böhm, P. Charlot, A. Collioud, J. Gipson, R. Haas, T. Hobiger, Y. Koyama, D. MacMillan, Z. Malkin, T. Nilsson, A. Pany,

- G. Tuccari, A. Whitney, and J. Wresnik (2009). Design Aspects of the VLBI2010 System. Progress report of the IVS VLBI2010 committee.
- Plag, H., R. Gross, and R. M. (2009). Global Geodetic Observing System for Geohazards and Global Change. *Geosci BRGM's J Sustain Earth* 9, 96103.
- Schlüter, W. and D. Behrend (2007). The International VLBI Service for Geodesy and Astrometry (IVS): Current Capabilities and Future Prospects. *Journal of Geodesy* 81(6-8), 379–387.
- Schuh, H. and J. Böhm (2013). Very Long Baseline Interferometry for Geodesy and Astrometry. In G. Xu (Ed.), *Sciences of Geodesy II, Innovations and Future Developments*, pp. 339–376.
- Schuh, H., P. Charlot, H. Hase, E. Himwich, K. Kingham, C. Klatt, C. Ma, Z. Malkin, A. Niell, A. Nothnagel, W. Schlüter, K. Takashima, and N. Vandenberg (2002). Product Specification and Observing Programs. Report of working group 2 to the IVS directing board.
- Steuftmeh, H. (1994). *Optimierung von Beobachtungsplänen in der Langbasisinterferometrie (VLBI)*. Ph. D. thesis, Verlag des Instituts für Angewandte Geodäsie.
- Sun, J., C. Dai, N. Jian, Y. Zhou, G. Wang, and J. Ping (2010). Investigation of stronger diurnal ERP signals in summer derived from the VLBI CONT08 campaign. *Chinese Science Bulletin* 55(29), 3274–3278.
- Sun, J., A. Pany, J. Böhm, and H. Schuh (2011). Status and Future Plans for the VieVS Scheduling Package. In W. Alef, S. Bernhart, and A. Nothnagel (Eds.), *Proceedings of the 20th Meetings of the European VLBI Group for Geodesy and Astrometry*, pp. 44–48.
- Teke, K., J. Böhm, H. Spicakova, A. Pany, L. Plank, H. Schuh, and E. Tanir (2009). Piecewise Linear Offsets for VLBI Parameter Estimation. In G. Bourda, P. Charlot, and A. Collioud (Eds.), *Proceedings of the 19th European VLBI for Geodesy and Astrometry Working Meeting*, pp. 63–67.
- Treuhaft, R. and G. Lanyi (1987). The Effect of the Dynamic Wet Troposphere on Radio Interferometric Measurements. *Radio Science* 22(2), 251–265.
- Vandenberg, N. (1997a). *Sked's Catalogs*. Goddard Space Flight Center. Program Reference Manual.
- Vandenberg, N. (1997b). *Standard Schedule File Format*. Goddard Space Flight Center. Program Reference Manual.
- Wresnik, J. (2009). *Simulationen für die neue Generation von VLBI-Systemen*. Ph. D. thesis, Technische Universität Wien.

- Wresnik, J., J. Böhm, A. Pany, and H. Schuh (2009). VLBI2010 simulations at IGG Vienna. In G. Bourda, P. Charlot, and A. Collioud (Eds.), *Proceedings of the 19th European VLBI for Geodesy and Astrometry Working Meeting*, pp. 147–150.
- Wresnik, J., J. Böhm, A. Pany, J. Wresnik, and H. Schuh (2008). VLBI2010 Simulations at IGG Vienna. In A. Finkelstein and D. Behrend (Eds.), *The 5th IVS General Meeting Proceedings*, pp. 421–426.
- Wresnik, J., J. Böhm, and H. Schuh (2006). Simulations for VLBI2010. In D. Behrend and K. Baver (Eds.), *International VLBI Service for Geodesy and Astrometry 2006 General Meeting Proceedings*, NASA/CP-2006-214140, pp. 93–97.
- Wresnik, J., J. Böhm, and H. Schuh (2007). Monte Carlo Simulations for VLBI2010. In J. Böhm, A. Pany, and H. Schuh (Eds.), *Proceedings of the 18th European VLBI for Geodesy and Astrometry Working Meeting*, ISSN 1811-8380, pp. 168–174.

Curriculum vitae

- 19.02.1980 Born in Shandong, China
- 1997-2001 Bachelor studies at the Department of Electronic and Informational Engineering,
Academy of Aeronautical Engineering, Qingdao, China
- 2001-2004 Master of Science (MSc) studies on Satellite Navigation
at the Communication and Information System Department,
Academy of Equipment Command and Technology, Beijing, China
- 2004- Engineer at the Beijing Aerospace Control Center,
Beijing, China
- 2008- Doctoral studies on astro-geodynamics at the Shanghai Astronomical Observatory,
Chinese National Academy of Sciences, Shanghai, China
- 2010- Doctoral studies at the Research Group Advanced Geodesy
of Department of Geodesy and Geoinformation,
Vienna University of Technology, Vienna, Austria

A. Appendices

A.1. Reference manual of VIE_SCHED program

In order to exploit the full power of the future VLBI2010 system and to derive the best possible geodetic parameters, a new scheduling package (VIE_SCHED) has been developed at Vienna University of Technology. It is one part of the Vienna VLBI Software (VieVS). This appendix serves as reference manual of VIE_SCHED program.

A.1.1. Overview of VIE_SCHED

Scheduling is the first step in preparation for a VLBI experiment. VIE_SCHED is such an program that helps you prepare schedules for VLBI observing sessions automatically. VIE_SCHED is normally used for geodetic VLBI sessions.

VIE_SCHED, as part of VieVS, was originally written by Jing Sun in 2010 from scratch. VieVS is a new geodetic VLBI analysis software developed at Vienna University of Technology, since 2008. VieVS has now reached a mature status and produces results with as high accuracy as other VLBI software package (Böhm et al., 2009, 2012). For more information about VieVS, see the VieVS webpage (<http://vievs.hg.tuwien.at.at>). To be consistent with VieVS, VIE_SCHED is also written in Matlab which makes it easy to use and modify and it is designed to run under Windows and Linux operating systems. Currently VIE_SCHED package is maintained by the advanced geodesy research group at Vienna University of Technology, and Jing Sun has primary responsibility for it. The latest version of VIE_SCHED (VIE_SCHED 2.0) was released together with VieVS 2.0 in August, 2012. This manual is based on VIE_SCHED 2.0 version. As constant changes and improvements will be made to VIE_SCHED, the manual will be updated and released correspondingly. As the initial developer, I am always eager to hear suggestion

from users for improving it. Questions, problems, and comments may be addressed at any time to Jing Sun at: jing.sun@tuwien.ac.at, that will be handled with high priority.

A.1.2. Distribution and installation

To get VieVS and VIE_SCHED, the external users are asked to send a letter describing the purpose they would like to use VieVS for. Then the user will be given username and password to access the webpage (<http://vievs.hg.tuwien.ac.at/>) using ftp. To install VieVS and VIE_SCHED you need to download the VieVS directory. If you do not need all NGS files (located in VieVS/DATA/NGS/) you do not need to download all of them. The structure of VIE_SCHED within VieVS is shown in Figure A.1.1.

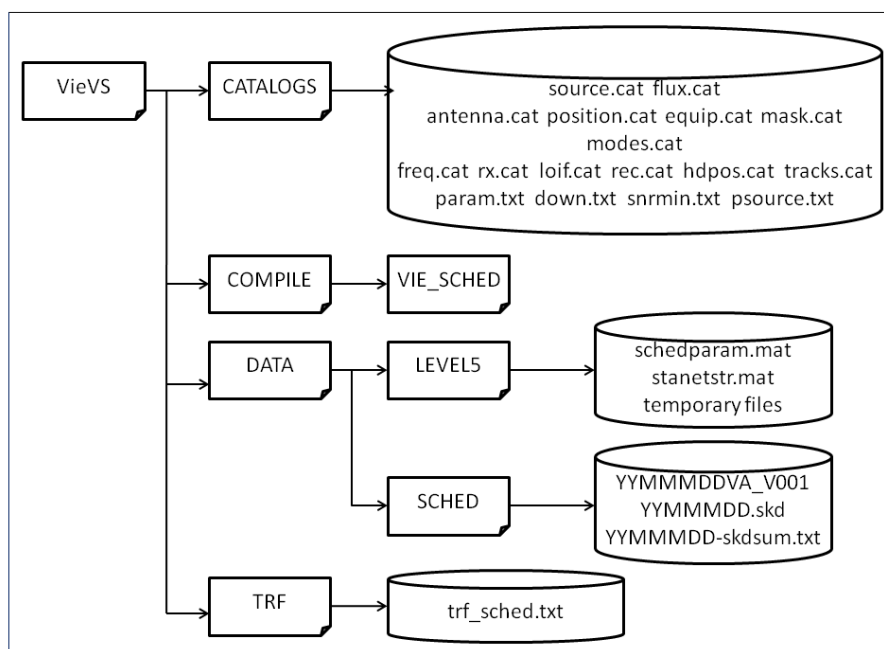


Figure A.1.1.: The structure of VIE_SCHED within VieVS.

In VieVS/CATALOGS/ directory, all input files consisting of catalog system files and local control files are located. The source code of VIE_SCHED is saved in VieVS/COMPILE/VIE_SCHED_V20/ folder. The “V20” indicates the version of VIE_SCHED. During the scheduling some temporary files are created and stored in VieVS/DATA/LEVEL5/ folder, which can be used for troubleshooting when you run into trouble. The output scheduling files are written into VieVS/DATA/SCHED/ folder. To keep station position consistent with that used in simulation and estimation, a

trf_sched.txt file is created by copying the station positions out of position.cat file and put in VieVS/TRF/ folder.

A.1.3. Input files

All the input files of VIE_SCHED are located in the area of VieVS/CATALOGS/, which consist of catalog system files (.cat files) and local control files (.txt files). The directory, path for the input files, and file names are fixed in VIE_SCHED.

Catalog system files

VIE_SCHED reads catalog system files for selection of sources, stations, and observing modes when creating a schedule for an VLBI experiment. The catalog system files are ASCII files controlled and maintained at Goddard Space Flight Center (GSFC) and are available via anonymous ftp (<ftp://gemini.gsfc.nasa.gov/pub/sked/catalogs/>). The catalog files contain only the most up to date information on sources, antennas, and equipments. These files should be refreshed by copying the latest versions via ftp to your local VieVS/CATALOGS/ directory whenever a change is announced. The information on the catalog files and the fields in each of the catalog files are described in document (Vandenberg, 1997a) at <ftp://gemini.gsfc.nasa.gov/pub/sked/docs/>. Table A.1.1 lists all the catalog files and their contents. The VIE_SCHED program can be run for either simulation research or real VLBI experiment. The usage of each catalog file is also given in the last column in Table A.1.1.

Table A.1.1.: Catalog system files.

Type	File Name	Contents	Used for
Sources:			
	source.cat	source positions	simu + real
	flux.cat	source fluxes	simu + real
Stations:			
	antenna.cat	antenna information	simu + real
	position.cat	station x,y,z locations	simu + real
	equip.cat	equipment IDs	simu + real
	mask.cat	horizon and coordinate masks	simu + real
Observing modes:			
	modes.cat	observing modes	simu + real
	freq.cat	frequency sequences	real

rx.cat	receiver setups	real
loif.cat	station LO and IF setups	real
rec.cat	recording modes	real
hdpos.cat	head offsets	real
tracks.cat	standard recorded tracks	real

It is also possible to maintain a personal copy of any of the catalogs and use that in VIE_SCHED by your requirement. Especially for the simulation studies, the catalogus files need to be extended by virtual stations at different locations and of different quality (station specifications). The task of editing the catalog file should be given great care, because each catalog file does not stand alone and there are cross references to other catalogs within some of the catalog files. The order of the entries is not irrelevant for VIE_SCHED because matching is done by name or by code which is required to be unique within a file. To change some catalog entries for real VLBI experiment, you can refer to catalogs manual (Vandenberg, 1997a) for detailed format descriptions or send the information to me and I will make the appropriate entries and create new ASCII catalog files for you. The next section outlines how to change information on sources, stations, and observing modes for simulation research. If you run into problems in the procedure for changing a catalog entry, please notify me via email and I will help you work through it.

(1) How to change information on sources.

The IAU names (and common names, if have) in the source.cat file are used to find the same-named entries in the flux.cat. To change the list of available sources, you should edit source.cat file giving IAU names (and common names, if available) of sources and positions (right ascension and declination) following the existing entries. Then edit the flux.cat file to enter the source fluxes and models by common names. If you make a change in source.cat file or flux.cat file, you must delete the current source.mat file (located in VieVS/DATA/LEVEL5/) before running VIE_SCHED. Then the new information on sources can be read and used by VIE_SCHED, otherwise the old information on sources saved in source.mat file will be loaded into VIE_SCHED. If no flux value is available for a given source, the source will not be used for scheduling.

(2) How to change information on stations.

VIE_SCHED reads the antenna names in the antenna.cat file to find the corresponding entries in the position.cat, equip.cat, and mask.cat catalog files. The four catalogs are linked together

by antenna name, which must be unique in each catalog. You can edit the ASCII catalog files on your computer and change the parameters following the original version. It will be good for backup to put a comment (line beginning with *) before or after your new/revised entry to indicate what you changed and why. To add a new station locally, you need to do the steps below to make sure all of the necessary catalogs and important parameters are updated.

Step 1: Edit the antenna.cat file to add the new antenna information including 8-character antenna name, axis type, slewing rate, constant, and limits for axis. In current version, two kinds of axis type (AZEL and HADC) can be processed in VIE_SCHED. For the other axis types, the user has to calculate and transform the antenna parameters correspondingly by himself.

Step 2: Edit position.cat file to enter the new position using the same name as antenna name. Geocentric XYZ coordinates of the site will be used in VIE_SCHED, while latitude and longitude are ignored.

Step 3: Make a new entry in equip.cat file, because the SEFD information of station will be used to calculate scan length automatically.

Step 4: Give a new entry in mask.cat file if the station has a horizon mask. Only this step is not requisite for scheduling.

As for the selection error conditions, if there are missing values for an antenna, this antenna will be excluded from the schedule and VIE_SCHED will issue warning message and proceed. Hence care must be taken in scheduling to ensure that the antenna parameters are complete.

(3) How to change information on observing modes.

All the possible observing modes for scheduling are listed in modes.cat file. You can edit the entry already defined or insert a new observing mode, but mode name is fixed to be "VLBI2010obsmodes" in VIE_SCHED. Be careful that the number of channels, sample rate, and 1 or 2 bits of quantification are specified for this observing mode, which will be used for calculation of scan length. The complete information on observing modes is checked thoroughly at the beginning. VIE_SCHED will not continue if the observing mode is not complete.

Local control files

Besides the catalog system files, four local control files are read and used by VIE_SCHED. Out of the four files described below, only param.txt file is a required input for VIE_SCHED, while the other three optional local control files are present if they are needed.

(1) param.txt file

VIE_SCHED automatically chooses scans using a rule-based approach. The major selecting options on the network, session time, scheduling strategy (source-based strategy or station-based strategy) can be specified on the graphical user interface (GUI) of VIE_SCHED. The various minor scheduling parameters are listed and set by user in param.txt file. For example, generally speaking, you do not want to observe the same source twice in a short interval. This leads to a rule saying “don’t observe a source if it has been observed in the last X minutes”, where X is user settable in param.txt file. The following Table A.1.2 presents an overview of each of the minor scheduling options and its brief description.

Table A.1.2.: Minor scheduling options.

Option	Description
PARA.WAVEL(1)	Wavelength of X band [meter]
PARA.WAVEL(2)	Wavelength of S band [meter]
PARA.RATE1A	Acceleration of AZ/HA axis [deg/s ²]
PARA.RATE2A	Acceleration of EL/DC axis [deg/s ²]
PARA.MARGEL1	Marge for AZ/HA axis [deg]
PARA.MARGEL2	Marge for EL/DC axis [deg]
PARA.MIN_SRCRP	The interval that the same source will not be observed twice [min]
PARA.SOURCE	Time for the antenna to settle down after slewing and before observation start time [sec]
PARA.TAPETM	Time for the tape after slewing and before observation start time [sec]
PARA.IDLE	Time allowed for idling after slewing and before observation start time [sec]
PARA.CALIBRATION	Time allowed for calibration after slewing and before observation start time [sec]
PARA.MAXSLEWTIME	Maximum time to allow an antenna to slew [sec]
PARA.MAX_WAIT	Maximum time to wait for the slow antenna [min]
PARA.CORSYNCH	Time to allow the correlator to synchronize tapes [sec]
PARA.MAX_SCAN	Maximum allowable scan time [sec]
PARA.MIN_SCAN	Minimum allowable scan time [sec]
PARA.FILLINMODE	If use fill-in mode (1/0)
PARA.FILLENDT	Maximum time for the end time of fill-in scan [min]
PARA.SCREEN	If print processing information on screen (1/0)

PARA.MIN_STANUM	Minimum subnet scheduled at one time
PARA.MIN_SRC2ANG	Minimum angle between two sources observed simultaneously [deg]
PARA.SKYDT	The interval for calculation of sky coverage [min]
PARA.EXPER	Experiment code
PARA.DESCRPTION	Description of the experiment
PARA.SCANDURA	The default scan length [sec]
PARA.TRACKSMODE	The formatter mode

(2) down.txt file

Frequently a station is unavailable for some part of the session. The most common, although not the only, reason is that it is participating in an intensive session. The down.txt file is used to indicate when some stations are unavailable for observing during a session. The scheduler specifies an interval when a station or subnet is unavailable (“down”), and VIE_SCHED will automatically ignore these stations during this interval. A station can have multiple downtimes in a schedule.

(3) snrmin.txt file

The minimum SNR targets for all stations are specified on the GUI of VIE_SCHED. In practice, some antennas are weaker, i.e. larger SEFD, so they will be given a lower minimum SNR target on all baselines involving this single station by band. The snrmin.txt file, if present, overrides the values from GUI.

(4) psource.txt file

As it is said above, VIE_SCHED is developed for geodetic VLBI experiments. On the other side, we are always observing new sources or particular sources with the VLBI technique. The psource.txt file is used to list the astrometric sources and set the observation density target.

A.1.4. How to run VIE_SCHED

After starting Matlab you should make the VieVS/WORK/ directory to current folder. Typing “VieVS” in the Matlab command window starts the interface of latest version of VieVS. After you select “Scheduling” menu label on the top of the interface, the interface of VIE_SCHED (see

Figure A.1.2) appears.

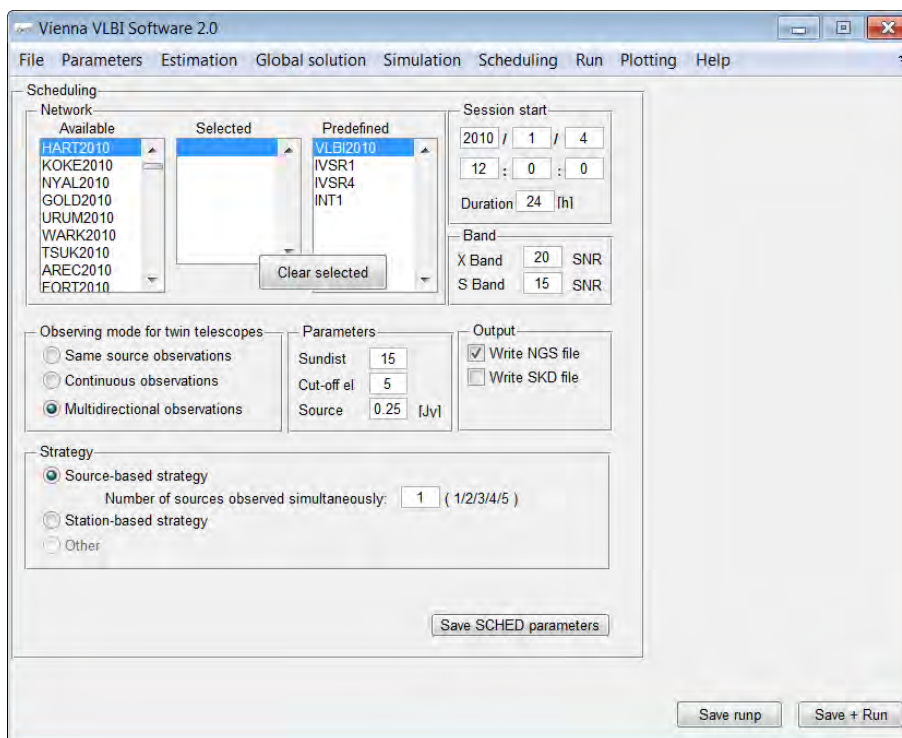


Figure A.1.2.: VIE_SCHED graphical user interface (GUI).

Here you can:

- Select the stations or use a predefined network. VIE_SCHED put the station names of all the entries in antenna.cat into the listbox of "Available". During the process of selecting stations you can add or remove stations from this list.
- Change the start time of the session and its duration.
- Set the SNR targets.
- Specify the observing mode for twin telescopes if there are twin telescopes in the network.
- Give the three basic parameters for scheduling (minimum angle distance to the Sun, cut-off elevation, minimum flux of source over all baselines).
- Specify the type of output file (NGS file or SKD file).

- Specify the strategy used for scheduling.

For a real VLBI experiment, the master file is the usual starting point for setting up a schedule. The masterfile is a table that lists all geodetic and astrometric sessions within the IVS. All IVS sessions have a unique experiment code associated with it. In addition to the session code, it includes the date of the session, the duration, the institution responsible for scheduling the session, the correlator, and other information.

Then go to “Run options” interface and select the “Run vie_sched” checkbox as shown in Figure A.1.3. Pushing “Save+Run” button starts running of VIE_SCHED.

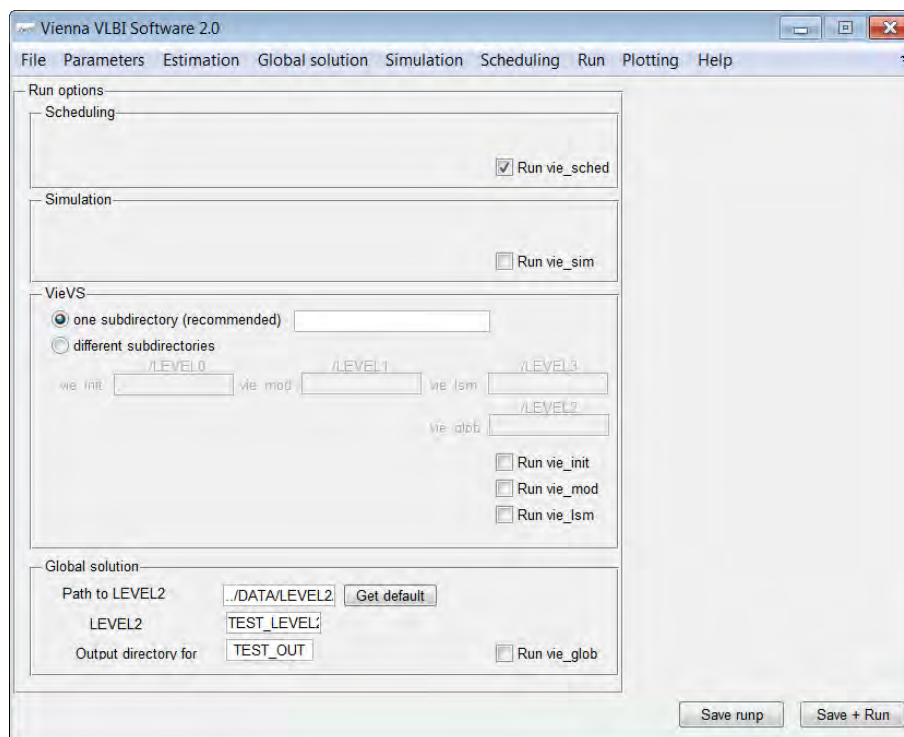


Figure A.1.3.: Run options for VIE_SCHED.

After announcing itself, VIE_SCHED reads all the input files and summarizes what it finds. VIE_SCHED will automatically select scans to fill up the schedule from the start time, stopping when time is reached. And you can also find detailed information on scheduled scans in the command window when VIE_SCHED is running. Expert users can use those message for judging its running status or debugging purposes. At the very end VIE_SCHED finishes with the ending time information.

A.1.5. Output files

As for output of VIE_SCHEM, it can generate standard NGS files for simulation and schedule files (.skd) for real VLBI experiment, which can be found in VieVS/DATA/SCHEM/. You can make the different types of output by setting the options on the GUI to meet your requirements. Additionally, a summary file (skdsum.txt) is also written in VieVS/DATA/SCHEM/, where you can get a preliminary evaluation of many aspects of the schedule. In VieVS/TRF/, trf_sched.txt file is generated and saved which contains the station positions used for scheduling.

(1) In output NGS file, the delay observations are set to zero in the data cards. VieVS simulation package (VIE_SIM) can read the empty NGS file directly, which provides a convenient way to connect scheduling with simulation and provides feedbacks on the quality of the schedule.

(2) The schedule file with a .skd extension is simply an ASCII file with different labeled sections. It contains a complete description of the session, the schedule, and the additional information needed to conduct the experiment for the complete network of stations and correlators. A description of the format of each schedule file section is contained in (Vandenberg, 1997b). The naming convention for IVS schedule files is “experiment code.skd”, where experiment code is listed in the master file. After you generate your schedule, the .skd file is copied to a central server location where the participating stations can access it electronically. The stations download the file and then run the Field System program drudg to make control files and listings for the experiment.

A.1.6. Analyzing tools

Some analyzing tools are developed (located in VieVS/DATA/SCHEM/) to obtain the statistics of schedule characteristics, to make plots of the distribution of scans and observations, plots of the distribution of sources on the celestial sphere in a short interval, plots of sky coverage at stations, displays of source-switching intervals, and so on. The graphical output will not be captured and incorporated in this manual. In a word, it is a good practice to always run analyzing tools after generating a schedule.

GEOWISSENSCHAFTLICHE MITTEILUNGEN

Bisher erschienen:

- Heft 1 Kolloquium der Assistenten der Studienrichtung Vermessungswesen. 1970 - 1973, Dezember 1973.
- Heft 2 EGGER-PERDICH-PLACH-WAGENSOMMERER, Taschenrechner HP 45 und HP 65, Programme und Anwendungen im Vermessungswesen. 1. Auflage, März 1974, Special Edition in English, Juli 1974, 2. verbesserte Auflage, November 1974.
- Heft 3 Kolloquium der Assistenten der Studienrichtung Vermessungswesen 1973 - 1974, September 1974.
- Heft 4 EGGER-PALFINGER-PERDICH-PLACH-WAGENSOMMERER, Tektronix-Tischrechner TEK 31, Programmbibliothek für den Einsatz im Vermessungswesen, November 1974.
- Heft 5 K. LEDERSTEGGER, Die horizontale Isostasie und das isostatische Geoid, Februar 1975.
- Heft 6 F. REINHART, Katalog von FK4 Horrebow-Paaren für Breiten von +30 bis +60, Oktober 1975.
- Heft 7 Arbeiten aus dem Institut für Höhere Geodäsie, Wien, Dezember 1975.
- Heft 8 Veröffentlichungen des Instituts für Photogrammetrie zum XIII. Internationalen Kongreß für Photogrammetrie in Helsinki 1976, Wien, Juli 1976.
- Heft 9 W. PILLEWIZER, Felsdarstellung aus Orthophotos, Wien, Juni 1976.
- Heft 10 PERDICH-PLACH-WAGENSOMMERER, Der Einsatz des programmierbaren Taschenrechners Texas Instruments SR-52 mit Drucker PC100 in ingenieurgeodätischen Rechentechnik, Wien, Mai 1976.
- Heft 11 Kolloquium der Assistenten der Studienrichtung Vermessungswesen 1974 - 1976, November 1976.
- Heft 12 Kartographische Vorträge der Geodätischen Informationstage 1976, Wien, Mai 1977.
- Heft 13 Veröffentlichung des Instituts für Photogrammetrie anlässlich des 80. Geburtstages von Prof. Dr.h.c. K. Neumaier, Wien, Januar 1978.
- Heft 14 L. MOLNAR, Self Checking Analytical Relative Orientation and Strip Formation, Wien, Dezember 1978.
- Heft 15 Veröffentlichung des Instituts für Landesvermessung anlässlich des 80. Geburtstages von Prof. Dr. Alois Bavir, Wien, Januar 1979.
- Heft 16 Kolloquium der Assistenten der Studienrichtung Vermessungswesen 1976 - 1978, Wien, November 1979.
- Heft 17 E. VOZIKIS, Die photographische Differentialumbildung gekrümmter Flächen mit Beispielen aus der Architekturbildmessung, Wien, Dezember 1979.
- Heft 18 Veröffentlichung des Instituts für Allgemeine Geodäsie anlässlich des 75. Geburtstages von Prof. Dipl.-Ing. Dr. F. Hauer, Die Höhe des Großglockners, Wien, 1981.
- Heft 19 H. KAGER, Bündeltriangulation mit indirekt beobachteten Kreiszentren, Wien, April 1981.
- Heft 20 Kartographische Vorträge der Geodätischen Informationstage 1980, Wien, Mai 1982.
- Heft 21 Veröffentlichung des Instituts für Kartographie anlässlich des 70. Geburtstages von Prof. Dr. Wolfgang Pillewizer: Glaziologie und Kartographie, Wien, Dezember 1982.
- Heft 22 K. TEMPFLI, Genauigkeitsschätzung digitaler Höhenmodelle mittels Spektralanalyse, Wien, Mai 1982.
- Heft 23 E. CSAPLOVICS, Interpretation von Farbinfrarotbildern, Wien, November 1982.

- Heft 24 J. JANSKA, Rektifizierung von Multispektral-Scanneraufnahmen - Entwicklung und Erprobung eines EDV-Programms, Wien, Mai 1983.
- Heft 25 Zusammenfassung der Diplomarbeiten, Dissertationen und Habilitationen an den geodätischen Instituten der TU Wien, Wien, November 1984.
- Heft 26 T. WUNDERLICH, Die voraussetzungsfreie Bestimmung von Refraktionswinkeln, Wien, August 1985.
- Heft 27 G. GERSTBACH (Hrsg.), Geowissenschaftliche/geotechnische Daten in Landinformationssystemen - Bedarf und Möglichkeiten in Österreich, Juni 1986.
- Heft 28 K. NOVAK, Orientierung von Amateuraufnahmen ohne Paßpunkte, Wien, August 1986.
- Heft 29 Veröffentlichung des Instituts für Landesvermessung und Ingenieurgeodäsie, Abt. Ingenieurgeodäsie, anlässlich des 80. Geburtstages von Prof. Dipl.-Ing. Dr. F. Hauer, Wien, Oktober 1986.
- Heft 30 K.-H. ROCH, Über die Bedeutung dynamisch ermittelter Parameter für die Bestimmung von Gesteins- und Gebirgseigenschaften, Wien, Februar 1987.
- Heft 31 G. HE, Bildverbesserung mittels digitaler Filterung, Wien, April 1989.
- Heft 32 F. SCHLÖGELHOFER, Qualitäts- und Wirtschaftlichkeitsmodelle für die Ingenieurphotogrammetrie, Wien, April 1989.
- Heft 33 G. GERSTBACH (Hrsg.), Geowissenschaftliche/geotechnische Daten in Landinformationssystemen - Datenbestände und Datenaustausch in Österreich, Wien, Juni 1989.
- Heft 34 F. HOCHSTÖGER, Ein Beitrag zur Anwendung und Visualisierung digitaler Geländemodelle, Wien, Dezember 1989.
- Heft 35 R. WEBER, Lokale Schwerefeldmodellierung unter Berücksichtigung spektraler Methoden zur Geländereduktion, Wien, April 1990.
- Heft 36 o.Prof. Dr. Hans Schmid zum 70. Geburtstag. Veröffentlichung der Abteilung für Landesvermessung, Wien, Oktober 1990.
- Heft 37 G. GERSTBACH, H. P. HÖLLRIEGL und R. WEBER, Geowissenschaftliche Informationsbörse - Eine Nachlese zu GeoLIS II, Wien, Oktober 1990.
- Heft 38 R. ECKER, Rastergraphische Visualisierungen mittels digitaler Geländemodelle, Wien, August 1991.
- Heft 39 Kartographische Forschungen und Anwendungsorientierte Entwicklungen, herausgegeben von W. Stams und F. Kelnhofer zum 80. Geburtstag von Prof. Dr. W. Pillewizer, Wien, Juli 1991.
- Heft 39a W. RIEGER, Hydrologische Anwendungen des digitalen Geländemodells, Wien, Juli 1992.
- Heft 40 K. STEINNOCHER, Methodische Erweiterungen der Landnutzungsklassifikation und Implementierung auf einem Transputernetzwerk, Wien, Juli 1994.
- Heft 41 G. FORKERT, Die Lösung photogrammetrischer Orientierungs- und Rekonstruktionsaufgaben mittels allgemeiner kurvenförmiger Elemente, Wien, Juli 1994.
- Heft 42 M. SCHÖNER, W. SCHÖNER, Photogrammetrische und glaziologische Untersuchungen am Gäsbre (Ergebnisse der Spitzbergenexpedition 1991), Wien, Mai 1996.
- Heft 43 M. ROIC, Erfassung von nicht signalisierten 3D-Strukturen mit Videotheodoliten, Wien, April 1996.
- Heft 44 G. RETSCHER, 3D-Gleiserfassung mit einem Multisensorsystem und linearen Filterverfahren, Wien, April 1996.
- Heft 45 W. DAXINGER, Astrogravimetrische Geoidbestimmung für Ingenieurprojekte, Wien, Juli 1996.
- Heft 46 M. PLONER, CCD-Astrometrie von Objekten des geostationären Ringes, Wien, November 1996.

- Heft 47 Zum Gedenken an Karl Killian "Ingenieur" und "Geodät" 1903-1991, Veröffentlichung der Fachgruppe Geowissenschaften, Wien, Februar 1997.
- Heft 48 A. SINDHUBER, Ergänzung und Fortführung eines digitalen Landschaftsmodelles mit multispektralen und hochauflösenden Fernerkundungsaufnahmen, Wien, Mai 1998.
- Heft 49 W. WAGNER, Soil Moisture Retrieval from ERS Scatterometer Data, Wien, Dezember 1998.
- Heft 50 R. WEBER, E. FRAGNER (Editoren), Prof. Bretterbauer, Festschrift zum 70. Geburtstag, Wien, Juli 1999.
- Heft 51 Ch. ÖHRENER, A Similarity Measure for Global Image Matching Based on The Forward Modeling Principle, Wien, April 1999.
- Heft 52 M. LECHTHALER, G. GARTNER, Per Aspera ad Astra, Festschrift für Fritz Kelnhofer zum 60. Geburtstag, Wien, Jänner 2000.
- Heft 53 F. KELNHOFER, M. LECHTHALER, Interaktive Karten (Atlanten) und Multimedia – Applikationen, Wien, März 2000.
- Heft 54 A. MISCHKE, Entwicklung eines Videotheodolit-Meßsystems zur automatischen Richtungsmessung von nicht signalisierten Objektpunkten, Wien, Mai 2000.
- Heft 55 Veröffentlichung des I.P.F. anlässlich der Emeritierung von Prof. Dr. Peter Waldhäusl, Wien.
- Heft 56 F. ROTTENSTEINER, Semi-automatic Extraction of Buildings Based on Hybrid Adjustment Using 3D Surface Models and Management of Building Data in a TIS, Wien, Juni 2001.
- Heft 57 D. LEGENSTEIN, Objektrekonstruktion aus perspektiven Bildern unter Einbeziehung von Umrisslinien, Wien, Mai 2001.
- Heft 58 F. KELNHOFER, M. LECHTHALER und K. BRUNNER (Hrsg.), Telekartographie und Location Based Services, Wien, Jänner 2002.
- Heft 59 K. BRETTERBAUER, Die runde Erde eben dargestellt: Abbildungslehre und sphärische Kartennetzentwürfe, Wien, 2002.
- Heft 60 G. GARTNER, Maps and the Internet 2002, Wien 2002.
- Heft 61 L. DORFFNER, Erzeugung von qualitativ hochwertigen 3D Photomodellen für Internetbasierte Anwendungen mit besonderem Augenmerk auf Objekte der Nahbereichsphotogrammetrie, Wien, Jänner 2002.
- Heft 62 K. CHMELINA, Wissensbasierte Analyse von Verschiebungsdaten im Tunnelbau, Wien 2002.
- Heft 63 A. NIESSNER, Qualitative Deformationsanalyse unter Ausnutzung der Farbinformation, Wien 2002.
- Heft 64 K. BRETTERBAUER, R. WEBER, A Primer of Geodesy for GIS-Users, Wien 2003.
- Heft 65 N. PFEIFER, 3D Terrain Models on the basis of a triangulation, Wien, Jänner 2002.
- Heft 66 G. GARTNER (Hrsg), Location Based Services & Telecartography, Wien 2004.
- Heft 67 I. KABASHI, Gleichzeitig-gegenseitige Zenitwinkelmessung über größere Entfernungen mit automatischen Zielsystemen, Wien 2004.
- Heft 68 J. BÖHM, Troposphärische Laufzeitverzögerungen in der VLBI, Wien 2004.
- Heft 69 R. WEBER, W. SCHLÜTER, U. SCHREIBER, O. TITOV Evolving Space Geodesy Techniques (EGS XXVII General Assembly, Nice, France, 2002), Wien 2004.
- Heft 70 G. WEINWURM, Amalthea's Gravity Field and its Impact on a Spacecraft Trajectory, Wien 2004.

- Heft 71 Forschungsgruppe Ingenieurgeodäsie, Festschrift anlässlich des 65. Geburtstages von Herrn o.Univ. Prof. Dr.-Ing. Heribert Kahmen, Wien 2005.
- Heft 72 A. REITERER, A Knowledge-Based Decision System for an On-Line Video-Theodolite-Based Multisensor System, Wien 2005.
- Heft 73 M. HABERLER, Einsatz von Fuzzy Methoden zur Detektion konsistenter Punktbewegungen, Wien 2005.
- Heft 74 G. GARTNER, Location Based Services & Telecartography, Proceedings of the Symposium 2005, Wien 2005.
- Heft 75 Th. HOBIGER, VLBI as a tool to probe the ionosphere, Wien 2006.
- Heft 76 E. KLAFFENBÖCK, Troposphärische Laufzeitverzögerung von GNSS-Signalen – Nutzen aktiver Referenzstationsnetze für die Meteorologie, Wien 2006.
- Heft 76a P. J. MENDES-CERVEIRA, Tidal and non-tidal contributions to surface loading processes on station coordinates, Wien 2006.
- Heft 78 G. KOSTOV, G. BOURDA, L. FERNANDEZ, T. KONDO, Research Projects at IGG Reports, Wien 2007.
- Heft 79 J. BÖHM, A. PANY, H. SCHUH (Editors), Proceedings of the 18th European VLBI for Geodesy and Astrometry Working Meeting, 12-13 April 2007, Wien 2007.
- Heft 80 J. BÖHM, Tropospheric Delay Modelling at Radio Wavelengths for Space Geodetic Techniques, Wien 2007.
- Heft 81 G. Retscher, Mobile Multi-sensor Systems for Personal Navigation and Location-based Services, Wien 2007.
- Heft 82 R. HEINKELMANN, Bestimmung des atmosphärischen Wasserdampfes mittels VLBI als Beitrag zur Klimaforschung, Wien 2008.
- Heft 83 F. ROTTENSTEINER, Automatic extraction of buildings from airborne laserscanner data and aerial images, Wien 2008.
- Heft 84 S. TODOROVA, Kombination geodätischer Weltraumverfahren für globale Karten der Ionosphäre, Wien 2009.
- Heft 85 J. WRESNIK, Simulationen für die neue Generation von VLBI-Systemen, Wien 2009.
- Heft 86 A. KARABATIC, Precise Point Positioning (PPP). An alternative technique for ground based GNSS troposphere monitoring, Wien 2011.
- Heft 87 K. TEKE, Sub-daily Parameter Estimation in VLBI Data Analysis, Wien 2011.
- Heft 88 G. THALER, Echtzeit Bahn- und Uhrberechnung der GPS-Satellitenkonstellation basierend auf Beobachtungsdaten des RTIGS-Stationsnetzwerkes, Wien.
- Heft 89 P. SWATSCHINA, Dynamic and Reduced-Dynamic Precise Orbit Determination of Satellites in Low Earth Orbits, Wien 2012.
- Heft 90 S. BÖHM, Tidal excitation of Earth rotation observed by VLBI and GNSS, Wien 2012.
- Heft 91 H. KRÁSNA, Estimation of solid Earth tidal parameters and FCN with VLBI, Wien 2013.



TECHNISCHE
UNIVERSITÄT
WIEN
Vienna University of Technology

GEOWISSENSCHAFTLICHE MITTEILUNGEN

Heft Nr. 92, 2013

**VLBI scheduling strategies
with respect to VLBI2010**

Jing Sun

Veröffentlichung des Departments für Geodäsie und Geoinformation
ISSN 1811-8380

Schriftenreihe der Studienrichtung VERMESSUNG UND GEOINFORMATION